

DISS. ETH NO. 28755

Automated Design of Additive Manufactured Flow Components

A thesis submitted to attain the degree of

DOCTOR OF SCIENCES
(Dr. sc. ETH Zurich)

presented by

Manuel Biedermann

M.Sc. Technical University of Munich
born on 01.04.1991
citizen of Germany

accepted on the recommendation of

Prof. Dr.-Ing. Mirko Meboldt, examiner
Prof. Dr.-Ing. Sandro Wartzack, co-examiner

2022

Manuel Biedermann
manuel.biedermann@mavt.ethz.ch

©2022

ETH Zurich
Product Development Group Zurich
Leonhardstrasse 21
8092 Zurich
Switzerland

pd | z Product Development Group Zurich
Produktentwicklungsgruppe Zürich

Acknowledgments

I express my sincere gratitude to a number of people who supported me during my doctoral studies.

First of all, I would like to thank my doctoral advisor, Prof. Mirko Meboldt, who gave me the opportunity to pursue my doctoral studies, supported my research through many inspiring and valuable discussions, and gave me the trust and freedom to explore my ideas and passion. I would also like to express my sincere gratitude to Prof. Sandro Wartzack for his interest in this work and for accepting to be my co-examiner.

I would like to thank all my colleagues at the Product Development Group Zurich (pd|z). In particular, I would like to thank Patrick Beutler for all the insightful discussions and his valuable support and critical feedback as a sparring partner. Furthermore, my sincere gratitude goes to Julian Ferchow, Aschraf Danun, Daniel Omidvarkarjan, Urs Hofmann, Jonas Conrad, Marcel Gort, Prof. Christoph Klahn, Filippo Fontana, Timon Heinis, Daniel Türk, Prof. Bastian Leutenecker-Twelsiek, Kai von Petersdorff-Campen, Jan Zimmermann, Julian Wolf, Felix Wang, Stephan Fox, Stephan Wegner, Sara Mettler, Stefanie Dennis, Carole Haerry, and Dario Fenner. I am deeply grateful to have been part of this inspiring, creative, and cheerful working environment at pd|z.

I would like to thank all research and industry partners for the exciting collaborations. In particular, I want to thank Prof. Daniel Schwendemann and Silvan Walker from the IWK at OST, Lukas Böni, Patrick Rühls, and Eric Stirnemann from Planted, Ralph Kussmaul, Georgios Pappas, and Prof. Paolo Ermanni from the CMASLab, Silvia Rohner, Jan Thomas Meyer, Prof. Rogert Gassert, and Prof. Christian Bermes from the Varileg exoskeleton project, and Ralph Rosenbauer.

I would like to thank all students that I supervised during their bachelor, semester, and master thesis projects. It was always a pleasure to pass on knowledge, explore new research ideas together, be challenged by creative students, and participate in hackathons.

Finally, I would like to thank all my friends and my whole family – in particular my parents, Maria and Albert – for their long-standing support and encouragement during the past years.

Contents

Acknowledgments	i
Abstract.....	v
Zusammenfassung	vii
Nomenclature	x
1 Introduction.....	1
2 Background.....	7
2.1 Process chain of AM and main advantages.....	7
2.2 Potential benefits of AM for flow components.....	10
2.3 Basic considerations in the design of AM parts	13
2.4 Key challenges of a manual design approach.....	15
2.5 Automated design approach and research gap	19
3 Goals and contributions	22
3.1 Goals	22
3.2 Contributions.....	24
4 Study I: Automated creation and nesting of flow channels.....	29
4.1 Introduction	30
4.2 Computational design synthesis framework.....	34
4.3 Case study	45
4.4 Discussion.....	50
4.5 Conclusion.....	53
4.6 Acknowledgment	53

5	Study II: Automated consideration of overhang constraint.....	55
5.1	Introduction	56
5.2	Computational design methods	62
5.3	Case study	75
5.4	Discussion	85
5.5	Conclusion	88
5.6	Acknowledgment	88
5.7	Appendix.....	89
6	Study III: Automated routing of multiple flow channels	93
6.1	Introduction	94
6.2	Computational design methods	100
6.3	Case study	124
6.4	Discussion.....	136
6.5	Conclusion	139
6.6	Acknowledgment	139
6.7	Appendix.....	140
7	Conclusion and outlook.....	145
7.1	Conclusion	145
7.2	Outlook	151
	Bibliography	156
	Curriculum vitae	181
	List of publications.....	183

Abstract

Many prior works demonstrate the potential of additive manufacturing (AM) for flow components. Examples include nozzles, flow distributors, hydraulic manifolds, and heat exchangers. Compared to conventional manufacturing methods, such as milling and drilling, AM offers a high degree of design freedom and enables the fabrication of organic-shaped and functionally optimized flow structures. Such parts can be produced without additional tooling at reduced lead times, allowing the rapid and iterative testing of many design variants. In addition, AM enables the cost-efficient production of customized parts that can be tailored to the individual needs of specific customers or applications.

Despite the potential of AM, a key challenge is to design complex parts for AM. In practice, a common approach is to manually create the 3D geometry of parts using computer-aided design (CAD) tools. However, a manual design process can lead to several challenges. First, it requires considerable expert knowledge of AM and skills with CAD tools, which can be a critical barrier for novice designers. Second, the design of organic-shaped parts can be time-consuming and require the creation of hundreds of design features. Third, designers must consider process-related restrictions of AM (e.g., prevention of critical overhangs) and may require several manual loops to analyze and modify design features for manufacturability (e.g., adaption of circular flow channels to droplet shapes). Fourth, the part development can involve many design changes, e.g., to include feedback from simulations and iterative tests, compare different production scenarios, and customize parts to specific needs. If such frequent design changes are performed manually, the manual effort, labor costs, and development time can significantly increase.

This work aims to automate the design of complex flow components fabricated using AM. For this purpose, this work follows a knowledge-based engineering approach and implements rule- and knowledge-based design algorithms for specific flow components. In particular, this work focuses on multi-flow nozzles and hydraulic manifolds produced using the AM process of laser powder bed fusion. This work presents three studies, each focusing on a specific design challenge.

Study I automates the design of complex AM multi-flow nozzles. The basic modeling idea is to decompose nozzles into a set of design elements that are used as the basic building blocks of nozzles and include recurring features, such as different cross-section shapes, flow channels, channel branches, guiding vanes, and reinforcement ribs. These design elements are organized using a hierarchical structure. This modeling approach allows to capture the hierarchical nature of complex nozzles and automate the design creation and nesting of multiple flow channels.

Study II focuses on the automated consideration of the AM overhang constraint during the design generation of AM parts, such as hydraulic manifolds. For this purpose, the study models the dependency between geometric parameters (e.g., inclination of flow channel cross-sections) and process-related parameters of AM (e.g., build direction, minimal build angle, and maximum diameter of horizontal cross-sections). Based on these relations, this study demonstrates how to automatically create flow channels without critical overhangs inside the channels by locally modifying the shape of circular cross-sections to adapted shapes (e.g., droplet). In addition, this study shows how to generate integrated and sacrificial supports. The result is a production-ready 3D part design that can be used to fabricate prototypes or conduct simulations.

Study III automates the routing of multiple flow channels for AM flow components, such as hydraulic manifolds. For this purpose, the study models flow channels as virtual cables defined by a chain of particles (= centerline of flow channels) and collision spheres (= required space of each flow channel). These cables are iteratively subjected to geometric-based constraints in order to impose different functional part requirements (e.g., minimizing the length of flow channels and preventing overlaps between different channels). In addition, the adaption of channel cross-sections for AM is taken into account by iteratively updating the radii of the collision spheres during the automated routing of flow channels.

Based on the presented studies, a key conclusion is that a rule- and knowledge-based approach can be applied successfully to automate the design of complex AM flow components, such as multi-flow nozzles and hydraulic manifolds. Potential future research directions include transferring the results to different applications, further simplifying the automated design process, and integrating machine learning techniques.

Zusammenfassung

Viele bisherige Arbeiten demonstrieren das Potenzial der additiven Fertigung („*Additive Manufacturing*“, AM) für Strömungskomponenten. Beispiele sind Düsen, Strömungsverteiler, Hydraulikverteiler, und Wärmetauscher. Im Vergleich zu konventionellen Fertigungsverfahren wie Fräsen und Bohren bietet AM ein hohes Maß an Gestaltungsfreiheit und ermöglicht die Fertigung organisch geformter und funktional optimierter Strömungsstrukturen. Diese Bauteile können ohne zusätzliche Werkzeuge und in kürzerer Zeit hergestellt werden, was das schnelle und iterative Testen vieler Designvarianten ermöglicht. Darüber hinaus ermöglicht AM die kosteneffiziente Herstellung individualisierter Bauteile, die auf die spezifischen Bedürfnisse bestimmter Kunden oder Anwendungen angepasst werden können.

Trotz des Potenzials von AM besteht eine zentrale Herausforderung darin, komplexe Bauteile für AM zu konstruieren. In der Praxis erfolgt die Konstruktion der 3D-Geometrie von Bauteilen oft manuell mit CAD-Werkzeugen („*Computer-Aided Design*“). Ein manueller Konstruktionsprozess kann jedoch mehrere Probleme mit sich bringen. Erstens erfordert er ein beträchtliches Fachwissen über AM und Erfahrung im Umgang mit CAD-Werkzeugen, was für unerfahrene Konstrukteure eine kritische Hürde darstellen kann. Zweitens kann die Konstruktion von organisch geformten Bauteilen zeitaufwändig sein und die Erstellung von Hunderten von Designelementen erfordern. Drittens müssen Konstrukteure prozessbedingte Restriktionen von AM berücksichtigen (z. B. die Vermeidung kritischer Überhänge) und benötigen unter Umständen mehrere manuelle Schleifen, um Designelemente im Hinblick auf die Fertigbarkeit zu analysieren und anzupassen (z. B. Anpassung kreisförmiger Strömungskanäle auf Tropfenform). Viertens können bei der Entwicklung von Bauteilen viele Designänderungen erforderlich sein, um die Ergebnisse von Simulationen und iterativen Tests einzuarbeiten, verschiedene Produktionsszenarien zu vergleichen und Bauteile an spezifische Anforderungen anzupassen. Wenn solche häufigen Designänderungen manuell durchgeführt werden, können der manuelle Aufwand, die Arbeitskosten und die Entwicklungszeit erheblich steigen.

Zusammenfassung

Das Ziel dieser Arbeit ist es, die Konstruktion von komplex geformten Strömungskomponenten zu automatisieren, die mit AM hergestellt sind. Hierzu verfolgt diese Arbeit einen wissensbasierten Konstruktionsansatz und implementiert regel- und wissensbasierte Konstruktionsalgorithmen für ausgewählte Strömungskomponenten. Insbesondere konzentriert sich diese Arbeit auf Mehrstoffdüsen und Hydraulikblöcke, die mit dem AM Verfahren des selektiven Laserschmelzens hergestellt werden. In der Arbeit werden drei Studien vorgestellt, die sich jeweils auf eine spezifische Konstruktionsaufgabe konzentrieren.

Studie I automatisiert die Konstruktion komplexer Mehrstoffdüsen. Die grundlegende Modellierungsidee besteht darin, Düsen in eine Reihe von Designelementen zu zerlegen, die als Grundbausteine für Düsen verwendet werden können und häufig wiederkehrende Elemente enthalten wie verschiedene Kanalquerschnitte, Strömungskanäle, Kanalverzweigungen, Strömungsleitbleche und Verstärkungsrippen. Diese Designelemente sind in einer hierarchischen Struktur organisiert. Dieser Modellierungsansatz ermöglicht den hierarchischen Aufbau komplexer Düsen zu beschreiben und die Erstellung und Verschachtelung von mehreren Strömungskanälen zu automatisieren.

Studie II konzentriert sich auf die automatisierte Berücksichtigung der Überhangsrestriktion von AM bei der Generierung von AM Bauteilen, wie etwa Hydraulikverteiltern. Zu diesem Zweck modelliert die Studie die Abhängigkeit zwischen geometrischen Parametern (z.B. Neigung von Kanalquerschnitten) und prozessbedingten AM Parametern (z.B. Baurichtung, minimaler Bauwinkel und maximaler Durchmesser horizontaler Querschnitte). Auf Basis dieser Beziehungen zeigt die Studie, wie man Strömungskanäle ohne kritische Überhänge im Inneren der Kanäle erzeugen kann, indem die Form kreisförmiger Querschnitte automatisch lokal angepasst wird (z. B. auf eine Tropfenform). Darüber hinaus zeigt die Studie, wie integrierte und entfernbar Stützstrukturen erzeugt werden können. Das Ergebnis ist eine fertigungsgerechte 3D Bauteilgeometrie, die für die Herstellung von Prototypen oder die Durchführung von Simulationen verwendet werden kann.

Studie III automatisiert die Anordnung mehrerer Strömungskanäle für Strömungskomponenten, wie z. B. Hydraulikverteiler. Hierzu modelliert die Studie Strömungskanäle als virtuelle Kabel, die durch eine Kette von

Partikeln (= Mittellinie der Strömungskanäle) und Kollisionskugeln (= benötigter Raum für jeden Kanal) definiert sind. Diese Kabel werden iterativ geometrischen Zwangsbedingungen ausgesetzt, um verschiedene funktionale Bauteilanforderungen aufzuprägen (z. B. Minimierung der Länge der Strömungskanäle und Vermeidung von Überlappungen zwischen verschiedenen Kanälen). Zudem wird die Anpassung von Kanalquerschnitten für AM berücksichtigt, indem die Radien der Kollisionskugeln bei der Kanalanordnung iterativ aktualisiert werden.

Auf Basis der vorgestellten Studien ist eine zentrale Schlussfolgerung dieser Arbeit, dass ein regel- und wissensbasierter Konstruktionsansatz erfolgreich angewendet werden kann, um die Konstruktion von komplexen AM Strömungskomponenten zu automatisieren, wie z. B. von Mehrstoffdüsen und Hydraulikverteilern. Mögliche zukünftige Forschungsrichtungen sind die Übertragung der Ergebnisse auf andere Anwendungsbereiche, die weitere Vereinfachung des automatisierten Konstruktionsprozesses und die Integration von Techniken des maschinellen Lernens.

Nomenclature

Acronyms and abbreviations

3D	3-Dimensional
ASTM	American society for testing and materials
AM	Additive manufacturing
CAD	Computer-aided design
CFD	Computational fluid dynamics
DFAM	Design for additive manufacturing
E-PBF	Electron powder bed fusion
FEA	Finite element analysis
ISO	International organization for standardization
KBE	Knowledge-based engineering
L-PBF	Laser powder bed fusion
RQ	Research question
TO	Topology optimization
VDI	Verein Deutscher Ingenieure

Symbols

A	[%]	Required adaption of flow channels
C_j	[-]	Constraint with index j
d	[-]	Damping factor for cable simulation
D	[mm]	Diameter of a flow channel
D_{end}	[mm]	Diameter of a flow channel at the end point
D_{start}	[mm]	Diameter of a flow channel at the start point
D_{max}	[mm]	Maximum diameter of a horizontal flow channel
H	[mm]	Build height of an AM part
i	[-]	Index for particle i
j	[-]	Index for constraint j
It	[-]	Number of solver iterations
It_{max}	[-]	Maximum number of solver iterations
k	[-]	Index for particle k
l	[-]	Index for particle l
L	[mm]	Total length of flow channels (or cables)

L^0	[mm]	Initial length of flow channels (or cables)
m_P	[g]	Mass of part
N	[-]	Number of particles for discretizing cables
N_{batch}	[-]	Maximum number of AM parts in build space
N_{total}	[-]	Total number of particles for all cables
\mathbf{P}_i	[-]	Position of the point closest to particle i
r	[mm]	Fillet radius for channel cross-sections
R_i	[mm]	Radius of collision sphere for particle i
R_S	[mm]	Search radius for bundling close flow channels
t	[mm]	Wall thickness
t_{min}	[mm]	Minimum required wall thickness
t_{Cables}	[s]	Time for convergence of cable simulation
$t_{Geometry}$	[s]	Time for generation of 3D part geometry
\mathbf{T}	[-]	Tangent vector of cable path
\mathbf{v}_i	[-]	Velocity of particle i
\mathbf{v}_i^0	[-]	Initial velocity of particle i
v_f	[%]	Volume fraction of sacrificial supports
V	[mm ³]	Volume of required build material
$V_{Enclosing}$	[mm ³]	Volume of body enclosing sacrificial supports
V_I	[mm ³]	Volume of integrated support structures
V_P	[mm ³]	Volume of part geometry
V_S	[mm ³]	Volume of sacrificial support structures
w_j	[-]	Scalar weight factor for constraint j
\mathbf{x}_i	[-]	Position of particle i
\mathbf{x}_i^0	[-]	Initial position of particle i
\mathbf{x}_i^{maxIt}	[-]	Position of particle i after solver convergence
$\Delta\mathbf{x}_i$	[-]	Weight-averaged move vector of particle i
$\Delta\mathbf{x}_{i,C_j}$	[-]	Move vector of particle i due to constraint C_j
X	[mm]	X-Dimension of part projected on the build plate
Y	[mm]	Y-Dimension of part projected on the build plate
α	[°]	Build angle
α_{min}	[°]	Minimum required build angle
β	[°]	Profile angle of channel cross-sections
γ	[°]	Local inclination angle of channel cross-sections
ε	[-]	Current solver threshold
ε_{min}	[-]	Minimum solver threshold
ρ	[g/cm ³]	Density of material
ψ	[°]	Angle between two cable segments

1 Introduction

Additive manufacturing (AM) refers to a class of manufacturing methods that fabricate a part or product by adding material layer-by-layer directly from a digital, three-dimensional (3D) model [1][2][3]. This layerwise process differs from conventional manufacturing methods that rely on subtractive (e.g., milling and drilling) or formative processes (e.g., casting and forging). The manufacturing restrictions of such conventional methods often limit the attainable complexity of parts. In contrast, AM allows the production of highly complex-shaped parts, which are often impossible or too costly to manufacture using conventional methods [1][2][3]. This advantage of AM is frequently referred to as "complexity for free" and makes it possible to create parts with enhanced performance and integrate several subcomponents and functions in a single part. Another key advantage is that AM does not require additional production aids such as tools and molds [1][2][3]. Thus, AM enables the cost-efficient production of parts in small batch sizes or even with lot size one. This advantage of AM enables the quick fabrication of prototypes for fast development iterations, shortens the time to market, and reduces the lead-time for part delivery. Moreover, this benefit of AM offers the possibility of cost-efficiently manufacturing customized parts that are tailored and designed for the individual needs and requirements of a specific customer or application [4][5][6][7].

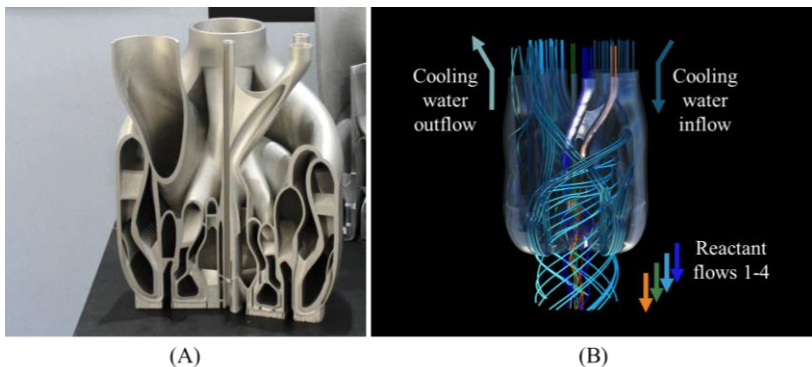


Fig. 1. (A) Complex burner nozzle fabricated using AM (developed by Siemens AG Technology); (B) Visualization of different fluid flows guided inside the nozzle.

The advantages and potential benefits of AM can be used in different industries, such as aerospace [8], automotive [9], tool-making [10], electric machines [11], medical devices [12], and construction [13]. The focus of this work is on applications in fluid and process engineering [14][15][16][17][18][19][20]. In this application area, many prior works demonstrate the potential of AM for flow components, such as nozzles [21][22][23], flow distributors [24][25], hydraulic manifolds [26][27][28] heat exchangers [29][30][31], reactors [32][33][34][35][36][37], and porous structures [38][39][40]. For example, Fig. 1 shows an organic-looking burner nozzle produced using AM [41]. This nozzle is used to produce synthesis gas from different reactants [42]. For this purpose, the nozzle integrates multiple flow channels that guide the reactants and distribute them from pipe inlets to ring-shaped outlets. In addition, the part incorporates flow channels that direct cooling water through the nozzle to protect it against process temperatures above 1300 °C. Previously, such nozzles had to be welded together from several subcomponents leading to increased manufacturing costs and lead-times. AM enables the integration of all flow channels into a single part. Moreover, the design freedom of AM allows the functional optimization of each flow channel to improve the uniform distribution of fluid flows and reduce pressure losses [41].

Therefore, AM has become sufficiently mature as a production technology for industrial applications, and the current landscape of AM offers a wide range of available processes and materials. However, a key challenge is to leverage these possibilities and design parts for AM [1][2][3]. One common approach is to create the 3D geometry of AM parts manually using computer-aided design (CAD) tools. Such a manual design process leads to several challenges [1][2][43][44][45][46][47]. Especially for complex-shaped parts, it requires advanced skills with CAD tools. This prerequisite can be an obstacle for CAD novices to take full advantage of AM. However, even for expert CAD users, manually designing AM parts can be tedious. One reason is that today's CAD tools were initially developed for conventional manufacturing methods, such as milling and drilling [43][44], and CAD tools are often still based on using low-level design features (e.g., sketches, curves, extrude, surfaces). Consequently, CAD users may require many manual and repetitive steps

to draw and combine such design features and design complex AM parts. In addition to the functional requirements of a part, CAD users must consider the restrictions of the chosen AM process and material [1][2][3]. For example, it can be necessary to prevent geometric features with critical overhangs [48][49][50][51]. Such process-related restrictions of AM may cause designers to perform multiple manual loops to check and modify design features for manufacturability. Another challenge is that the iterative development of an AM part often requires many changes to the part design, as designers need to include feedback from iterative tests and simulations [35][52][53]. The customization of parts to specific needs can be a further reason for many design changes [4][5][6][7]. If CAD users perform such design changes manually, these manual steps can cause increased manual effort and labor costs and prevent innovative business models such as the customization of parts.

Given the challenges of a manual design approach, many prior works aim to automate the design of AM parts using digital design tools [1][2][54][55]. Prior works use various design tools such as topology optimization (TO) [56][57][58] or techniques from knowledge-based engineering (KBE) [59][60][61][62][63], such as feature databases, CAD templates, design configurators, and design synthesis tools [64][65][66][67][68][69][70]. An automated design approach offers several benefits [1][2][71]. It enables novice and expert CAD users to create complex part designs and explore different concepts with reduced manual effort. In addition, users can make rapid design changes as required during an iterative part development or for customizing parts to specific needs.

In general, design automation for AM is a growing area of research [1][2][55]. In the case of TO, many prior works use structural TO to generate lightweight AM parts [72]. However, research is still required to automate the design of AM parts in other application areas, such as flow components [14][19]. In this application area, prior works use fluid-based TO [73] to generate the design of flow components, such as flow manifolds and heat exchangers [74][75][76][77] and mostly consider one or two fluid flows. However, complex AM flow components, such as multi-flow nozzles and hydraulic manifolds, often integrate multiple flow channels to guide several fluid flows. For such AM parts, the design and arrangement of several flow channels are still a challenge [14][19]. In the

case of a KBE approach, prior works present automated and knowledge-based design tools for various AM parts, such as structural components, compliant elements, and mechanical mechanisms [64][65][66][67][68][69][70]. However, an automated and knowledge-based design approach has yet to be demonstrated for complex AM flow components.

This work aims to address this research gap and present novel design algorithms to automate the design of AM flow components, such as multi-flow nozzles [21][22][23] and hydraulic manifolds [26][27][28]. For this purpose, the work follows a KBE approach and implements rule- and knowledge-based design algorithms for AM flow components. In this regard, the work focuses on three specific research questions (RQs):

- **RQ I:** What framework can be used to automatically generate the design of complex AM multi-flow nozzles, considering the creation and nesting of multiple flow channels?
- **RQ II:** What procedures can be used to consider the overhang constraint of AM when generating the geometry of flow channels for AM parts such as hydraulic manifolds?
- **RQ III:** What approach can be used to automate the routing of multiple flow channels guiding separate fluid flows, as required for AM parts such as hydraulic manifolds?

This work is structured, as shown in Fig. 2. After this introduction, Chapter 2 provides a background on the basic process chain of AM and the potential benefits of AM for flow components, such as multi-flow nozzles and hydraulic manifolds. In addition, the chapter introduces the field of design for AM and describes key challenges in the manual design of AM parts. The chapter then introduces the use of an automated design approach for AM, describes the limitations of prior works, and specifies the research gap. Chapter 3 outlines the goals of this work, motivates each RQ and provides a brief description of the contributions. Each RQ is assessed in a separate study. Chapter 4 presents the results of Study I for RQ I. Chapter 5 describes the results of Study II for RQ II. Chapter 6 presents the results of Study III for RQ III. Chapter 7 concludes by summarizing the studies and drawing the main conclusions. Finally, the chapter provides an outlook for potential future research directions.

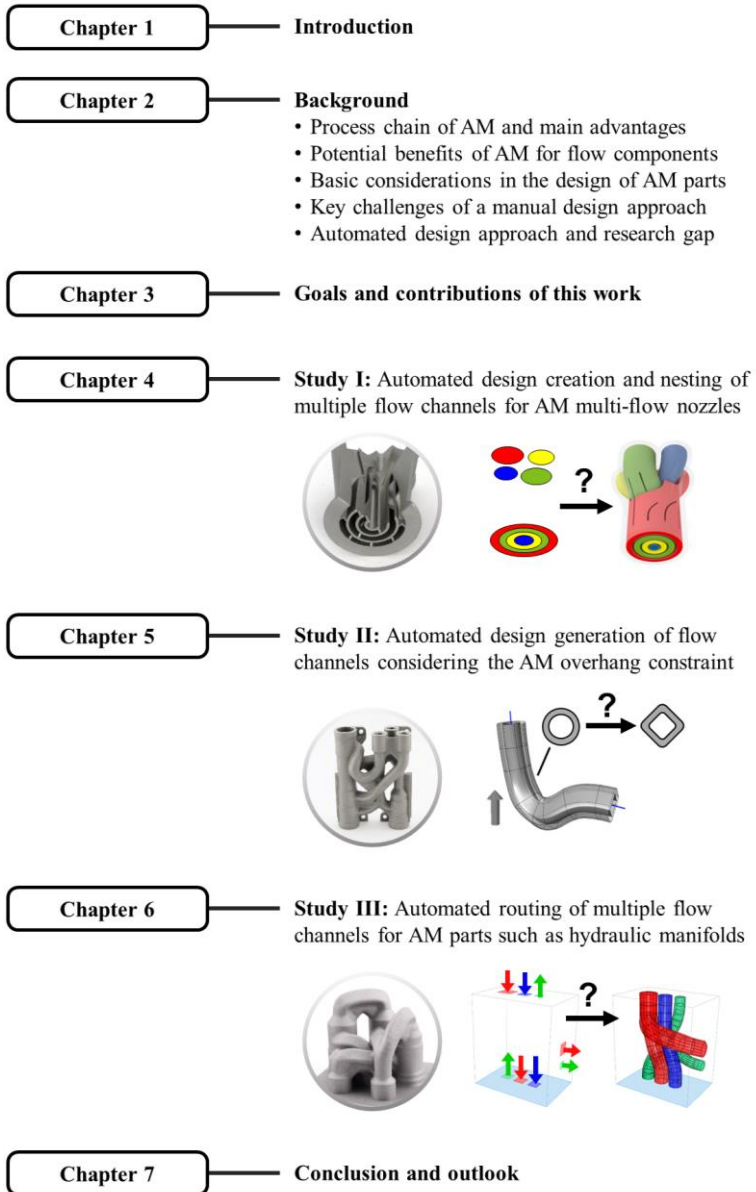


Fig. 2. Overview of this work and content of each chapter.

2 Background

2.1 Process chain of AM and main advantages

Over the past decades, AM has been increasingly used in various industries for applications, such as prototyping, tool making, series parts, customization of products, and repair of parts [1][2][3]. AM parts can be fabricated from materials, such as metals, polymers, ceramics, and composites. According to standard ISO/ASTM 52900:2021 [78], AM is a "process of joining materials to make parts from 3D model data, usually layer upon layer, as opposed to subtractive and formative manufacturing technologies". In general, different processes exist that follow an additive shaping process to fabricate parts. AM processes are divided into seven categories: powder bed fusion, directed energy deposition, binder jetting, material jetting, material extrusion, vat photopolymerization, and sheet lamination. Prior works provide a comprehensive review of different AM processes and materials [1][2][3]. This work focuses on the AM process of laser powder bed fusion (L-PBF). The process of L-PBF allows the fabrication of parts made from metals, such as stainless steel, aluminum, titanium, copper, and many other alloys [3][8][79]. Fig. 3 shows the basic steps of the process chain for L-PBF from the part design to the final part using an example of a nozzle.

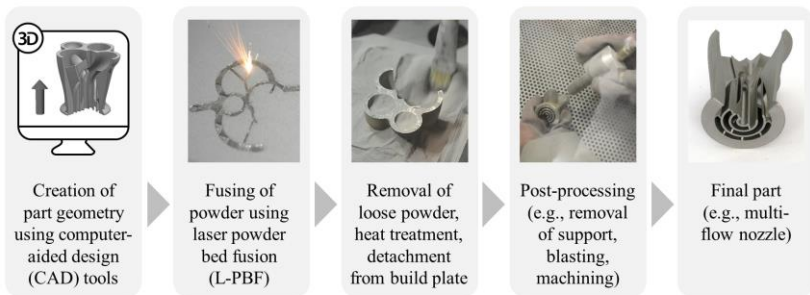


Fig. 3. Basic steps for production of a part using the AM process of L-PBF.

The first step in the overall process chain is to create a 3D geometry of the part using CAD tools. Next, special software tools are used to pre-process the part geometry for AM and add sacrificial support structures. These supports anchor the part to the build plate and prevent deformations due to increased thermal residual stresses [3][80][81]. The layerwise process of L-PBF makes it necessary to slice the part geometry into layers. The orientation of these layers is determined by the user-defined build direction indicated by the gray arrow in Fig. 3.

In the next step, the AM machine is prepared (e.g., mounting of the build plate and filling the powder chamber), and the fabrication process can start. For each layer, powder is first distributed by a coater on the build plate. In the second step, thermal energy is used to locally melt and solidify the powder at the sliced cross-sections of the part. Energy is induced either through a laser beam (laser powder bed fusion, L-PBF) or an electron beam (electron powder bed fusion, E-PBF) [3][78]. The two steps of coating the build plate with powder and melting powder are repeated cyclically for all layers of the part.

During the fabrication, the support structures dissipate excessive heat from the local melt pool through the solid material to the base plate [3][80][81]. As a result, the support structures avoid an increased thermal distortion of the fabricated structure and prevent process failures during the AM fabrication (e.g., collisions between the built part and the coater, occurrence of cracks, and excessive warpage of the part).

After layerwise fabrication, the next steps are to remove the non-molten powder, apply heat treatment steps, and detach the part from the build plate. Further post-processing steps include the removal of the supports and blasting the part. After AM, parts may possess an increased surface roughness and deviate in shape due to thermal warpage. Therefore, it is necessary to further post-process parts using subtractive manufacturing methods to achieve high precision on interfaces (e.g., threads, sealing surfaces) or decrease the surface roughness of internal regions using methods such as abrasive flow machining [82].

The described process chain illustrates the basic steps of L-PBF. Compared with conventional methods, such a digital and layerwise AM process offers two key advantages, often referred to as the "complexity for free" and the "small lot size" advantage [1][2][3][83].

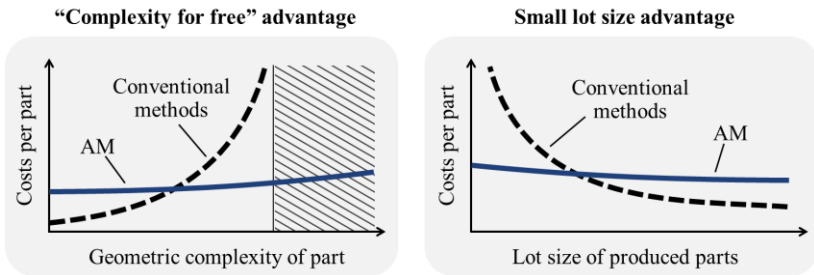


Fig. 4. Visualization of "complexity for free" and small lot size advantage of AM compared to conventional manufacturing methods (modified based on [83]).

Fig. 4 visualizes both advantages. The term "complexity for free" refers to the fact that AM allows the production of almost any shape based on the layerwise build-up of material [1][2][3][83]. The costs per part for AM remain constant or increase only slightly, even for parts with complex geometries, which is a key advantage over conventional manufacturing methods. For conventional processes, parts with increased complexity may lead to increased effort and costs per part or may not be possible to produce (see the hatched area in Fig. 4).

The small lot size advantage refers to the fact that AM processes do not require additional tooling aids for the layerwise production of parts, thus making it possible to use AM to cost-efficiently produce parts with small lot sizes or as customized parts with lot size one [1][2][3][83]. In contrast, conventional manufacturing processes, such as injection molding, often require upfront investments in tooling aids, such as molds. Such initial costs typically increase the costs per part for small lot sizes. Consequently, conventional methods are often economically viable, particularly for large lot sizes, when the initial fixed costs for tooling can be distributed over a higher number of parts [83].

The break-even point between AM and conventional methods depends on the specific case and AM production technology [83][84][85][86][87]. In the case of AM, the costs per part for AM only decrease slightly with an increasing lot size. One way to decrease the costs per part for AM is to fabricate multiple parts in a single build job. This batch processing reduces the costs per part related to the machine setup, idle times during the recoating of layers, and de-powdering of the parts.

2.2 Potential benefits of AM for flow components

This work focuses on applying AM for flow components. Examples of such parts include nozzles, flow distributors, hydraulic manifolds, heat exchangers, injection molding molds, and reactors [14][15][16][17][18][19][20]. As an illustration, Fig. 5 shows selected examples of multi-flow nozzles and hydraulic manifolds fabricated using L-PBF.

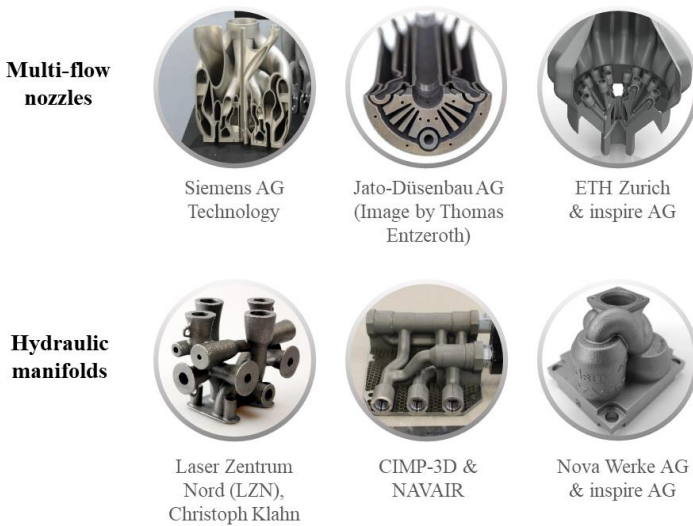


Fig. 5. Selected examples of flow components fabricated using AM, in particular multi-flow nozzles and hydraulic manifolds.

Such complex-shaped flow components are often impossible or too costly to fabricate using conventional manufacturing methods. For instance, the shape of the flow channels is restricted to straight holes fabricated using conventional methods such as milling or drilling. In addition, conventional parts must be welded and assembled from multiple subcomponents, such as tubes, flanges, and fittings. By contrast, AM makes it possible to rethink the design of conventional flow components. In this regard, AM can provide several benefits. In the following, Table 1 describes the potential benefits of applying AM for flow components. For this purpose, the work makes use of a framework presented in [88], which categorizes the potential benefits of AM into seven value clusters.

Table 1. Overview of potential benefits of AM for flow components based on [88]

Value cluster	Potential benefits of AM for flow components
Prototyping	AM enables the fast and cost-efficient fabrication of prototypes. These prototypes can be used to conduct experimental tests and validate the performance of parts and flow simulations. Companies can apply such a rapid prototyping approach to fabricate and test multiple design variants iteratively. This benefit allows companies to achieve a faster time-to-market and ensure the performance of parts [88].
Enhanced designs	AM makes it possible to create highly functionally optimized flow components. For example, parts can be optimized to improve the distribution of fluid flows or to reduce pressure losses. In addition, parts can integrate multiple flow channels tightly nested in each other, leading to compact parts with reduced part mass and size. Moreover, parts may integrate design features to combine functions such as static mixing, heat treatment, and chemical reaction [15][16]. These advantages make AM a promising enabler in advancing the field of process intensification for process engineering devices [89][90]. These potential benefits allow companies to develop and sell flow components with enhanced performance and new functionalities.
Custom products	The small lot size advantage of AM enables the cost-efficient production of customized parts with a lot size one. Instead of selling standard components, companies can use this advantage to tailor parts to the individual needs of a specific customer or application [91][92][93]. Flow components can be customized depending on the specific use case, operating conditions, desired process output and yield, mounting, and available installation space. This benefit allows companies to improve their product differentiation and offering to customers.

<p>Process concentration</p>	<p>AM allows integrating several features such as flow channels, connectors, attachments, sensors, and stiffening ribs into a single part. Previously, such subcomponents had to be joined and assembled using many separate manufacturing steps [41]. AM allows concentrating such separate manufacturing steps in one integral manufacturing process. Consequently, companies can reduce the costs, manual effort, and time required to produce functionally integrated parts [88].</p>
<p>Improved delivery</p>	<p>The layerwise process of AM does not require additional tooling. Parts can directly be produced based on a digital model. This advantage enables companies to establish localized and flexible supply chains, fabricate parts on demand, and deliver parts at a reduced lead-time. In addition, companies can operate with less inventory, quickly deliver spare parts, and can use AM processes to repair parts [94][95][96].</p>
<p>Incremental product launch</p>	<p>As AM does not require additional tooling, the design of a part can be changed flexibly. Companies can use this advantage to make design changes, even after selling the first batch of a part [88]. This flexibility allows companies to integrate feedback from initial customers. Especially for new products, this benefit enables companies to improve the design of parts continuously [53].</p>
<p>Production tools</p>	<p>Established process engineering methods such as extrusion and injection molding offer the advantage that goods can be produced efficiently with very high throughput at low costs. For such established production methods, AM can be used to fabricate production tools such as molds and extrusion dies [10][97]. This indirect use of AM allows companies to combine the advantages and potential benefits of established production methods and AM.</p>

2.3 Basic considerations in the design of AM parts

As described in the previous section, AM offers several benefits for rethinking the design, functionality, and manufacturing of flow components. However, the design of AM parts is often mentioned as a challenge to leverage the potential benefits of AM [4][98][99]. The research field of design for AM (DFAM) aims to support the design of AM parts by providing design methods and frameworks for AM [4][100][101][102][103][104][105][106][107]. In this regard, prior works emphasize that AM designers need to consider the opportunistic aspects (e.g., increased design freedom, potential for part customization) and restrictive aspects of AM (e.g., restrictions and limitations of AM processes, part costs, need for post-processing) [100][102][106][108]. Fig. 6 illustrates the two aspects. This section describes both aspects and provides a brief overview of previous works in the area of DFAM.

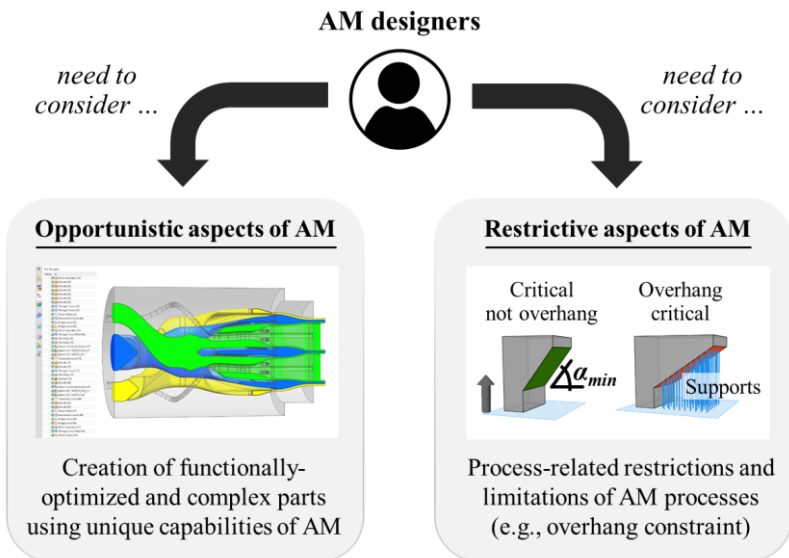


Fig. 6. Consideration of opportunistic and restrictive aspects in design for AM.

Opportunistic aspects relate to the possibilities and design freedom of AM. Based on [100], the unique capabilities of AM enable parts with the following types of complexities: *shape complexity* (production of nearly any shape), *material complexity* (fabrication of parts made of one or more materials with distinct or gradual transitions), *hierarchical complexity* (integration of design features at different length scales), and *functional complexity* (integration of multiple functions in a single part).

Restrictive aspects refer to the manufacturing restrictions of AM processes that limit the design freedom. These restrictions are specific for each AM production technology and depend on parameters, such as the selected material, AM machine, and process parameters [1][2][3]. In addition, the post-processing and post-machining of parts may impose restrictions on the part design [82]. This work focuses on the AM process of L-PBF of metals [3][8][79]. For this AM process, the overhang constraint is one important manufacturing restriction. As shown in Fig. 6, this constraint states that inclined surfaces with overhangs require a minimum build angle α_{min} to the build plate [48][49][50][51]. Otherwise, such overhangs are critical, and additional support structures must be added to prevent process failures during AM.

Prior works support the design of functional and manufacturable AM parts using various techniques. For example, prior works present design rules that provide threshold values for the restrictions of different AM processes and materials. Based on experimental studies, prior works recommend values for the minimum build angle α_{min} that allow the production of overhangs without additional supports [48][49][50][51]. Other works support designers by providing design guidelines for AM, for example, to select a suitable build orientation of a part to the build plate [109][110][111]. Prior works also present design heuristics to make designers aware of the design potential of AM [112][113]. In addition, prior works aim to make knowledge of AM more accessible to designers by providing worksheets [114][115]. Others works aim to structure AM knowledge using ontologies [116][117][118]. Previous works also present design methods that guide designers through a structured design process for AM [106][119][120]. Prior works in the area of DFAM also use software-based design tools such as TO and techniques from KBE to design parts for AM (see brief overview in Sec. 2.5) [54][55].

2.4 Key challenges of a manual design approach

Therefore, many design rules, guidelines, and methods exist for supporting the design of AM parts. Nevertheless, the design of complex-shaped parts is oftentimes still a key barrier to implementing AM parts, especially for novice AM designers [4][98][99][121]. One reason is that, in today's practice, AM parts are often designed by manually creating and combining design features using CAD tools [1][2][43][44][45][46][47]. Such a manual and CAD-based design process can be challenging for several reasons. As shown in Fig. 7, key challenges include the required expert knowledge and experience, manual creation of many low-level design features with CAD tools, manual consideration of restrictions for AM, and manual implementation of frequent design changes.

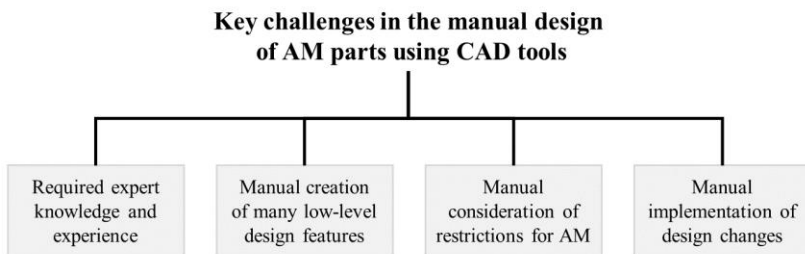


Fig. 7. Key challenges in the manual design of AM parts using CAD tools.

Required expert knowledge and experience

One key challenge is that the manual design of AM parts often requires considerable expert knowledge and skills in different areas [46][105][121][122]. For example, designers must have experience with CAD tools to create complex 3D part geometries. In addition, they require in-depth knowledge of the examined application to translate the part requirements into a 3D part geometry. Designers also need experience with simulation tools to optimize part designs (e.g., finite element analysis (FEA) and computational fluid dynamics (CFD)) [35][37][41]. Moreover, they must understand DFAM rules and guidelines to ensure the manufacturability of part designs. Furthermore, designers must consider the entire process chain and understand the possibilities and limitations of conventional

manufacturing methods to plan the post-processing and post-machining of AM parts [82]. Therefore, a manual design process relies heavily on the expertise and experience of AM designers. This required expert knowledge can be a barrier for novice AM designers in creating complex parts and leveraging the potential benefits of AM.

Manual creation of many low-level design features

Another challenge is related to the basic functionality of traditional CAD tools. Classical CAD tools were initially developed for conventional manufacturing methods, such as milling and drilling [43][44][45][46]. Today, they are often still based on the approach of manually creating and combining design features, such as planes, sketches, splines, surfaces, extrudes, and boreholes. Such basic design features are sufficient to design simple-shaped parts for conventional manufacturing processes. However, AM enables new design possibilities and allows the production of parts with increased complexity. Such complex AM parts can be composed of hundreds of design features [43][44][45][46]. In this case, the manual creation of many low-level design features makes it necessary to perform several repetitive design steps. As an example, Fig. 8 shows the CAD-based design of flow channels. Consequently, the manual design of AM parts may often be time-consuming, even for experienced CAD users. In addition, the complex parameterization between design features can make it challenging to apply major changes to the part design because it requires manual restructuring of many design features.

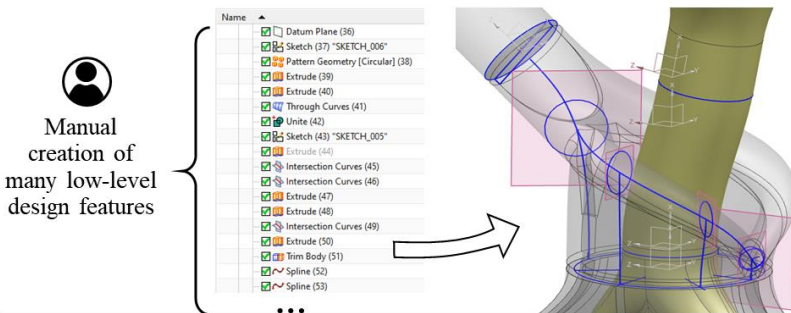


Fig. 8. Design of flow channels by manually creating and combining many low-level design features (e.g., planes, sketches, extrudes, surfaces, edge blends).

Manual consideration of restrictions for AM

Another challenge in the manual design of AM parts is to consider the restrictions of the chosen AM process and material [1][2][3]. The overhang constraint is one important restriction for L-PBF [48][49][50][51]. Critical overhangs and the use of sacrificial supports can be avoided by modifying the part design. For example, as shown in Fig. 9 (A), a droplet-shaped cross-section can be used instead of circular cross-sections to prevent critical overhangs and inaccessible supports [14][110][123][124]. A circular cross-section needs to be modified if it is oriented horizontally to the build plate, and its diameter D lies above D_{max} . This threshold D_{max} marks the maximum diameter of a horizontal circular cross-section that can be produced without supports [48][49][50][51]. As shown in Fig. 9 (B), this technique allows the fabrication of support-free flow channels for parts, such as hydraulic manifolds [26][82]. The manual consideration of such production-related restrictions is easy to implement for simple-shaped parts. However, this task can be more challenging for complex AM parts. For example, for hydraulic manifolds with many flow channels, designers may need to check and modify the cross-section shape of several channels. However, such design changes can lead to overlaps between different flow channels, and further design changes are required to resolve the intersections between channels. Consequently, designers may require several manual loops to implement restrictions for AM. In addition, manual consideration of restrictions can lead to human-related errors. Designers may overlook overhangs, which can lead to process failures during AM and cause further development cycles.

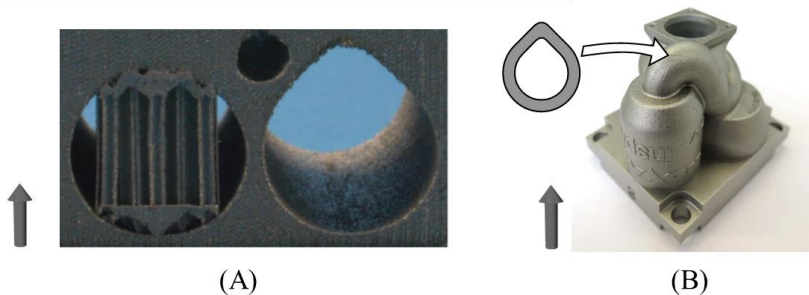


Fig. 9. (A) Adaption of a circular horizontal cross-section to droplet shape to avoid internal support structures [124]; (B) Hydraulic manifold with droplet-shaped flow channel (developed by Nova Werke AG and inspire AG) [82].

Manual implementation of frequent design changes

As described above, the manual design of AM parts can require an increased manual effort. The manual effort can significantly increase if it is necessary to create multiple design variants or make frequent design changes. For example, an iterative development approach can make it necessary to integrate feedback from simulations and experimental tests over multiple development cycles [35][52][53]. Another reason for frequent design changes is the comparison of different AM processes, materials, and production scenarios (e.g., changes in build direction). Such production-related changes can demand major changes in the part geometry to fulfill the specific restrictions of the chosen production technology and material [1][2][3]. The customization of AM parts can be another reason for frequent design changes. It requires the creation of many different design variants that must be tailored to application- or customer-specific requirements [4][5][6][7].

If CAD users perform such design changes manually, these manual steps can cause an increased manual effort, longer iteration cycles, and high labor costs. Fig. 10 further illustrates this challenge. The execution of simulations can be automated using modern software-based tools. Using AM enables the digital and automated production of parts without the need for extra tooling. However, a manual design approach requires manual steps by CAD users to create the initial part design and make subsequent design changes. Consequently, a manual design process prevents a fully digital and automated process chain for AM. In addition, it can hinder novel business models enabled by AM, such as the cost-efficient design and production of customized parts [4][5][6][7].

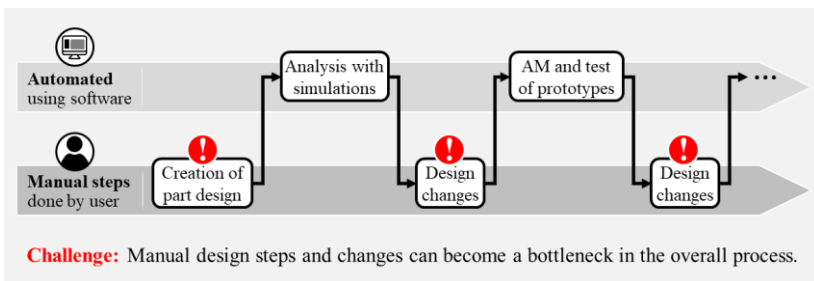


Fig. 10. Development process using a manual design approach for AM.

2.5 Automated design approach and research gap

Given the challenges of a manual design process, many prior works aim to automatically generate the design of AM parts. In general, different techniques can be used to automate the design of AM parts [1][2][54][55]. This section introduces two approaches relevant to this work. In particular, this section describes the use of TO and techniques that follow a KBE approach. Based on this, the section outlines the limitations of prior works and specifies the research gap addressed in this work.

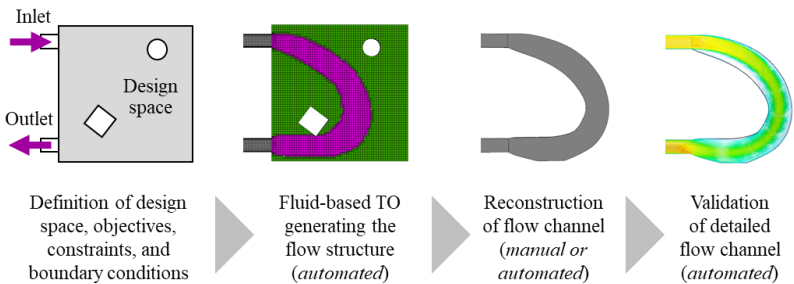


Fig. 11. Fluid-based TO for generating a flow-optimized channel (based on [125]).

Many prior works use structural TO for the design of lightweight AM parts [72]. However, TO can also be used to generate the design of AM flow components, such as flow manifolds and heat exchangers [74][75][76][77]. Fig. 11 shows the basic process of a fluid-based TO using an example of a flow channel. User inputs include the available design space, objectives, constraints, and boundary conditions (e.g., inlets and outlets). Based on these inputs, TO uses a simulation-driven design process to generate a structure that optimizes the guidance of the fluid flow while considering objectives, such as minimizing pressure losses or improving the uniform flow distribution. In addition, the TO can consider restrictions of AM, such as the overhang constraint [126][127][128]. In this case, the TO automatically modifies the shape of flow channel cross-sections to avoid critical overhangs and non-accessible supports inside the channels [74][75][129]. After the TO, the next steps are to interpret and reconstruct the design concept of the generated flow structure and perform additional flow simulations to validate the detailed design of the flow channel.

Another approach for automating the design of AM parts is to use techniques that follow a KBE approach [59][60][61][62][63]. A KBE approach aims to capture the required expert knowledge and implement manual and recurring design tasks as automated and reusable design algorithms. The required knowledge can be obtained from case studies, expert interviews, technical documents, and standards. The standard VDI 5610-2 [130] and KBE methodologies such as MOKA [131], KNOMAD [132], and CommonKADS [133] provide structured procedures for implementing and operating KBE applications. In general, various techniques can be used to build automated and knowledge-based design tools for AM parts. Common techniques include rule-, constraint- and object-based design systems, custom feature libraries, CAD templates, configurators, and design synthesis tools [64][65][66][67][68][69][70].

As an example, Fig. 12 shows a feature library for polymer-based AM parts [66], which consists of frequently recurring mechanical interfaces, such as connectors, joints, and snap-fits. During the development of the feature library, the different design elements are validated using physical prototypes, for instance, to determine the influence of different AM processes, materials, and build orientations on clearance parameters. In the design phase, CAD designers can then use and quickly integrate these application-specific and knowledge-based design features as high-level building blocks [134][135]. This approach reduces the manual effort required to create the detailed 3D geometry of such frequently recurring features [66]. In addition, such an automated and knowledge-based design approach reduces the number of iterations required to produce and test multiple prototypes before achieving a functional part [66].

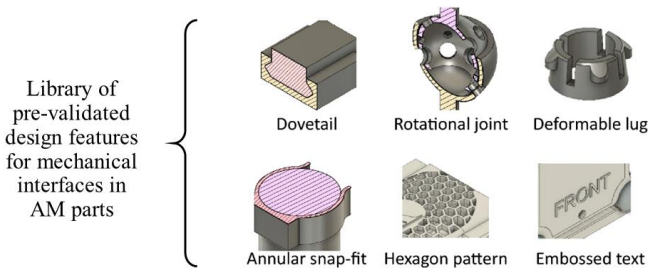


Fig. 12. Feature library with mechanical interfaces for AM parts as an example of an automated and knowledge-based design tool for AM [66].

In general, both fluid-based TO and techniques from KBE can be used to automate the design of AM flow components. However, prior works that apply these approaches have some limitations.

In the case of fluid-based TO, many prior works generate the design of flow components, such as flow manifolds and heat exchangers. Nevertheless, most works consider only one or two fluid flows [74][75][76][77]. However, flow components produced using AM can integrate multiple flow channels to guide several fluid flows. In this case, multiple TOs can be performed sequentially to generate a flow structure for each fluid flow. However, this process can lead to semi-optimal designs that favor the initially created flow channels and disfavor the subsequently generated channels [136][137]. Very few works on fluid-based TO exist that consider several separate fluid flows simultaneously [136][137]. Another drawback of TO is that the generated result is a design concept in the form of a rough material distribution. Prior works aim to reconstruct such design concepts automatically in a detailed 3D part geometry [138][139][140]. However, as reported in prior works, a manual design process is often still necessary to interpret and refine such design concepts and reconstruct them as detailed 3D part geometries that are ready for production with AM [2][58][141][142].

In the case of a KBE approach, the broad applicability is a key advantage of the approach. In fact, many works in the area of KBE exist that demonstrate knowledge-based techniques to automate the design of systems such as aircraft, cars, trains, and robots [59][134][143][144]. Specifically for AM parts, prior works describe design frameworks that include aspects of a KBE approach by integrating AM-related knowledge [62][65][96][116][117][118][145][146][147]. Prior works also present automated design tools for different application areas of AM, such as structural components, compliant elements, springs, snap fits, interface elements, and mechanical mechanisms [64][65][66][67][68][69][70]. However, an automated and knowledge-based design approach has yet to be implemented for AM flow components. In particular, the design and arrangement of several flow channels remain a challenging task [14][19] that is frequently required for AM flow components, such as multi-flow nozzles [21][22][23] and hydraulic manifolds [26][27][28].

3 Goals and contributions

3.1 Goals

This work aims to address the outlined research gap and automate the design of complex-shaped flow components produced using AM. For this purpose, this work follows a KBE approach and implements rule- and knowledge-based design algorithms for AM flow components. More specifically, this work aims to achieve the following *goals*:

- The first goal is to develop design algorithms that capture and integrate the application-specific knowledge required to generate the design of AM flow components, such as multi-flow nozzles and hydraulic manifolds.
- The second goal is to develop these design algorithms to consider process-related manufacturing restrictions of AM, such as the overhang constraint.
- The third goal is to demonstrate the implementation of the developed design algorithms and show their functionality and benefits through illustrative case studies.

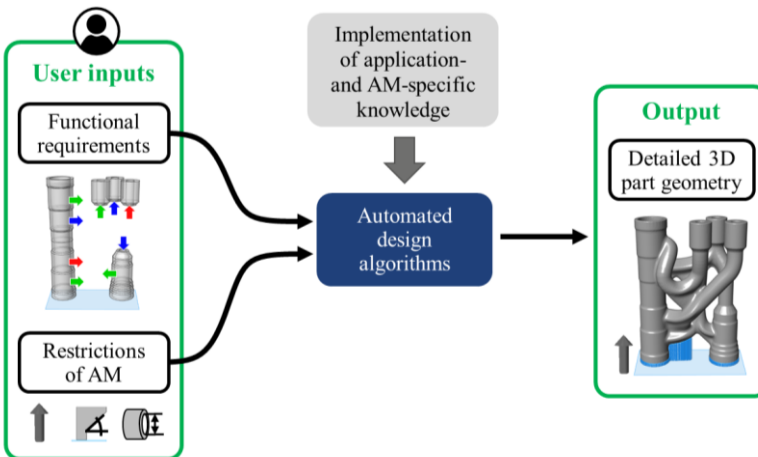


Fig. 13. Envisioned process for automating the design of AM flow components.

The *basic approach* of this work is to capture application- and AM-specific knowledge and implement manual and frequently recurring design tasks as rule- and knowledge-based design algorithms. Fig. 13 illustrates the envisioned automated design process using an example of a hydraulic manifold. In the envisioned design process, novice or expert CAD users can apply the design algorithms by defining the design intent using top-level user inputs. These inputs include functional requirements of a part (e.g., inlets and outlets of flow channels, dimensions of channels) and restrictions of the chosen AM production technology (e.g., build direction, minimum build angle). The developed design algorithms automatically transfer these user inputs into a detailed 3D part geometry that is ready for AM production and does not need manual editing steps of the geometry. The generated part geometry serves as a basis for further steps in the part development (e.g., conduction of simulations, fabrication of prototypes for experimental tests).

The *scope* of this work is narrowed by two factors. First, it focuses on specific flow components. This restriction makes it possible to identify specific design challenges that can be addressed using novel automated design algorithms. In this work, the focus lies on multi-flow nozzles and hydraulic manifolds. For both applications, many case studies highlight the potential of AM compared to conventional manufacturing methods [21][22][23][26][27][28]. These case studies can be used to analyze the existing manual design process and identify recurring and challenging design tasks. Furthermore, these case studies serve as an important knowledge base for the development of automated design algorithms.

Second, the work focuses on a specific AM process and targets metal parts produced using L-PBF. One reason for this choice is that the basic capabilities and limitations of L-PBF are well reported in the literature. Many prior works describe the process-related restrictions of L-PBF, such as the minimum required build angle for different metals. Knowledge of these manufacturing restrictions is essential for developing design algorithms. Another reason is that L-PBF has reached a high level of maturity for industrial applications [3][8][79]. Many prior case studies on nozzles and hydraulic manifolds use L-PBF as it allows the production of nearly fully dense parts suitable for high-pressure and high-temperature applications [21][22][23][26][27][28].

3.2 Contributions

This work presents three studies to automate the design of AM flow components. Fig. 14 shows an overview of these studies. Each study addresses a specific design challenge that is investigated in the context of multi-flow nozzles or hydraulic manifolds. The research questions and contributions of each study are described below.

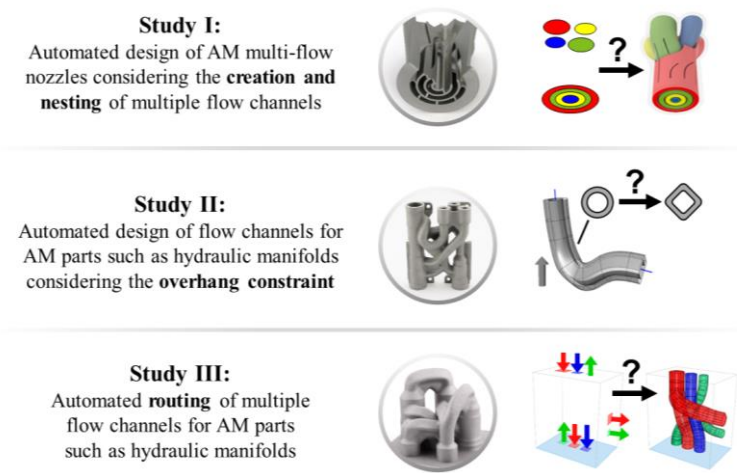


Fig. 14. Overview of contributions of this work, including studies I, II, and III.

Study I: Automated design of AM multi-flow nozzles considering the creation and nesting of multiple flow channels (Chapter 4)

AM enables the fabrication of complex nozzles that can integrate multiple flow channels into a single part. However, designing such multi-flow nozzles can be challenging and effortful when using a manual design approach with CAD tools. Designers must manually create the geometry of multiple flow channels, which can have different cross-section shapes and require complex transitions between the inlets and outlets. In addition, designers must nest several flow channels for different fluid flows. Typically, this design task requires many manual Boolean operations to combine the different flow channels into a single part. This design challenge leads to the following question:

RQ I:

What framework can be used to automatically generate the design of complex AM multi-flow nozzles, considering the creation and nesting of multiple flow channels?

Study I [148] presents a computational framework to automate the design of AM multi-flow nozzles. The study automates the creation and nesting of multiple flow channels into a single part. For this purpose, the study i) models a generic part architecture (or blueprint) of multi-flow nozzles, ii) describes the necessary design elements (or building blocks) of nozzles, and iii) defines a design synthesis process for generating manufacturable and functionally optimized nozzle geometries.

Study I:

[148] M. Biedermann, M. Meboldt, Computational design synthesis of additive manufactured multi-flow nozzles. *Additive Manufacturing* (2020).

Study II: Automated design of flow channels for AM parts such as hydraulic manifolds considering the overhang constraint (Chapter 5)

When designing parts for AM, designers must consider process-related restrictions. In particular, the overhang constraint can require several production-related design changes to obtain manufacturable part geometries. For example, it can be necessary to change the circular cross-section of flow channels to adapted shapes (e.g., droplet, diamond) to prevent critical overhangs and inaccessible supports inside channels. The manual consideration of such design adaptations can be challenging, especially for complex flow components. AM hydraulic manifolds can integrate several flow channels oriented in different directions to the build plate. In such cases, designers may require many manual iterations to create all flow channels, analyze their manufacturability, and make design changes for AM. This challenge raises the following question:

RQ II:

What procedures can be used to consider the overhang constraint of AM when generating the geometry of flow channels for AM parts such as hydraulic manifolds?

Study II [149] presents a set of automated CAD procedures that automatically generate and modify design features to fulfill the AM overhang constraint. These procedures avoid a manual implementation of production-related design changes and enable users to automatically transfer the layout design of a hydraulic manifold (e.g., centerlines of flow channels) into a production-ready 3D part geometry. Specifically, the study describes procedures that automatically generate i) support-free flow channels by locally adapting the shape of flow channel cross-sections for AM, ii) integrated and sacrificial supports for critical overhangs below horizontal channels, and iii) manufacturable detailed features, such as boreholes, part interfaces, and ribs.

Study II:

[149] M. Biedermann, P. Beutler, M. Meboldt, Automated design of additive manufactured flow components with consideration of overhang constraint. *Additive Manufacturing* (2021).

Study III: Automated routing of multiple flow channels for AM parts such as hydraulic manifolds (Chapter 6)

AM enables the integration of many intertwined and branched flow channels with multiple crossings in a single part. However, a key challenge is to define the paths (or centerlines) of several flow channels and route them between different inlets and outlets. In this regard, designers must consider functional requirements, such as minimizing the length of the channel paths and avoiding sharp bends to reduce pressure losses. Additionally, different channels that guide separate fluid flows are not allowed to intersect. In addition to functional requirements, designers must consider restrictions of AM, such as the potential modification of

channel cross-sections due to the overhang constraint. However, such design changes in the channel cross-sections may lead to new overlaps between different flow channels and require several readjustments of the channel paths. Therefore, the manual routing of multiple flow channels is often a very challenging and tedious design task, even for experienced CAD users. This challenge leads to the following question:

RQ III:

What approach can be used to automate the routing of multiple flow channels guiding separate fluid flows, as required for AM parts such as hydraulic manifolds?

Study III [150] presents a computational approach to automatically create the paths of multiple flow channels guiding separate fluid flows. This study further advances the automated design workflow for hydraulic manifolds (Study II). In particular, the study i) describes a computational approach to enable the automated routing of multiple branched flow channels guiding separate fluid flows, ii) considers different functional part requirements (e.g., minimized length of flow channel paths, avoidance of sharp bends in channel paths, prevention of overlaps between different channels), and iii) considers the potential adaption of channel cross-sections for AM during the routing process.

Study III:

[150] M. Biedermann, P. Beutler, M. Meboldt, Routing multiple flow channels for additive manufactured parts using iterative cable simulation. *Additive Manufacturing* (2022).

4 Study I: Automated creation and nesting of flow channels

The content of this chapter has been published in the journal of *Additive Manufacturing* [148] under the title “*Computational design synthesis of additive manufactured multi-flow nozzles.*”

Abstract

Additive manufacturing (AM) enables highly complex-shaped and functionally optimized parts. To leverage this potential, the creation of part designs is necessary. However, as today’s computer-aided design (CAD) tools are still based on low-level geometric primitives, the modeling of complex geometries requires many repetitive, manual steps. As a consequence, the need for an automated design approach is emphasized and regarded as a key enabler to quickly create different concepts, allow iterative design changes, and customize parts with reduced effort. Topology optimization exists as a computational design approach but usually demands a manual interpretation and redesign of a CAD model and may not be applicable to problems such as the design of parts with multiple integrated flows. This work presents a computational design synthesis framework to automate the design of complex-shaped multi-flow nozzles. The framework provides AM users a toolbox with design elements, which are used as building blocks to generate finished 3D part geometries. The elements are organized in a hierarchical architecture and implemented using object-oriented programming. As the layout of the elements is defined with a visual interface, the process is accessible to non-experts. As a proof of concept, the framework is applied to successfully generate a variety of customized AM nozzles that are tested using co-extrusion of clay. Finally, the work discusses the framework’s benefits and limitations, the impact on product development and novel AM applications, and the transferability to other domains.

4.1 Introduction

Based on the layerwise adding of build material, additive manufacturing (AM) enables the fabrication of intricate, organic-shaped structures with high complexity [4][98][99]. A part can be complex because of its shape, material composition, functionality, and hierarchically organized features [100]. As an example, Fig. 15 shows a redesigned AM burner nozzle that is produced using laser powder bed fusion (L-PBF) [41]. It integrates multiple flow channels for cooling water and different reactants. The part demonstrates that AM processes have become mature enough to fabricate highly integrated and functionally optimized structures. However, to create such complex part designs, it is necessary to provide suitable design tools, which is considered a major barrier to the implementation of AM [4][55][98][99][119].

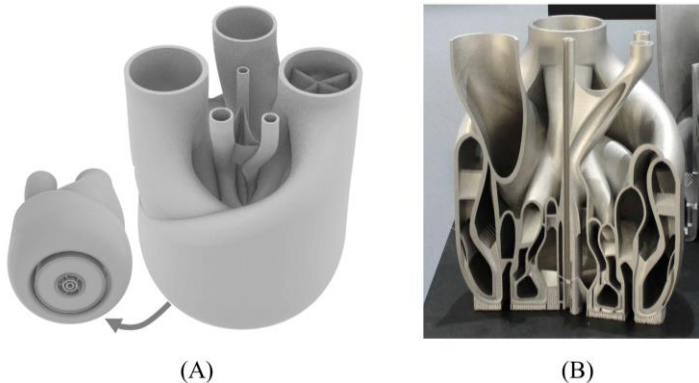


Fig. 15. (A) AM burner nozzle with multiple flow channels (developed and provided by Siemens AG Technology, further described in [5]); (B) Section cut of part fabricated with L-PBF.

Especially complex AM parts are based on profound application-specific knowledge of experts and oftentimes require a time-consuming manual process of modeling with computer-aided design (CAD) tools. The reason is that today's CAD tools were originally developed for conventional manufacturing processes such as milling and are still based

on combining low-level geometric primitives [43]. CAD tools have evolved over the past decades, but since the introduction of *SketchPad* as the first CAD system, geometric modeling has remained a manual process with a low degree of abstraction [43]. In the case of the burner in Fig. 15, the CAD model was created within six months and contains over 2500 features. Especially for such a complex design, a manual, low-level process limits rapid and iterative design changes as well as the quick embodiment of a variety of design concepts.

Therefore, with the rise of AM, the need for improved design tools and an automated design approach is seen as a decisive factor in design for AM (DFAM) and applications such as customization [4]. To capture the design intent of a user on a higher level, one commonly applied tool of computational design synthesis [54][55][119] is topology optimization (TO), in which a designer defines high-level requirements like design space, loads, and boundary conditions. TO algorithms are used for specific problems like lightweight parts and compliance mechanisms [54][72], parts for heat transfer [151][152], or problems with one or two mixing flows [153][154][155]. Although TO allows creating very complex structures, the raw result is a non-parametric design proposal in the form of a discretized material distribution. Therefore, the result of a TO usually represents a rough concept, which demands a manual interpretation and redesign of a CAD model [141][142][156] or a reverse engineering approach [157][158].

Besides computational design tools, another approach to assist DFAM is to capture and store design knowledge using expert systems and databases, for which prior works focus on feature taxonomies [65][108] and ontologies for AM [116][117]. In general, the use of a knowledge-based engineering (KBE) approach for design automation in AM is highlighted, but proposed frameworks are yet to be implemented [55][159] or exist only for domains such as lightweight parts [67][160]. Although KBE offers many benefits for an automated design approach [59][134], prior works focus only on larger assemblies like aircraft or robots [143], and a lack of cases is criticized [144]. Likewise, many techniques exist in computational design synthesis [161][162][163], but the implementation for DFAM is yet to be fostered and demonstrated for AM applications [54][106].

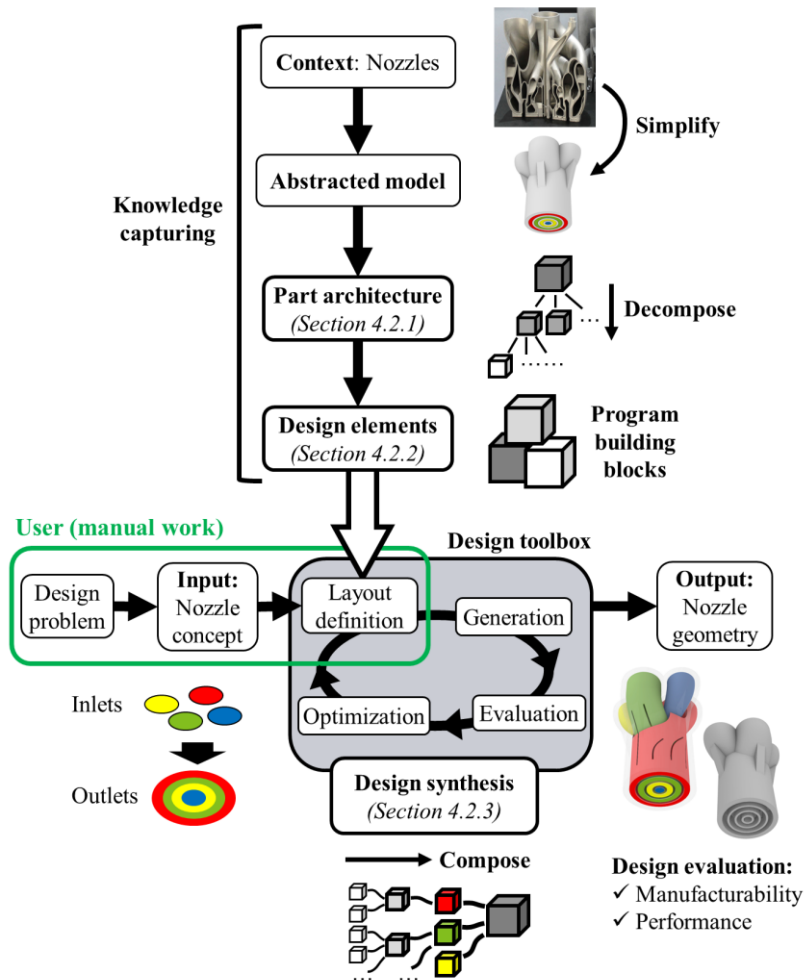


Fig. 16. Overview of computational design synthesis framework including knowledge capturing of part architecture and design elements as well as steps of the design synthesis process for the creation of 3D nozzle geometry.

The aim of this work is to present and implement a computational design synthesis framework that enables the automated design of AM nozzles that guide multiple fluid flows. An overview of the framework is given in Fig. 16. Similar to prior works [67][68][161], the main idea is to provide users with a software-based design toolbox with a set of design elements, which function as high-level building blocks. Given the concept of a nozzle including inlets and outlets, a user specifies the layout design of a part, meaning the arrangement of design elements. The layout serves as an input for the toolbox that automatically translates it into the corresponding 3D nozzle geometry. To analyze manufacturing restrictions of AM [48][51], the toolbox provides functions to check wall thickness values and critical overhang angles. These allow detecting and excluding non-manufacturable AM designs. Furthermore, a nozzle can be evaluated for its performance using computational fluid dynamics (CFD) analysis. Overall, the framework is based on

- a *part architecture* that organizes an AM nozzle with multiple integrated flows as a hierarchy of design elements (Sec. 4.2.1),
- a set of *design elements* that are implemented through object-oriented programming and represent building blocks of multi-flow nozzles (Sec. 4.2.2), and
- a *design synthesis process* that enables novice users through a visual interface and CAD plugin to define a layout, generate a nozzle geometry, and evaluate it for manufacturability and performance (Sec. 4.2.3).

After outlining the framework, a case study in Sec. 4.3 demonstrates its use to automatically generate a variety of customized AM nozzles that are tested using co-extrusion of clay. Sec. 4.4 discusses the framework's benefits and limitations and emphasizes the impact on product development and novel AM applications. In addition, the discussion comments on the transferability of the approach to other domains. Sec. 4.5 finishes with a summary and the conclusions of the work.

4.2 Computational design synthesis framework

4.2.1 Part architecture

To capture the design logic of a system or part, a common step in the area of knowledge-based design is to decompose it into its individual components and design elements, which have different functions and properties [59][109][134][164]. As shown in Fig. 17, a nozzle part with multiple integrated flow channels can be decomposed into a number of building blocks or design elements. The depicted nozzle represents a simplified version of the burner nozzle depicted in Fig. 15.

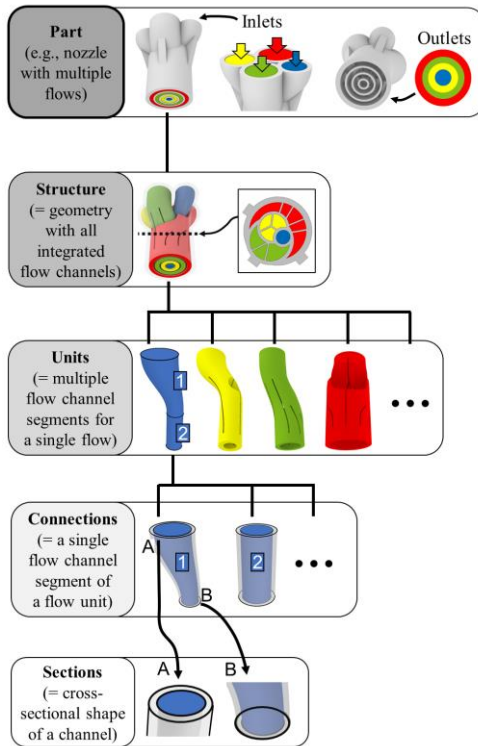


Fig. 17. Top-down decomposition of a nozzle geometry with multiple integrated flow channels into its individual design elements within a hierarchical part organization.

The nozzle in Fig. 17 has four pipe inlets and four ring-shaped outlets. It guides four different fluid flows that are marked by the colors blue, yellow, green, and red. As mentioned, the nozzle represents one single example to visualize the developed part architecture for multi-flow nozzles. Other nozzle variants with a similar architecture may differ in the number, shape, and positionings of the inlets and outlets, as well as other design features and characteristics.

The part architecture in Fig. 17 results from a top-down decomposition of the nozzle and is defined by a hierarchy of design elements. The geometry of a nozzle is modeled in such a way that it consists of a structure that integrates multiple flow channels that guide different fluid flows within a monolithic geometry.

Within the structure, multiple flow channels are interlaced and nested in each other. Units are introduced to model the separate flow channels that correspond to the different fluid flows. In the example, the nozzle integrates four units to guide the four separate flows. Other nozzle variants may integrate a different number of units.

A unit can be composed of multiple flow channel segments. Connections are introduced to model the individual flow channel segments of a unit. Multiple connections can be aligned as a series or parallel network within a unit. To describe the geometry of a connection, it is necessary to specify its start and end section conditions. For this purpose, sections are used to define the start and end position of a connection together with the cross-sectional shape.

As a whole, the hierarchical part architecture represents a form of a master model or blueprint design [53][59][134][143] to generate different multi-flow nozzle designs. The design elements function as object-oriented building blocks. Instead of low-level CAD primitives, the design elements can be seen as predefined, high-level objects. To implement the design elements, this work applies object-oriented programming to instantiate design elements as objects and synthesize nozzles from them.

4.2.2 Design elements

Object-oriented programming is used to implement each design element as a class. In the following, the blueprint of each design element is described to program the functions and properties of its class.

4.2.2.1 Section class

As shown in Fig. 18, a section is defined by a local coordinate system and two planar, non-intersecting, and closed curves. The inner curve specifies the flow domain. A wall thickness parameter t determines the offset between the inner and outer curves. Based on a type parameter, the section curves are created from analytical curves (ellipsoids, rectangles), Unicode characters and letters, and custom input curves.

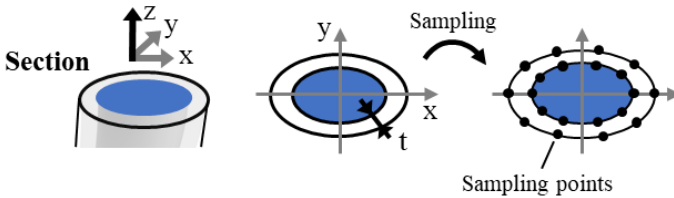


Fig. 18. Blueprint for section object to define the cross-sectional shape of flow channel segments.

Examples for various sections are visualized in Fig. 19. To further process a section, its shape is discretized by performing a sampling operation. As depicted in Fig. 19 (A), sampling points are placed on the curves of a section and divide these curves into smaller curve pieces. Section objects are also used to integrate threads, as shown in Fig. 19 (B).

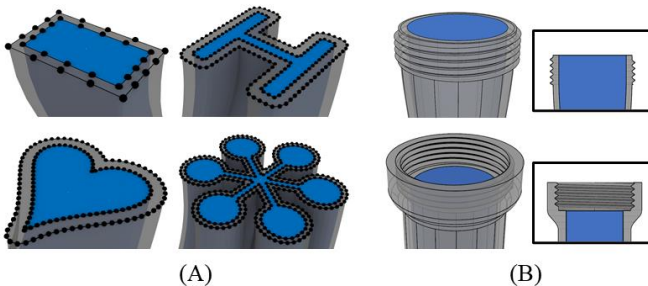


Fig. 19. (A) Example for sections with different curve types and generation of sampling points for further processing; (B) Integration of threads at sections.

4.2.2.2 Connection class

A connection represents one single flow channel segment and connects two sections. The inner body defines the flow domain, and the shell body corresponds to the wall. The geometry of a connection is determined by the orientation and shape of its start and end section. The bodies of a connection are defined by a surface-based boundary representation (BREP).

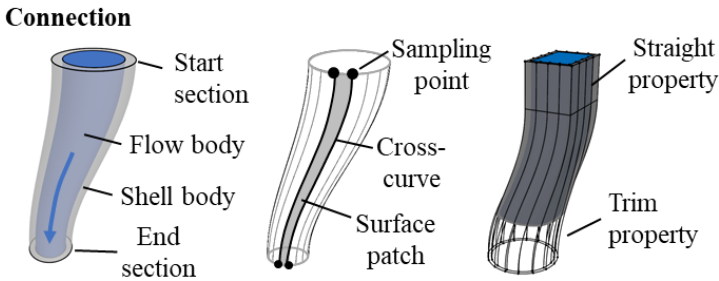


Fig. 20. Blueprint for connection object to represent one single flow channel segment.

As visualized in Fig. 20, the surfaces are lofted using a wireframe that is created from the curve pieces of the sections and additional cross-curve splines. The cross-curves start perpendicular to each section and connect the sampling points of both sections. In case two sections differ in their sampling number, the larger number is chosen for the sampling operation. To further modify a connection, its sections can be assigned with a straight or a trim property.

As shown in Fig. 21, within a connection, it is possible to integrate vanes for flow guidance and stiffening ribs as a reinforcement. The geometry of the generated vanes and ribs is defined by a set of design parameters, which are depicted in Fig. 21. The shape of each vane is parametrized by its start and end positions, thickness, opening angles, pitch angles, and trim angles. Ribs are parametrized using a wall thickness parameter as well as the width at the rib start and end positions. Similar to a connection, the geometry of vanes and ribs is generated using cross-curves and surface patches, as shown in Fig. 20.

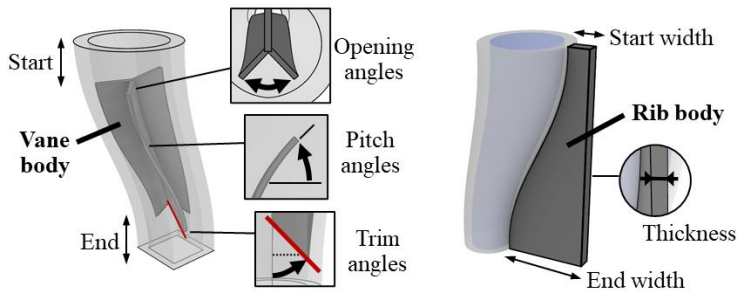


Fig. 21. Integration of flow guiding vanes and stiffening ribs into a connection object.

4.2.2.3 Unit class

A unit consists of multiple connections that form a network of flow channels to guide one single flow. A unit has a flow body and a shell body, which are composed of the flow and shell bodies of the contained connections. Connections can be arranged in series or parallel networks, as illustrated in Fig. 22. To define the layout of connections, a connectivity matrix in the form of an adjacency matrix is used, which stores all sections of a unit. In the matrix, non-weighted entries refer to the flow direction between two sections and determine the connections and their layout within a unit.

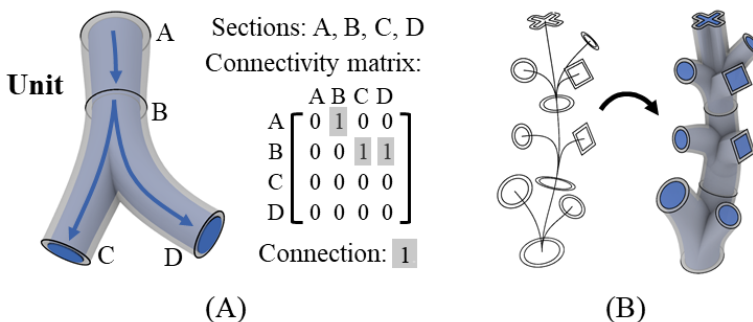


Fig. 22. (A) Blueprint for unit defined by a network of sections and their connections; (B) Example for a unit object containing connections in series and parallel.

4.2.2.4 Structure class

A structure integrates multiple units into a single part geometry. For this purpose, the geometric overlap between different flow regions needs to be detected and resolved. This is achieved by using Boolean operations between the bodies of units. As an example, Fig. 23 shows one blue and one green unit. In the original state, the flow bodies of both units overlap, and thus the resulting structure does not guide the flows in separated flow channels. To resolve this overlap, the flow body and shell body of the blue unit are subtracted from the bodies of the green unit. After this subtraction, the flow regions of both units no longer overlap, and a structure can be generated, which guides both flow domains in separated channels. Different rules can be implemented to resolve overlaps between different units. The example illustrates a rule where units with a smaller flow body (e.g., blue) are prioritized over units with a larger flow body (e.g., green).

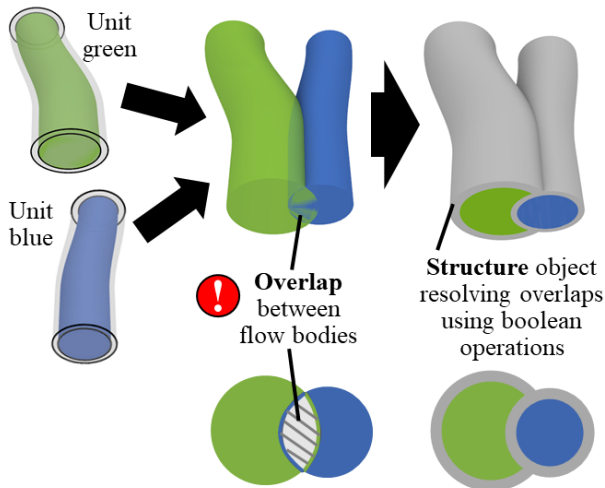


Fig. 23. Integration of units into a structure by resolving overlaps between different flows.

4.2.3 Design synthesis

The presented design elements function as predefined building blocks to automate the generation of multi-flow nozzles. Fig. 24 gives an overview of the design synthesis process. Starting from a specification of the design problem (e.g., conceptual definition of nozzle inlets and outlets), the design synthesis process requires a number of user inputs (regarding the employed design elements, fabrication data, performance evaluation, and design optimization) to generate a manufacturable and optimized 3D nozzle geometry.

The main steps of the design synthesis process include the user-based definition of a parametric nozzle layout using the design toolbox and its preprogrammed design elements, the generation of a 3D nozzle geometry, and the evaluation of manufacturability and performance. The use of an additional parametric optimization offers the possibility to iteratively change the parametric nozzle layout and optimize a nozzle design (see details in Sec. 4.2.3.4).

4.2.3.1 Parametric layout

To synthesize the design elements, a custom CAD plugin was programmed in the 3D-CAD software *Rhinoceros*® and its parametric design environment *Grasshopper*®. *Grasshopper* offers the possibility to specify the parametric layout of a nozzle using a visual, node-based editor. As shown in Fig. 25, a user selects a design element (e.g., section, connection, unit, structure, vane, rib object) from a toolbar and drags it into the *Grasshopper* canvas. Each element is assigned a set of parameters that define its shape and properties. To specify the relation between elements, they are connected using wires. For instance, as depicted for the yellow-colored unit in Fig. 25, two sections serve as an input for a connection object, which is extended with a vane and a rib object. In a similar manner, other units of a nozzle layout can be defined. Furthermore, this interface is used to specify user inputs from Fig. 24, such as build material, build direction, and thresholds for AM process parameters (e.g., minimum build angle α_{min} , minimum wall thickness t_{min}).

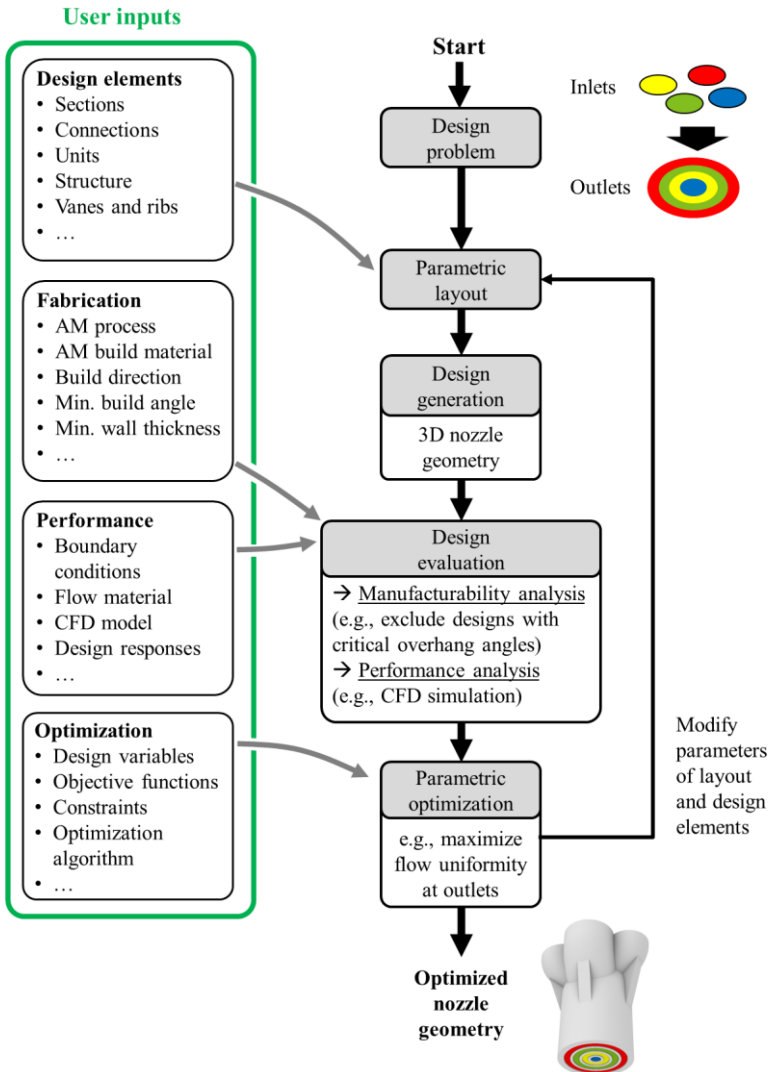


Fig. 24. Detailed overview of design synthesis process for multi-flow nozzles showing required user inputs (design elements, fabrication data, performance evaluation, design optimization) and process steps.

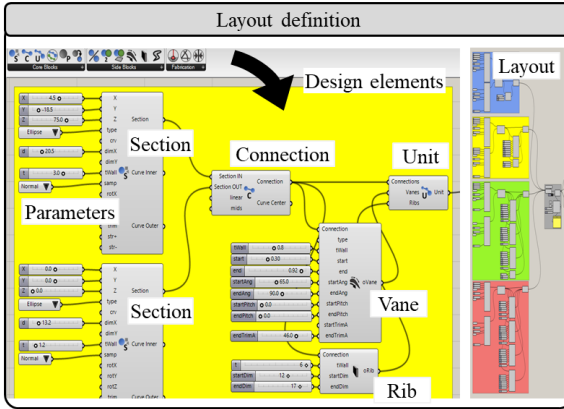


Fig. 25. Definition of a layout of design elements using the visual, node-based editor of Grasshopper.

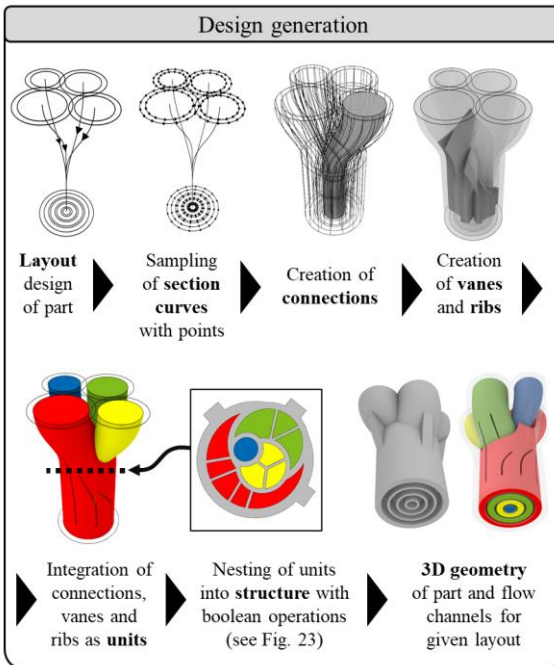


Fig. 26. Steps of design generation starting with a nozzle layout as an input leading to 3D nozzle geometry.

4.2.3.2 Design generation

Once the layout is defined, it can be automatically translated into the corresponding 3D nozzle geometry based on the preprogrammed design elements. As an example, Fig. 26 shows the generation for the nozzle variant with four flow channels. The process starts with the sampling of sections and continues with the creation of connections, vanes, ribs, and units. Overlaps between units are identified and Boolean operations are performed to interlace different units within a monolithic structure. The result is a surface-based 3D geometry of the nozzle and flow channels. If the geometry generation aborts due to geometrical CAD errors, the user is notified.

4.2.3.3 Design evaluation

The design generation step itself does not prevent the creation of designs that violate AM manufacturing restrictions. Design elements are only translated into the corresponding 3D geometry but do not adapt themselves. Therefore, it is necessary to evaluate the designs for AM restrictions and exclude non-manufacturable designs. As shown in Fig. 27 custom-programmed functions are used to detect critical wall thickness values or critical overhangs for a given build direction using a mesh-based description. Critical process parameters such as the minimum build angle α_{min} and minimum wall thickness t_{min} need to be defined by the user. These depend on the select AM process, build material, and machine and can be defined based on prior studies on AM processes [48][51]. Non-manufacturable AM designs are detected and marked. To evaluate the nozzle performance, a CFD analysis can be conducted. An interface was programmed to the external CFD tool *STAR-CCM+* to automatically export 3D geometries of flow channels and evaluate a CFD model for design responses such as pressure drop or flow velocity uniformity at a section outlet. Besides a CFD analysis, the reduction in cross-sectional area between two sections of a flow channel can be calculated.

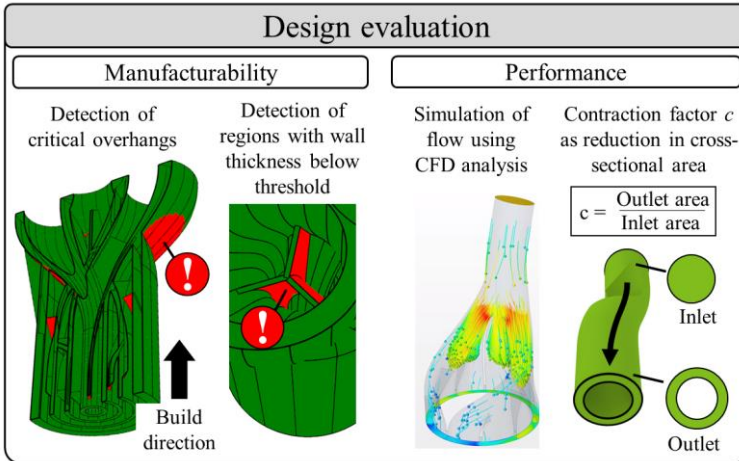


Fig. 27. Evaluation of nozzle design for AM manufacturing restrictions and performance.

4.2.3.4 Parametric optimization

Design elements make it possible to automate the generation of 3D nozzle geometries. To optimize a nozzle design, a parametric optimization can be performed, in which an algorithm automatically modifies the parameters of the nozzle layout and its design elements, generates and evaluates 3D designs, and improves these in an iterative procedure. For instance, as an objective function, the flow uniformity at a flow channel outlet can be maximized by changing the parameters of design elements such as guiding vanes. If the optimization generates non-manufacturable AM designs (e.g., vanes with critical overhang angles), such design variants are filtered out in the design evaluation and thus excluded during an optimization. A parametric optimization can be set up in *Grasshopper* using plugins such as *Galapagos*, *Optimus*, or *Wallacej* that provide different algorithms for design space exploration.

4.3 Case study

The following case study demonstrates the application of the framework and shows that it can be used to generate a variety of nozzle designs. Fused deposition modeling (FDM) of polylactide (PLA) is applied for the fabrication of nozzles. Their function is examined by extruding modeling clay as a viscous flow material. To study the generated nozzle designs, the approach is to use a cross-head extruder as a standardized part and mount customized generated nozzles with a thread interface. Different colors refer to flows of differently colored clays. As shown in Fig. 28, the cross-head extrudes four flows of clay into each other as concentric rings, whereas the nozzle tip merges the concentric flows and defines the shape of the extrudate that exits at the nozzle outlet.

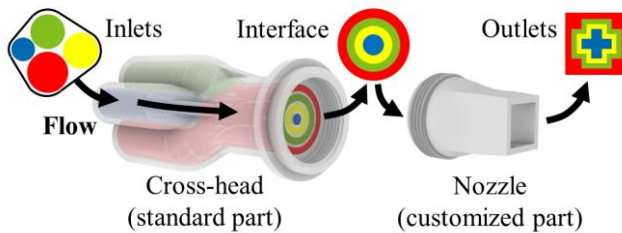


Fig. 28. Modular assembly consisting of automatically generated cross-head and nozzle.

Table 2 lists the studied nozzles. The inlets of each nozzle equal the interface of the cross-head. The outlets have various shapes. The selection of the outlet shapes is motivated by applications of a co-extrusion process. Similar shapes are used to co-extrude wires, tubes, profiles, heat sinks, packaging films, fuel cells, food, hydrogels, and other products and processes [165–173]. The design synthesis process is used to generate the nozzle geometries. As shown in Fig. 29, the first step is to define the layout of each nozzle. The design elements and their assigned parameters are then automatically translated into the corresponding 3D nozzle geometry within 5 to 10 s.

Table 2. Overview showing inlet and outlet, layout preview, and generated designs

ID	Nozzle inlet	Nozzle outlet	Layout design	Generated nozzle geometry (cut view and full model)
1				
2				
3				
4				
5				
6				
7				

The generated designs are evaluated for manufacturing restrictions of FDM. The build direction is defined in the z-axis. The nozzle design is checked for a minimum required build angle of $\alpha_{min} = 45^\circ$. If necessary, the layout is modified by the user to adapt regions with critical overhangs and recreate and reanalyze the 3D geometry. In addition, for the co-extrusion process, the flow channels are evaluated regarding the reduction in cross-sectional area in each channel. The generation of the nozzles is conducted without the use of a parametric optimization.

The resulting nozzle designs are fabricated using FDM and assembled with the cross-head part. The inlets of the cross-head are filled with modeling clay (e.g., *Play-Doh*). A hand press and plungers are used to push the clays through the cross-head and each nozzle. At the nozzle outlet, the co-extruded clay materials exit, as shown in Fig. 30 (A). The extruded strands are cut using a thin wire. The sliced samples are shown in Fig. 30 (B).

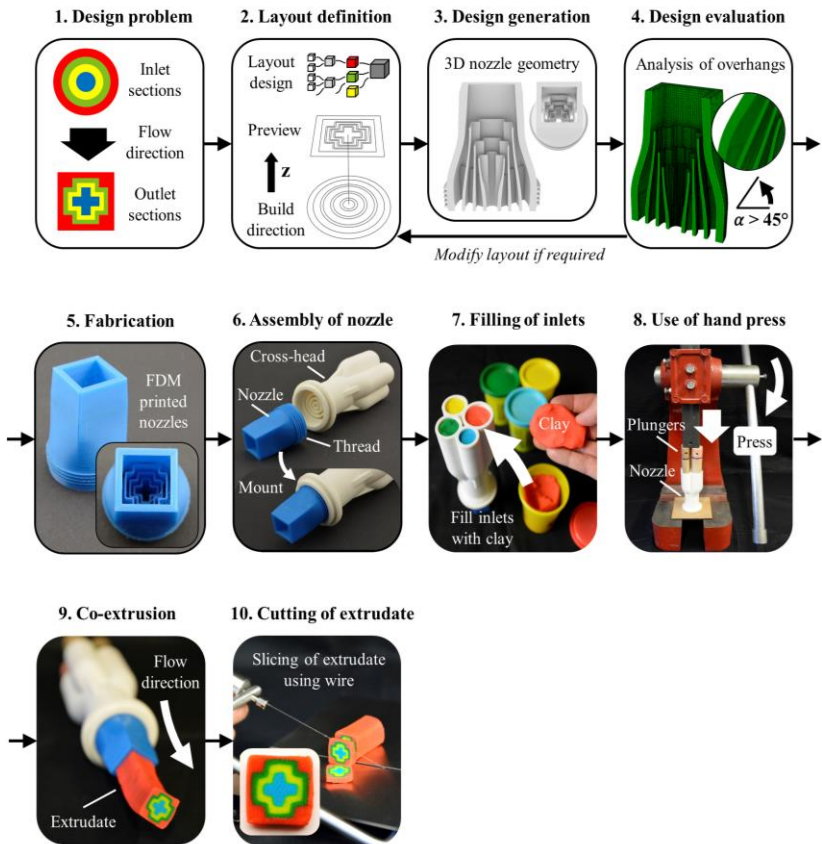
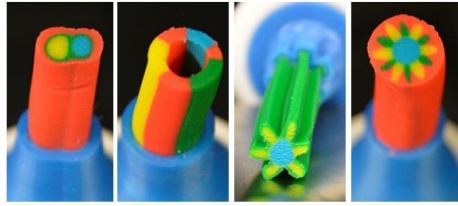
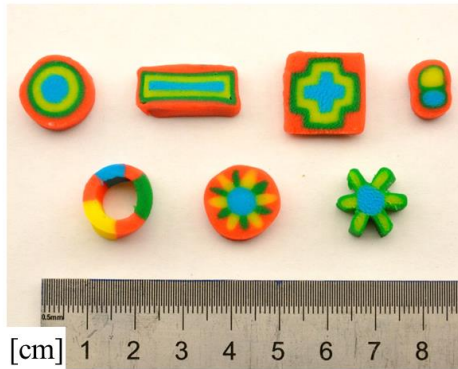


Fig. 29. Visualization of procedure to design and test customized nozzles showing steps of design generation and evaluation, fabrication of nozzles using FDM, preparation and filling of nozzles with soft clay material, use of a hand press to perform co-extrusion process, and resulting extrudate sample and slicing with wire.



(A)



(B)

Fig. 30. (A) Visualization of extrudate flows exiting nozzle outlets; (B) Sliced extrudate samples produced using FDM printed nozzles from Table 2.

As shown in Fig. 31, the positioning of vanes is critical to homogeneously distribute the flow material to a ring-shaped outlet. To maximize the velocity uniformity of the red flow channel, a CFD-driven parametric optimization can be used [41]. The red channel integrates four pairs of vane elements that are each defined by four parameters.

The initial, user-defined positioning of vanes leads to an outlet velocity uniformity of 69 % (baseline). To improve this objective, an optimization is applied that iteratively changes the vane parameters (16 in total), creates the 3D channel geometry, excludes non-manufacturable AM designs (e.g., vanes with overhangs) and runs a CFD analysis for manufacturable designs. The flow material is modeled as a laminar, incompressible flow with an inlet velocity of 4 mm/s and dynamic viscosity of 1500 Pa*s.

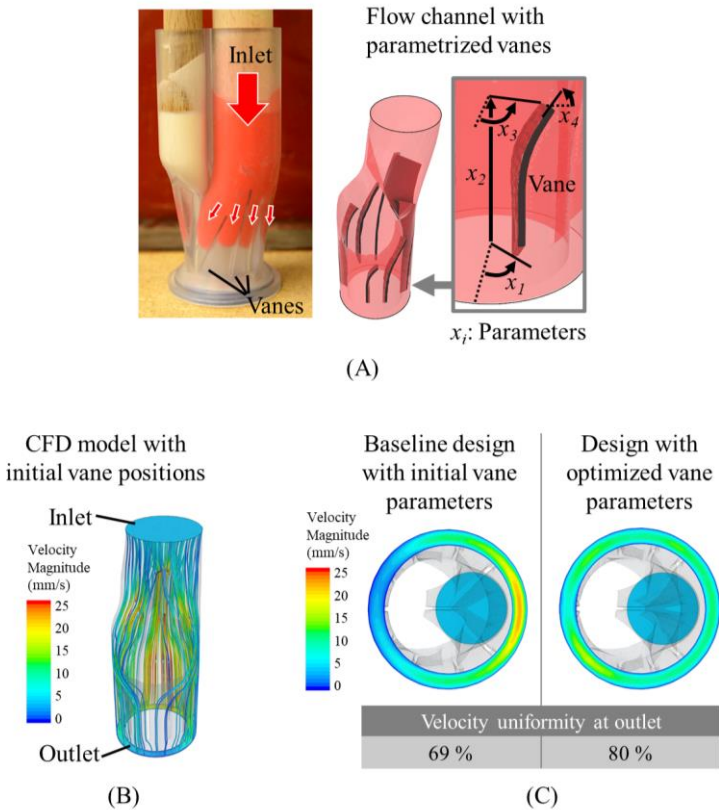


Fig. 31. (A) Uniform distribution of red clay material using four pairs of vanes that are each parametrized with four variables; (B) CFD model and streamlines; (C) Comparison of velocity profiles for baseline and optimized design.

In *Grasshopper*, the parametric optimization is set up using the *Opossum* plugin and its unconstrained, single objective optimization algorithm *RBFOpt* [174]. During the optimization, 325 design variants are successfully generated, of which 173 fulfill the FDM overhang constraint (minimum build angle of $\alpha_{min} = 45^\circ$), and a CFD analysis is performed. After 8 hours (AMD Ryzen, 32 cores, 64 GB RAM), the optimization converges with an optimized set of vane parameters and an improved outlet velocity uniformity of 80 %, as shown in Fig. 31.

4.4 Discussion

4.4.1 Advantages of object-oriented design elements

The design elements serve as a blueprint to enable the automated design of complex, additive manufactured flow components. The elements leverage the benefits of knowledge capturing and object-oriented programming. Compared to prior works [65], knowledge is not stored as explicit rules, heuristics, or databases but provided as (re-)usable, high-level building blocks. This makes it possible to capture the logic of AM parts and synthesize AM part designs with hierarchical complexity, such as nozzles with multiple integrated flow channels, for which a metallic prototype is shown in Fig. 32.

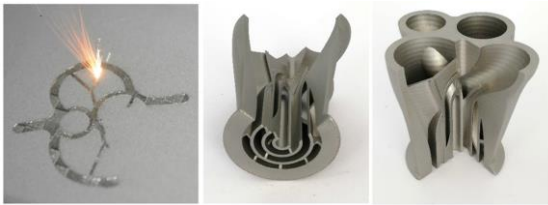


Fig. 32. Section cut of steel nozzle with multiple integrated flow channels fabricated with L-PBF.

4.4.2 Benefits for the user and iterative design development

Compared to a manual CAD process, low-level and time-consuming routine tasks such as the creation of geometric primitives are automated. Users can focus on creative tasks, generate 3D geometries for many different design concepts and make changes with reduced effort. This is especially beneficial for the iterative design, fabrication, and testing of AM parts. As design elements are provided through a graphical interface, the design process is also accessible for non-expert users. They can define, reuse, and copy layout designs without deep CAD knowledge. This provides a viable alternative to existing strategies for modeling and reusing CAD models [175].

4.4.3 Impact on novel AM-enabled applications

Besides benefits in iterative development, an automated design approach with design elements can be leveraged for AM-enabled, digital process chains. Especially for the customization of many part variants, design automation acts as an enabler for efficient design adaptations and as a key value driver for new, innovative business models. The case illustrates this opportunity for co-extrusion nozzles. In this respect, the importance of software engineering rises in the area of DFAM, and hardware products become like software-based services with the possibility for frequent design updates [53][176].

4.4.4 Comparison of approach to topology optimization

When performing a design exploration and exploitation, design elements have the disadvantage that they limit the searchable design space. The reason is that elements like sections predefine geometric features. This is a limitation compared to TO, in which design elements correspond to discretized finite elements and density values, and thus no prior features are specified. In combination with the proposed approach, TO may be utilized to identify new or improved high-level design elements. Furthermore, also for TO, the use of building blocks is examined in the context of moving morphable components [177][178].

4.4.5 Further integration of manufacturability for AM

In this work, manufacturability restrictions of AM, such as overhang constraints and minimum wall thickness values, are evaluated after the design generation. Therefore, design elements are not actively modifying themselves during the design generation step. Instead, non-manufacturable designs are detected and excluded (or filtered out) during a parametric optimization.

An improvement of this approach is to carry out a manufacturability adaption, for instance, for regions with overhangs already during the design generation step. Design elements such as sections and vanes would recreate and modify themselves according to a given build direction. For

example, an elliptical cross-section of a flow channel may automatically transform into a droplet-shaped curve to fulfill the overhang constraint.

Instead of classifying designs as manufacturable or non-manufacturable, other metrics can be used to better quantify the manufacturability for AM. For instance, the required amount of support structures [179], the part height, manufacturing costs, or thermal distortions [180] can be used as measures. In a multi-objective parametric optimization, such manufacturability measures can be combined with objective functions on the part performance. The weighting depends on the specific design problem and preferences of the designer.

4.4.6 Transfer to other AM application domains

This work implements a set of parametric design elements to synthesize a variety of multi-flow nozzles that integrate multiple flow channels. In general, the approach may be applied to similar flow components, such as dies with cooling channels, valves, manifolds, heat exchangers, and reactor designs [19][35]. Such parts also require the design of one or multiple flow channels, for which the design elements can be reused. Furthermore, the same part architecture and design synthesis process may be employed. However, more case studies are needed to investigate the applicability.

Besides flow components, other possible application domains include, for instance, heat sinks [152], compliance elements [181], truss structures [178], or antenna components [182]. For such application domains, the required design elements and part architecture may differ and require adaptations and additional programming effort. However, major steps of the approach may be reused and serve as an implementation basis. These are 1) the decomposition of a part into its individual design elements, 2) the object-oriented programming of design elements as building blocks, and 3) the application of a design synthesis process and parametric optimization using a visual, node-based editor such as *Grasshopper*. Furthermore, different forms of design representations can be investigated, such as voxel-based geometries [183].

4.5 Conclusion

This work presents a computational design synthesis framework for the automated generation of AM multi-flow nozzles based on high-level, object-oriented building blocks. The preprogrammed design elements allow AM users to quickly translate a layout design into a 3D nozzle geometry, which is analyzed for AM manufacturability and functional performance using CFD analysis. Furthermore, a nozzle design may be improved using a parametric optimization. As a demonstration, a case study successfully shows the generation and test of a variety of co-extrusion nozzles. Next research steps include the implementation of design elements that dynamically adapt themselves for AM restrictions instead of being excluded during a parametric optimization, as well as the transfer of the approach to other application domains of AM.

4.6 Acknowledgment

This work was supported by the initiative “*ETH Strategic Focus Area: Advanced Manufacturing.*” The authors would also like to thank Daniel Erne for conducting a series of prior tests on clay co-extrusion.

5 Study II: Automated consideration of overhang constraint

The content of this chapter has been published in the journal of *Additive Manufacturing* [149] under the title “*Automated design of additive manufactured flow components with consideration of overhang constraint.*”

Abstract

When designing parts for additive manufacturing (AM), users must consider manufacturing restrictions specific to the chosen AM production technology. For material extrusion or laser powder bed fusion (L-PBF), users need to follow design rules such as avoiding geometries with critical overhangs. If users create the 3D part geometry manually using computer-aided design (CAD), the consideration of design rules can be challenging and time-consuming. Especially for complex-shaped parts, novice designers may need multiple loops to analyze and modify CAD features for manufacturability. This manual process prevents users to quickly transfer the layout design of a part into the corresponding production-ready 3D part geometry. Therefore, it is highly desirable to automate the manual CAD process, including the consideration of AM restrictions. This work aims to automate the CAD-based design of AM parts with fluid flow channels. For this purpose, the work presents automated procedures that generate and modify design features such that they automatically comply with the AM overhang constraint. The procedures focus on flow components, such as hydraulic manifolds, and include design features such as support-free flow channels, integrated and sacrificial supports, and other features such as boreholes, interfaces, ribs, and channel branches. To enforce the overhang constraint in the generation of features, users define the part orientation to the build direction and values for the minimum build angle and maximum allowed diameter of horizontally oriented circular cross-sections. As a benchmark, the work demonstrates the procedures by revisiting an earlier AM hydraulic manifold. Given restrictions of L-PBF of stainless steel, the study uses the procedures to generate manufacturable 3D manifold

designs for different part orientations. One of the manifold variants is fabricated to show the manufacturability of the generated 3D part designs. The work finishes by discussing the benefits of the procedures, their transferability, and enhancements to generate manufacturable and functionally optimized designs.

5.1 Introduction

As highlighted in a recent review [14], the design and additive manufacturing (AM) of parts with fluid flow channels is relevant for a wide variety of applications. These include flow components, such as hydraulic manifolds, nozzles, valves, actuators, molds with conformal cooling channels, heat exchangers, and devices for process engineering [16][26][27][28][184][185][186][187][188][189][190][191].

As an example, Fig. 33 shows a hydraulic manifold with multiple flow channels, which an earlier study redesigned for laser powder bed fusion (L-PBF) of stainless steel [26].

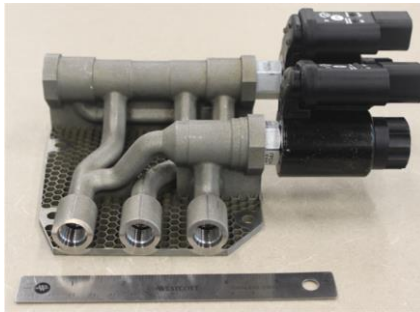


Fig. 33. Hydraulic manifold redesigned and fabricated using L-PBF of stainless steel [26] (CIMP-3D and NAVAIR Lakehurst).

When designing such parts for AM, users need to consider manufacturing restrictions for AM, which depend on factors such as the examined AM production technology, material, machine, and process parameters [1][4][98][99]. As illustrated in Fig. 34, one important manufacturing restriction for AM processes such as material extrusion and L-PBF concerns design features with geometric overhangs.

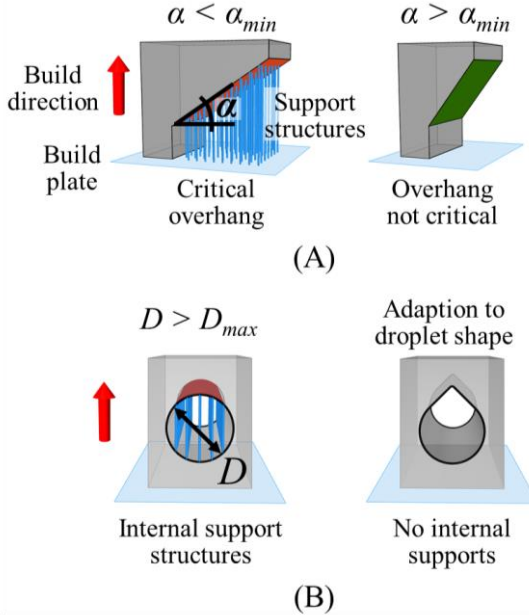


Fig. 34. (A) Minimum required build angle α_{min} to avoid supports; (B) Maximum allowed diameter D_{max} of circular cross-sections with a horizontal orientation before it requires internal supports or adaption of the cross-section shape.

Prior works analyze the manufacturability of critical overhangs using the minimum build angle α_{min} and the maximum diameter D_{max} of circular cross-sections with horizontal orientation to the build plate [48][49][50][51][81][123][192][193][194][195][196][197][198][199].

As shown in Fig. 34 (A), it is possible to fabricate critical overhangs that violate α_{min} and D_{max} using sacrificial support structures. Supports are added during AM and removed from the final part during post-processing. As depicted in Fig. 34 (B), the use of supports for internal features such as flow channels can lead to supports with limited or no accessibility for removal. One solution to avoid such internal supports is to modify the part design and change channel cross-sections from a circular to a modified shape, such as a droplet shape.

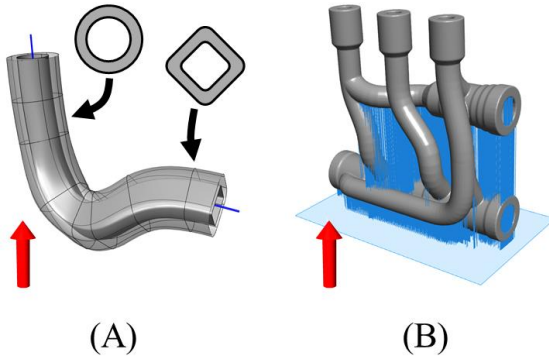


Fig. 35. (A) Design of support-free flow channels with a local adaptation of cross-sections to avoid internal supports; (B) Excessive sacrificial supports below flow channels with horizontal orientation to the build plate.

In general, the use of AM offers a high degree of design freedom [1][4][98][99]. However, if the 3D part design is created in a manual process using computer-aided design (CAD) tools, the consideration of AM restrictions can be challenging and time-consuming. Fig. 35 shows two common challenges relevant to the design of parts with flow channels, such as hydraulic manifolds [26]. As depicted in Fig. 35 (A), one challenge is creating support-free flow channels with curved pathways, which may require an adaption of the local cross-section to avoid internal supports. As illustrated in Fig. 35 (B), another challenge is to prevent critical overhangs and excessive sacrificial supports below horizontally aligned flow channels, for instance, by modifying pathways of flow channels or changing the orientation of the part to the build direction. For such kinds of design tasks, users may need multiple loops in a manual CAD process to analyze and modify design features to comply with AM restrictions.

Previous works provide users with design rules, guidelines, principles, and worksheets to support design for AM (DFAM) [105][109][114][115]. Furthermore, the application of software-based design tools is regarded as key to automate and accelerate the creation of part designs [4][55][71][98][99][119]. An automated design process offers many benefits compared to a manual CAD process. It enables users to generate

and explore an increased number of design variants, exploit them through design optimization, and individualize parts cost-efficiently for custom requirements. Moreover, it allows users to quickly implement design changes and shorten the development phase of an AM part, which often involves simulating, manufacturing, and testing several design iterations.

Topology optimization (TO) is one common approach to automate the creation of manufacturable and functionally optimized part designs [54][57][72]. Prior works account for AM restrictions such as the overhang constraint by implementing constraints and filters for density-based and level-set TO [126][127][128][200][201][202][203][204]. A recent review provides an overview of TO methods for fluid flow problems [73]. Prior works apply TO to generate AM part designs for different flow components, such as manifolds and heat exchangers [74][75][76][205][206].

Another approach to automate the design of AM parts is motivated by the field of knowledge-based engineering (KBE) [59][134]. The basic idea is to identify frequently recurring and time-consuming CAD tasks and automate them using design templates, feature databases, and design synthesis toolkits [161][162]. Compared to low-level CAD primitives, such design tools provide high-level and knowledge-based design features that allow capturing and sharing knowledge specific to the application, design, and production. Prior works use this approach for parts, such as structural components, compliant elements, mechanisms, and nozzles [67][68][69][148][207].

This work follows a KBE approach and aims to automate the CAD-based design of AM parts with fluid flow channels, including an automated consideration of the AM overhang constraint. The goal is to primarily support novice CAD users in the generation of production-ready 3D part designs. For this purpose, the work presents a set of automated procedures that generate and modify design features such that they automatically comply with the AM overhang constraint (e.g., generation of support-free flow channels). The automated CAD procedures are described in the context of hydraulic manifolds. However, they can also be reused for other AM flow components.

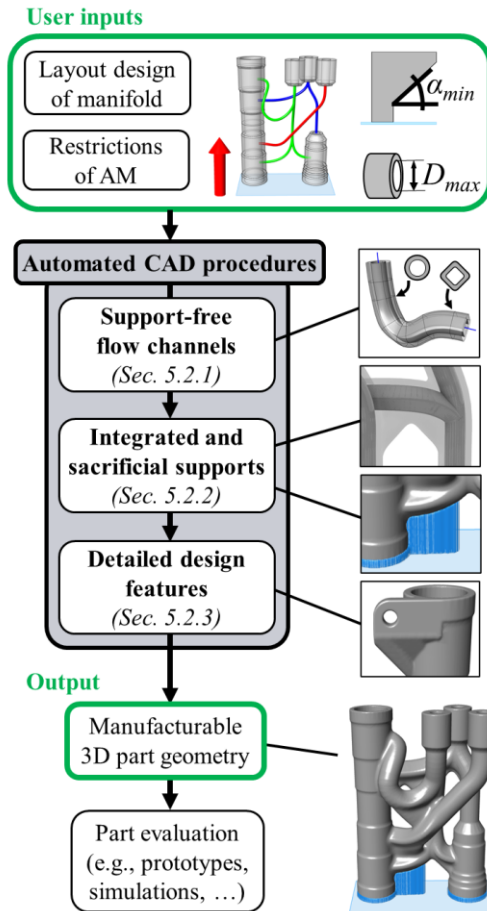


Fig. 36. Overview of automated CAD procedures used for the design generation of AM hydraulic manifolds.

The goal of the presented procedures is to enable users to automatically transfer the layout design of a manifold into a detailed 3D part geometry that is manufacturable using AM. Fig. 36 shows the user inputs and output of the overall process. One type of user input concerns the layout design [208] of a manifold specified by the pathways and dimensions of flow channels and features such as valve bodies and part

interfaces. Another type of user input concerns restrictions of AM. Within this work, the focus lies on the automated generation and modification of design features such that they comply with the AM overhang constraint. For this constraint, users define the orientation of the part to the build direction and values for the minimum build angle α_{min} and the maximum diameter D_{max} of circular cross-sections with horizontal orientation (see Fig. 34). The specific values for α_{min} and D_{max} are set by users and depend on the examined AM process, material, machine, and process parameters [1][4][98][99]. Given the user inputs, the procedures generate a production-ready 3D part design by creating

- *support-free flow channels* using a local adaption of the shape of channel cross-sections (Sec. 5.2.1),
- *integrated and sacrificial supports* for critical overhangs below horizontal channels (Sec. 5.2.2), and
- *manufacturable detailed features* such as boreholes, part interfaces, ribs, and channel branches (Sec. 5.2.3).

The generated 3D part design serves as a basis for further steps in the development process of a part. As shown in many prior works [26][188][191][209][210], the 3D part geometry can be used to fabricate prototypes for physical tests or simulate the part performance with computational fluid dynamics (CFD) and finite element analysis (FEA). Within the scope of this work, the focus lies on describing the automated procedures used to generate and adapt design features such that they comply with the overhang constraint, as described in Sec. 5.2. As a benchmark, the work demonstrates the functionality of the procedures in Sec. 5.3 by revisiting the AM hydraulic manifold [26], shown in Fig. 33. In the case study, the automated procedures are used to generate production-ready 3D manifold designs considering restrictions of L-PBF of stainless steel. As a proof of concept, different design variants are generated by varying the part orientation to the build direction and modifying the pathways of flow channels as user inputs. Sec. 5.4 discusses the benefits of the procedures, their transferability to other applications, and enhancements to generate manufacturable and functionally optimized part designs. Sec. 5.5 summarizes the work and concludes.

5.2 Computational design methods

5.2.1 Generation of support-free flow channels

This procedure generates a flow channel by placing cross-sections along a path curve. The cross-sections are used to construct the channel surface and walls. The basic idea is to adapt the shape of the cross-sections from a circular to an adapted shape (e.g., droplet, diamond) to prevent critical overhangs and internal supports at the inner surface of the flow channel. In this regard, a circular cross-section is only modified to a non-circular shape if it is required to fulfill the overhang constraint. Otherwise, the cross-section shape remains circular to minimize pressure losses and avoid peaks in the hoop stress distribution acting on the channel walls due to fluid pressure loading [26].

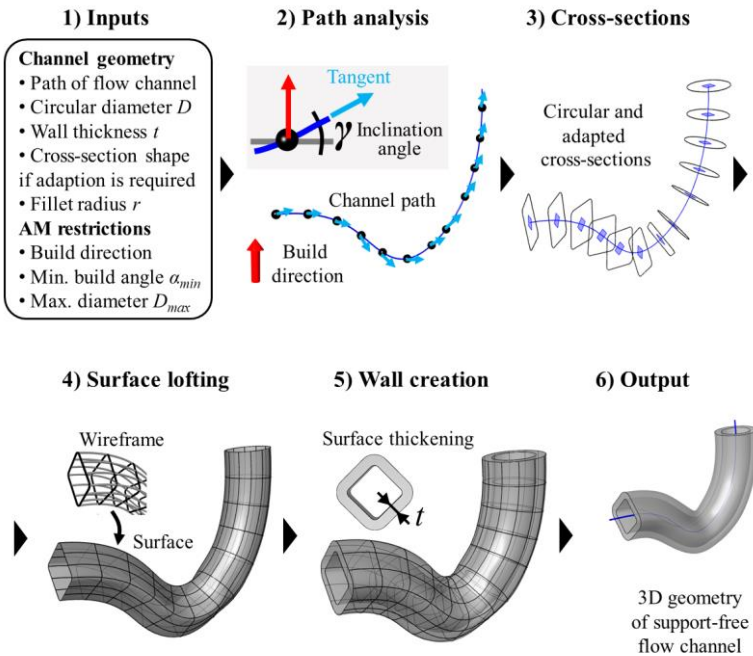


Fig. 37. Generation of support-free flow channels using a local adaption of cross-section shapes.

5.2.1.1 Overview of the procedure

Fig. 37 shows the main steps to generate support-free channels. User inputs in step 1 include settings on the channel geometry (channel path, diameter D , wall thickness t , fillet radius r) and AM restrictions (build direction, minimum build angle α_{min} , maximum diameter D_{max} of circular cross-sections with horizontal orientation to the build plate). In addition, it is necessary to define the cross-section shape (e.g., droplet, diamond, triangle, house), which should be used instead of a circular shape to avoid critical overhangs at the inner channel surface.

Step 2 analyzes the trajectory of the channel path to the build direction. At a predefined number of points along the channel path, the procedure calculates the local inclination angle γ measured between the tangent vector of the path and the build plate. The procedure also identifies special points at which the tangent is aligned horizontally to the build plate ($\gamma = 0^\circ$), or the inclination angle equals the minimum build angle ($\gamma = \alpha_{min}$). The number of points is predefined using a ratio of the diameter D and channel length.

Step 3 places local coordinate systems at the points. These are constructed based on the local tangent vector and the build direction. The local coordinate systems are used to place cross-sections along the channel path, as shown in Fig. 37. The cross-sections are instantiated from an object-oriented library of cross-sections containing different shapes (circular and self-supporting profiles). Sec. 5.2.1.2 provides further details on the library.

For each cross-section, the procedure determines if a circular shape can be used or if it is necessary to apply a non-circular, adapted cross-section to fulfill the overhang constraint. The decision depends on the local inclination angle γ of the cross-section, diameter D , and specified AM restrictions. Sec. 5.2.1.3 describes this dependency between the inclination angle γ , required cross-section shape, and degree of adaption in more detail. It serves as a basis for the automatic selection and parametrization of cross-sections, further outlined in Sec. 5.2.1.4. The procedure analyzes if cross-sections of the same flow channel overlap after the adaption step. If overlaps occur, they are detected and resolved by substituting the intersecting cross-sections with a single cross-section.

Step 4 creates the surface of the channel. For this purpose, a set of cross-curves are guided through the cross-sections. The resulting wireframe of curves is used to perform a loft operation and create the channel surface. Step 5 thickens the surface to create the channel walls. Step 6 shows the generated 3D geometry of a support-free flow channel.

The output also returns a percentage of the channel length for which the cross-section shape is adapted. Fig. 38 shows further examples of support-free flow channels generated using different adapted cross-section shapes to avoid internal critical overhangs.

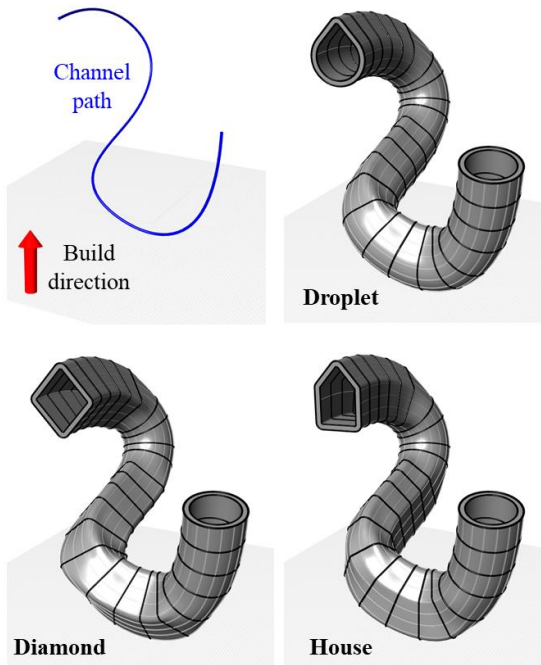


Fig. 38. Support-free flow channels generated using different cross-section shapes (droplet, diamond, house).

5.2.1.2 Library of cross-sections

As shown in Fig. 39, this work uses a library of cross-sections to generate channels with different adapted cross-section shapes. A cross sign defines the centroid for each cross-section shape and corresponds to the origin of the local coordinate system at which the cross-section is placed. A red arrow marks the orientation of a cross-section towards the build direction. Each type of self-supporting cross-section (droplet, diamond, triangle, house) avoids a critical overhang using a hat-like shape at the upper part of the cross-section curve. The hat is parametrized with the profile angle β . The self-supporting cross-sections are assigned with a fillet radius r to avoid sharp corners and stress peaks in channel walls. When users specify the fillet radius r , they must ensure that it complies with the overhang restriction of the examined AM process, material, machine, and process parameters. The library can be extended with other cross-section shapes or design parameters using object-oriented programming.

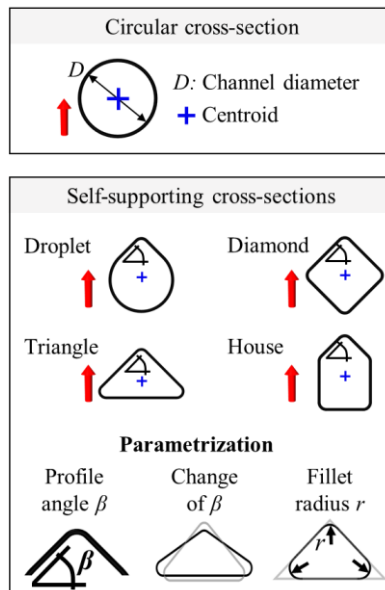


Fig. 39. Library of cross-sections containing circular and self-supporting shapes.

5.2.1.3 Influence of cross-section inclination

For each cross-section, the local inclination angle γ measured between the channel path tangent and the build plate has an important influence. It determines the required type of the cross-section shape and its parametrization. Fig. 40 illustrates this relationship. Depending on the inclination γ , the cross-section can remain circular or must be adapted (e.g., droplet shape). Suppose an adapted shape needs to be placed. In that case, the inclination angle γ defines the minimum profile angle β such that the inner surface of a channel does not possess a critical overhang.

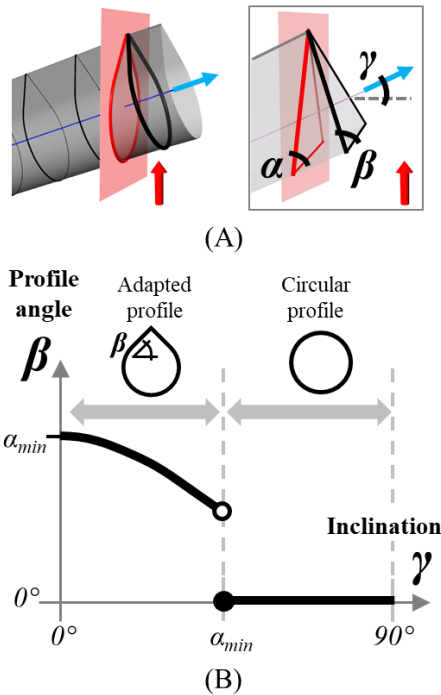


Fig. 40. (A) Definition of angles using a plane with vertical orientation to build plane; (B) Influence of inclination angle γ on the required cross-section shape and the minimum profile angle β given a minimum build angle α_{min} .

If a cross-section is aligned horizontally ($\gamma = 0^\circ$), it needs to have an adapted shape and the profile angle β should equal or be greater than the minimum required build angle α_{min} . If the inclination γ increases ($0^\circ < \gamma < \alpha_{min}$), the minimum value for β decreases. This relation can be shown by intersecting the channel with a plane that is oriented vertically to the build plate and examining the resulting build angle α . As further described in appendix Sec. 5.7.1, this allows deriving a formula for the minimum value of β , which is in the interval ($0^\circ \leq \gamma < \alpha_{min}$) as follows:

$$\beta = \arctan(\tan(\alpha_{min}) \cdot \cos(\gamma)) \quad (\text{Eq. 1})$$

If the inclination γ exceeds the minimum build angle α_{min} , it is no longer necessary to use an adapted cross-section shape, and it is possible to apply a circular profile. Within this interval ($\alpha_{min} \leq \gamma \leq 90^\circ$), the inclination γ of the channel segment is sufficiently large such that the channel walls are self-supporting and comply with α_{min} . This is also the case if a cross-section is aligned vertically to the build plate ($\gamma = 90^\circ$).

5.2.1.4 Selection and creation of cross-sections

The procedure automatically selects and creates a cross-section at a particular position along the channel path. As shown in Fig. 41, inputs include cross-section properties and AM restrictions. The output is either a circular or an adapted, self-supporting cross-section.

If the diameter D is smaller than D_{max} , it is not necessary to modify the cross-section shape. In this case, it is possible to place a circular profile. If D is larger than D_{max} , the procedure analyzes the cross-section inclination γ . As described in the prior section, the inclination angle γ decides if an adapted cross-section is required to prevent critical overhangs ($0^\circ \leq \gamma < \alpha_{min}$). Alternatively, the cross-section can remain a circular shape ($\alpha_{min} \leq \gamma \leq 90^\circ$).

If a self-supporting shape needs to be inserted, the user-specified type of cross-section shape is instantiated with the profile angle β (Eq. 1) and fillet radius r . The cross-section is rescaled such that its area equals the area of a circle with diameter D . This allows keeping a constant cross-sectional area along the channel. Alternatively, cross-sections can be rescaled to the hydraulic diameter.

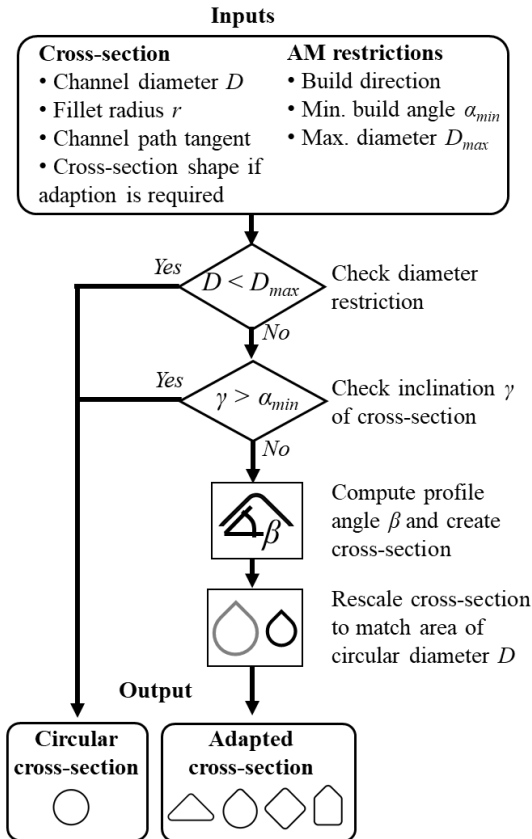


Fig. 41. Procedure for selection and creation of cross-sections.

5.2.2 Generation of integrated and sacrificial supports

The local adaption of cross-section shapes avoids critical overhangs at the inner surfaces of flow channels. The next step is to analyze the outer surfaces of channels for critical overhangs and, if required, place support structures that ensure the manufacturability for AM. This section describes an automated procedure to generate integrated and sacrificial supports for flow components, such as manifolds containing multiple flow channels.

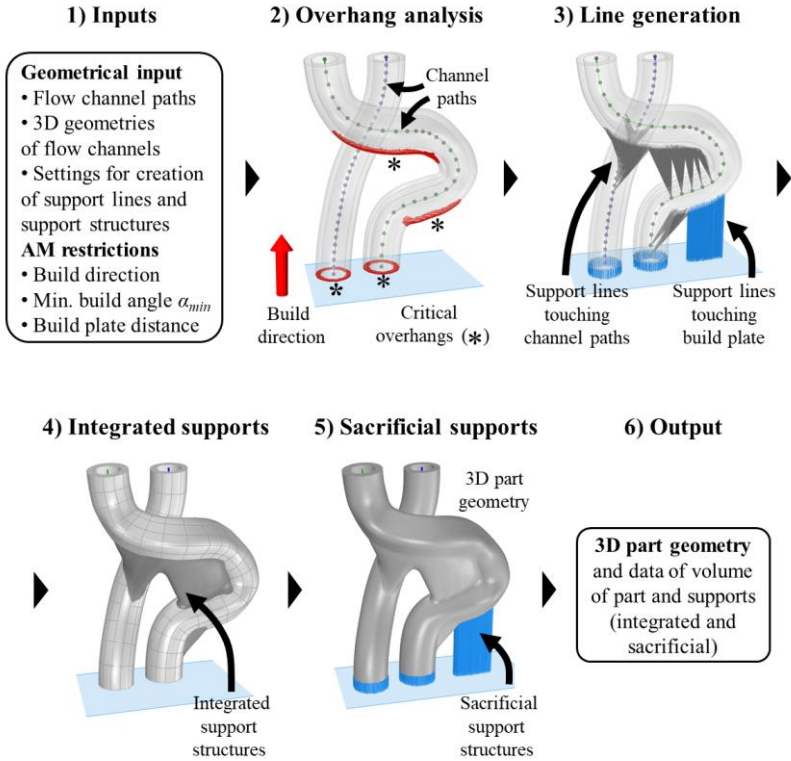


Fig. 42. Automated design of integrated and sacrificial supports.

5.2.2.1 Overview of the procedure

Fig. 42 shows the main steps of the procedure. Inputs in step 1 include the channel paths, 3D geometries of the channels (see Sec. 5.2.1), and settings for the generation of integrated and sacrificial supports. Further inputs are the minimum build angle α_{min} , build direction, and distance of the part to the build plate.

Step 2 detects critical overhangs that lie on the outer surfaces of channels. For this purpose, the procedure creates a mesh of the flow channels. The normal of each mesh face is compared to the build direction. A mesh face is identified as a critical overhang if the face orientation does not comply with the minimum build angle α_{min} .

Step 3 generates a set of support lines. Each support line is created by connecting the centroid of a critical mesh face with an associated support point, automatically identified by the procedure. A support point can either lie on one of the channel paths or the build plate. For each critical mesh face, the support point is determined based on two conditions. Firstly, the support point must lead to a feasible support line with an inclination angle equal to or larger than the minimum build angle α_{min} . Secondly, among all possible support points, the procedure selects the point with the closest distance to the critical mesh face to minimize the length of the support line.

The procedure leads to two groups of support lines. The first group, colored in gray, supports critical overhangs with support points located on a channel path. These support lines lie between channel paths and are used to create integrated supports, as shown in step 4 and further described in Sec. 5.2.2.2. The second group contains lines that start at a critical mesh face and end at a support point lying on the build plate. These lines are used to generate sacrificial supports, as shown in step 5 and further outlined in Sec. 5.2.2.3.

Therefore, the procedure makes use of integrated supports and sacrificial supports. Integrated supports are united with the channels and part geometry. They do not require additional effort for removal. However, they increase the part mass, which can decrease the part performance. Sacrificial supports are removed from the final part and only needed during AM. However, they require additional post-processing and sufficient access for removal.

Step 6 outputs a manufacturable 3D part geometry. This step also returns the volume of the required sacrificial supports V_S , integrated supports V_I , and part geometry V_P (which includes the volume V_I of integrated supports).

5.2.2.2 Integrated supports

Integrated supports are generated based on the first group of support lines, which connect critical mesh faces to support points located on the channel paths. As an example, Fig. 43 (A) shows a channel segment with a critical overhang.

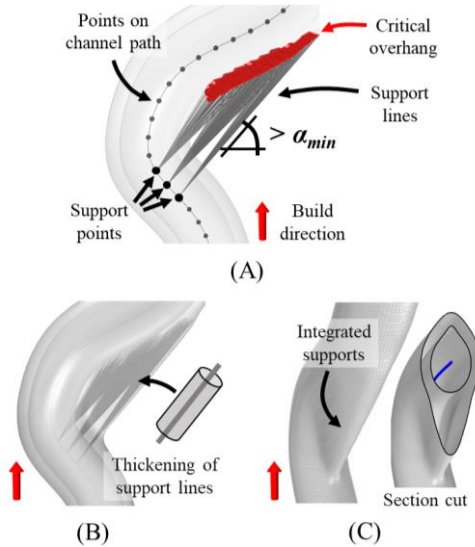


Fig. 43. (A) Creation of support lines for mesh faces with critical overhang; (B) Thickening of support lines to place support material; (C) Flow channel united with integrated supports.

The generated lines support critical mesh faces with associated support points that are sampled on the channel path. One support point can be assigned to multiple critical overhanging faces. This process leads to the fan-shaped alignment of support lines, as shown in Fig. 43 (A).

As displayed in Fig. 43 (B), the support lines are thickened to place material along the lines to support the critical overhang. A voxel-based modeling approach [211] is employed to computationally efficiently thicken the lines and unite them with the channel geometry. The area between the integrated supports and channel is smoothed to avoid sharp corners, as depicted in Fig. 43 (C).

In Fig. 43, the critical overhang is supported by a lower segment of the same channel. However, a critical overhang of a channel can also be supported by support lines, which end on the path of other channels. For instance, in Fig. 42, the support lines of the curved channel are connected to the path of the straight channel. The lines are used to create integrated supports between adjacent channels and increase the part's structural integrity.

5.2.2.3 Sacrificial supports

The second group of support lines, which connect critical mesh faces with associated support points lying on the build plate, are used to create sacrificial supports. Fig. 44 (A) shows an example of a channel segment with a critical overhang. As illustrated in Fig. 44 (B), an enclosing body is created that surrounds the support lines. For this purpose, the procedure uses voxel-based modeling [211] to thicken the lines and unite them as a single body. The enclosing body can be used to estimate the volume of sacrificial supports V_S by multiplying the volume of the enclosing body $V_{Enclosing}$ with the volume fraction v_f of the type of sacrificial supports:

$$V_S = V_{Enclosing} \cdot v_f \quad (\text{Eq. 2})$$

Fig. 44 (C) shows commonly used sacrificial supports such as block, lattice, and gyroid type [80][212]. Their volume fraction v_f depends on parameters such as the thickness of the lattice struts and walls. Again voxel-based modeling is applied to generate the geometry of sacrificial support structures. Cellular structures are created in the build space and then intersected with the enclosing body. As an alternative, sacrificial supports may also be generated using specialized software packages for build preparation (e.g., *Materialise Magics*).

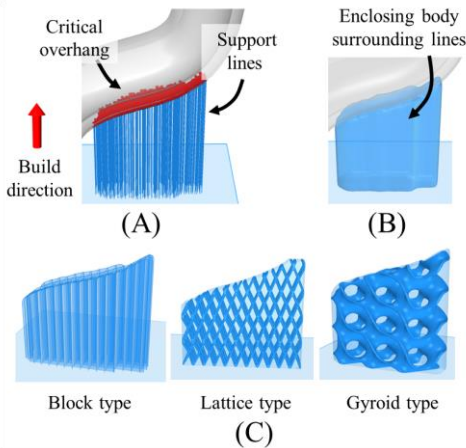


Fig. 44. (A) Support lines generated between the critical overhang and build plate; (B) Creation of enclosing body surrounding support lines; (C) Different types of sacrificial support structures.

5.2.3 Generation of detailed design features

Flow components such as hydraulic manifolds often integrate detailed design features such as boreholes for threads, interfaces for part attachment, and stiffening ribs for reinforcement. This section describes how such detailed design features can be automatically created and adapted to comply with the overhang constraint.

The first discussed design feature concerns the design of boreholes, for instance, to integrate and machine thread connections at flow channel inlets. In the following, it is assumed that a borehole is aligned horizontally to the build plate, and its diameter D is larger than the maximum allowed diameter D_{max} for horizontally oriented circular cross-sections. As shown in Fig. 45 (A), a borehole with a circular cross-section leads to a critical internal overhang. One option is to detect the critical overhang inside the borehole and generate sacrificial supports. However, these have to be removed and are difficult to access in internal structures. Another approach is to fabricate the borehole with an adapted cross-section shape such as a diamond profile, as illustrated in Fig. 45 (B). For this purpose, the automatic adaption of cross-section shapes from Sec. 5.2.1 is reused. This approach has the advantage that it prevents internal sacrificial supports. An alternative is to reduce the diameter of the borehole. However, this increases the required build material and material waste that results from machining.

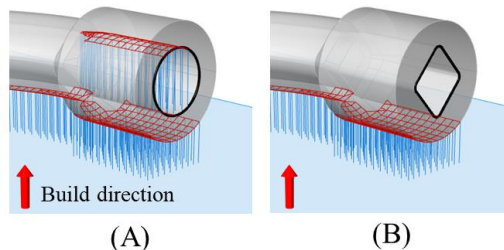


Fig. 45. (A) Borehole with circular cross-section requiring internal sacrificial supports; (B) Adapted cross-section to avoid internal supports.

Fig. 46 shows how other features such as interfaces and ribs can be automatically adapted for manufacturability by reusing the procedure for integrated supports from Sec. 5.2.2. Features such as interfaces and ribs are meshed to detect mesh faces with critical overhang. For each critical mesh face, an associated support point is identified on a channel path or the build plate. The support lines are thickened and integrated with the part design to support critical overhangs at detailed design features. This automated procedure is also used to generate internal supports for critical overhangs that can occur at the inner surfaces of flow channel branches. As an example, Fig. 47 (A) shows a branch with three merging channels. As illustrated in Fig. 47 (B), the automatic procedure detects critical overhangs, generates support lines, thickens the lines, and unites the integrated supports with the channel walls.

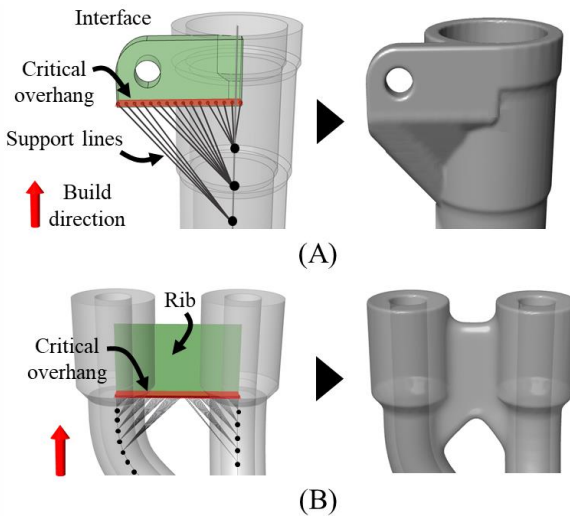


Fig. 46. (A) Creation of support lines and thickening to generate integrated supports for interface feature; (B) Procedure applied for reinforcement rib.

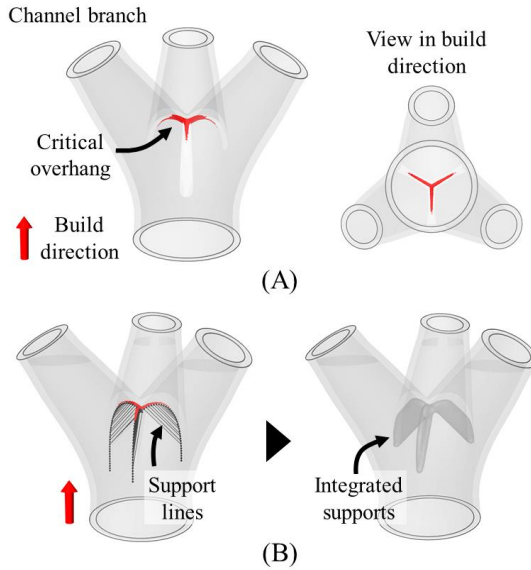


Fig. 47. (A) Critical overhang at the inner surface of flow channel branch; (B) Generation of integrated supports.

5.3 Case study

This case study demonstrates the application of the automated CAD procedures. The hydraulic manifold in Fig. 33 serves as a benchmark example. The goal is to show the generation of manufacturable 3D part geometries for different part orientations. The procedures are implemented using the CAD software *Rhinoceros*® with its parametric tool *Grasshopper*® and the *Dendro* plugin for voxel-based modeling. As shown in Fig. 48, the starting point is to extract the layout design from the original manifold, which includes channel paths and design features such as valve bodies and thread connections. The basic geometric dimensions of the manifold are taken from figures and X-ray images provided in the original study of the manifold [26]. The channels are defined with a diameter of $D = 8$ mm, a wall thickness of $t = 2.5$ mm, and the connectors have a thread size of ISO-M12. The inner diameters of the valve bodies lie between 15 and 21 mm, and the wall thickness is specified with 3 mm.

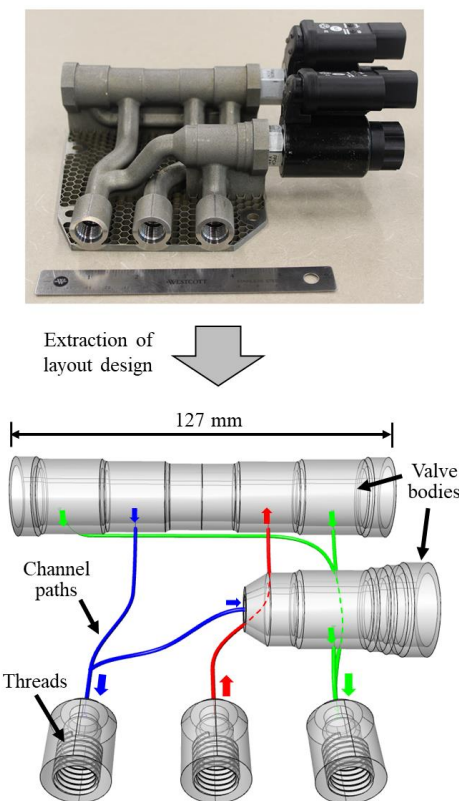


Fig. 48. Layout design extracted from original hydraulic manifold part presented in [26].

Like the original hydraulic manifold [26], the part should be manufactured in stainless steel using L-PBF. Within this case study, the manufacturing restrictions are chosen based on an earlier study that experimentally analyzed limitations for L-PBF of stainless steel [49]. Based on this study [49], the minimum build angle is chosen as $\alpha_{min} = 45^\circ$, and the maximum allowable diameter of circular cross-sections with horizontal orientation to the build plate is defined as $D_{max} = 7$ mm. It is important to note that α_{min} and D_{max} are user-defined values and can differ depending on the chosen AM production technology, material, machine, and process parameters [1][4][98][99].

Within this case study, circular cross-sections of channels, boreholes, and valve bodies should be adapted to diamond shapes with a fillet radius of $r = 0.5$ mm if it is required to fulfill the overhang constraint. The distance between the part and the build plate is chosen with 3 mm to attach the part using sacrificial supports and remove it after fabrication. Block type supports are selected and specified with a volume fraction of $v_f = 15\%$ [80][212] to estimate the volume of sacrificial supports. Again, these specific settings are chosen to demonstrate the automated CAD procedures but can vary depending on the examined AM process, material, machine, and process parameters.

The part orientation for AM is changed as a manual input. The automated procedures are applied to create manufacturable 3D manifold designs. Fig. 49 shows five design variants (V1 - V5) generated for different part orientations. The orientations are selected to align the main design features of the part to the build direction, as suggested in [109]. They are chosen to reduce the build height (V1) and to align the axes of the valve bodies (V2 and V3) or thread connections (V4 and V5) to the build direction.

For each variant, the layout design is automatically transferred into the corresponding 3D part geometry under the automated consideration of the overhang constraint. The procedures generate support-free flow channels (see Sec. 5.2.1), integrated and sacrificial supports (see Sec. 5.2.2), and adapt circular cross-sections of valve bodies and boreholes for threads (see Sec. 5.2.3). The overall design generation takes between 10 and 15 s for a single variant of a 3D part design. As shown in Fig. 49, each part orientation leads to a different 3D part geometry. Fig. 50 provides a detailed view of the generated design features using the example of V4.

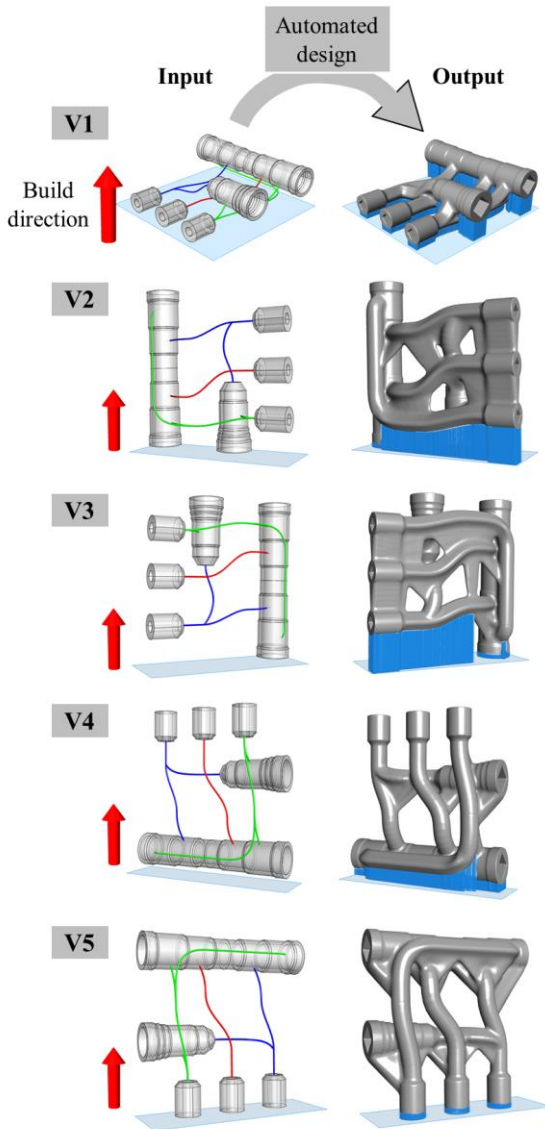


Fig. 49. Automated transfer of layout design into manufacturable manifold designs (including integrated and sacrificial supports) for five different part orientations (design variants V1-V5).

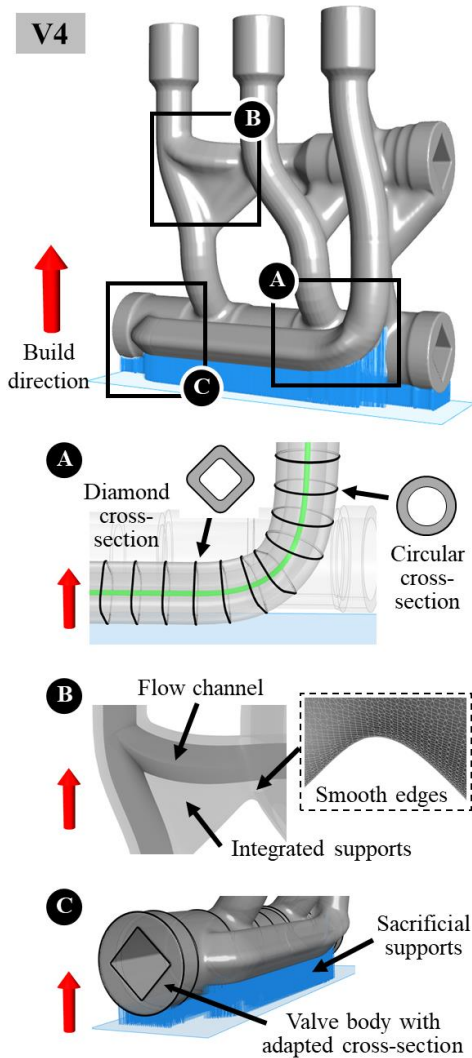


Fig. 50. Design features generated for variant V4; (A) Channel with smooth transition between circular and adapted cross-sections; (B) Integrated supports for critical overhangs of channel walls; (C) Sacrificial supports at the build plate and adaption of the inner cross-section of the valve body to avoid internal sacrificial supports.

In the original layout design of the manifold in Fig. 48, the valve bodies and thread connections are not oriented along parallel axes. This layout design makes it challenging to choose a part orientation without leading to trade-off situations. For example, for variant V4 the specified part orientation reduces the necessary adaption of channels to comply with the overhang constraint. However, it requires modifying the inner cross-sections of the valve bodies, thereby adding additional build material for integrated supports. Therefore, within this study, the idea is to modify the original layout design of the hydraulic manifold, as shown in Fig. 51 (A).

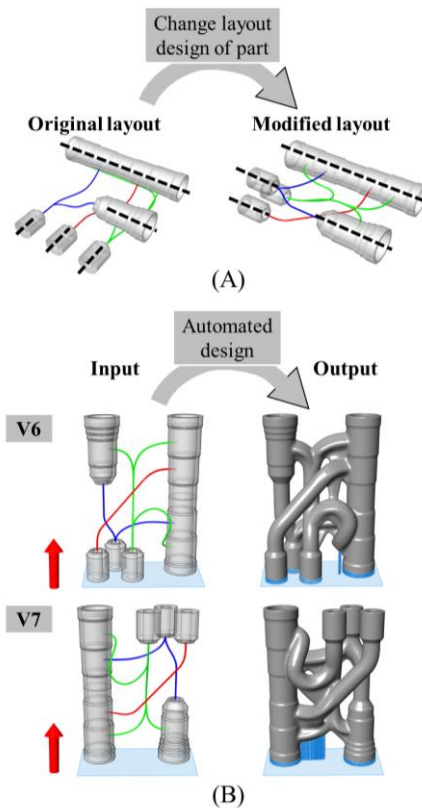


Fig. 51. (A) Modification of original layout design by aligning valve bodies and threads along parallel axes; (B) Automated transfer of modified layout design into manufacturable manifold designs (V6 & V7).

5 Study II: Automated consideration of overhang constraint

The thread connections are repositioned such that they lie on axes that are parallel to the axes of the valve bodies. The channel pathways are changed accordingly and routed to reduce the required adaption of channels and the occurrence of critical overhangs. The part orientation can be defined either in the direction of the parallel axes or opposite to it. These two variants lead to V6 and V7, for which Fig. 51 (B) displays the generated 3D part geometries, including integrated and sacrificial supports.

For each design variant, the generated 3D part geometries are used to extract a series of data values given in Table 3. These include the build height H , projected dimensions on the build plate X and Y , and the required adaption of flow channels A as a percentage of the total channel length. Furthermore, the table provides the volume of required sacrificial supports V_S and the volume of integrated supports V_I . The part volume V_P equals the volume of the part geometry with the integrated supports.

Table 3. Data values extracted from generated 3D part geometries

Design variant	Build height of part H [mm]	Dimensions projected on build plate $X \times Y$ [mm]	Adaption of channels along length A [%]	Sacrificial support volume V_S [mm ³]	Integrated support volume V_I [mm ³]	Part volume (with V_I) V_P [mm ³]
V1	41	127 x 127	96	7019	16143	98141
V2	130	38 x 127	71	2792	16998	98288
V3	130	38 x 127	71	2791	18867	100157
V4	130	38 x 127	32	3047	24772	104822
V5	130	38 x 127	32	468	48590	128640
V6	130	38 x 90	36	641	3561	82302
V7	130	38 x 90	36	635	4086	82827

This study applies simple analytical criteria calculated with a reduced computational effort to evaluate and compare different variants. They are given in Table 4. The performance is rated with the part mass m_P based on the part volume V_P and a material density of $\rho = 7.9$ g/cm³. The total length of all flow channels L serves as an indicator for pressure losses, as described in an earlier study of a hydraulic manifold [27]. Concerning

part production, the material volume V (sum of V_P and V_S) is used as an indicator for material costs. Furthermore, the table lists the maximum number of parts N_{batch} that can be placed in a single build job. The number N_{batch} serves as an indicator for the attainable platform utilization of a machine to produce a design variant as a series part. In this study, the build space of an EOS M 400 machine is populated, as shown in Fig. 52. An increased number of parts per batch N_{batch} reduces manufacturing costs related to machine setup, distribution of idle times during recoating of layers, and de-powdering parts. For a batch job, this allows reducing manufacturing costs, measured per part. It is important to note that other evaluation criteria can also be used to rate design variants besides the stated criteria. For instance, the generated 3D part geometry can be used as a basis to fabricate prototypes for experimental tests, conduct numerical simulations to evaluate part performance or apply cost calculations for production. Regarding these methods, the reader is referred to previous works [26][87][188][191][209][210][213].

Table 4. Evaluation criteria for selection of design variant

Design variant	Mass of part ($= \rho * V_P$) m_P [g]	Total length of flow channels L [mm]	Material volume ($= V_S + V_P$) V [mm ³]	Maximum number of parts in build space N_{batch} [-]
V1	775	463	105160	9
V2	776	463	101080	38
V3	791	463	102948	38
V4	828	463	107869	28
V5	1016	463	129108	28
V6	650	422	82943	42
V7	654	422	83462	42

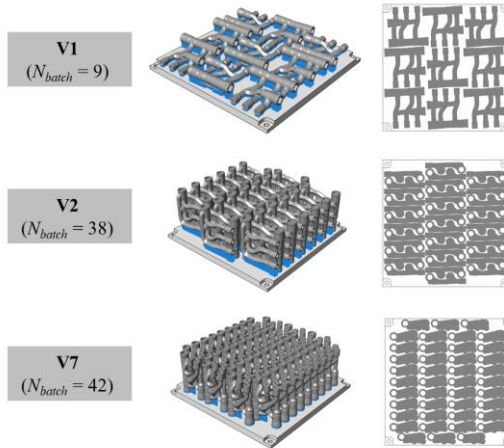


Fig. 52. Platform utilization of an EOS M 400 machine with a build space of $400 \times 400 \times 400$ mm.

Based on Table 4, variants V6 and V7 show a reduced part mass m_P and have a shorter total length of flow channels L . Moreover, both variants require a smaller amount of material volume V for fabrication and possess a very compact part design, which allows populating the build space with an increased number of parts N . Out of these two variants, V7 is chosen for further examination. However, also other variants may be selected and further studied. The main goal of this study is to show the manufacturability of the generated 3D part geometry and demonstrate the fabrication of the design variant as a physical prototype using L-PBF of stainless steel.

As displayed in Fig. 53, the part design is extended with detailed features. These include interfaces for the assembly of the part and stiffening ribs to increase the part integrity and stability against vibrations during post-machining. The features and required integrated supports are generated with the automated procedure described in Sec. 5.2.3. Clamping faces are added to fixate the part during machining.

Fig. 54 (A) and (B) show the manifold part, which was successfully produced using a Concept Laser M2 UP1. Fig. 54 (C) and (D) depict the part during the machining of interfaces and threads. The final mass of the produced part shown in Fig. 54 is 731 g.

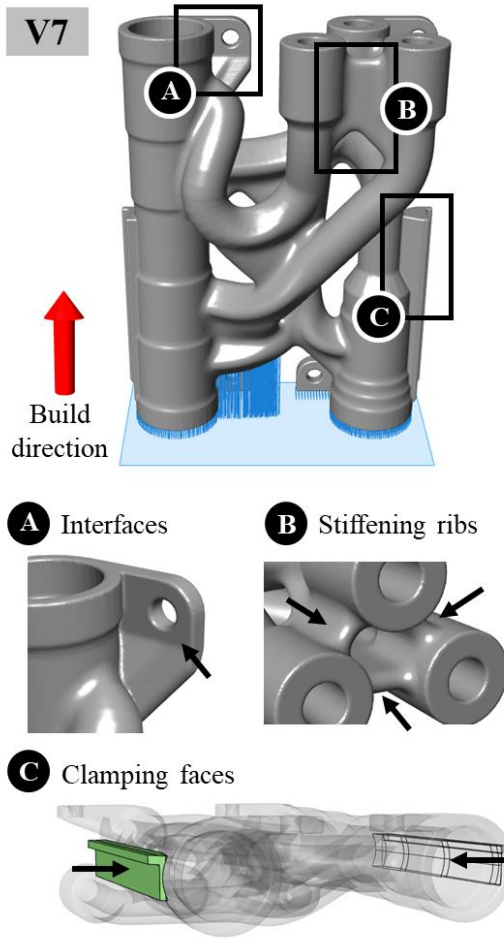


Fig. 53. Final part design of variant V7, including detailed features such as interfaces for part attachment, stiffening ribs for reinforcement, and clamping faces for machining.

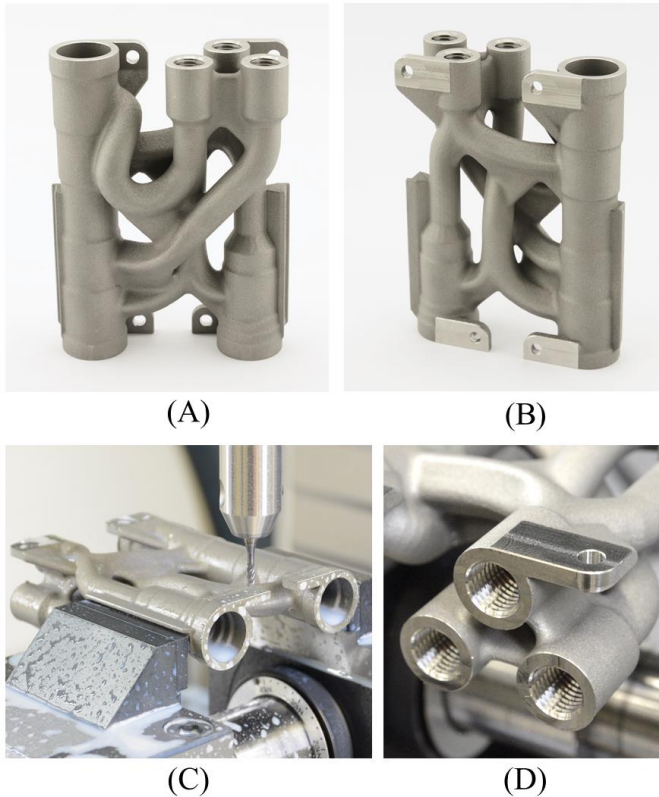


Fig. 54. (A) Front view of design variant V7 fabricated in stainless steel using L-PBF; (B) Rear view of part; (C) Part clamped for machining; (D) Detailed view of machined interfaces and thread connections.

5.4 Discussion

5.4.1 Benefits for the development process

Based on the automated CAD procedures, novice users can quickly transfer the layout design of an AM part, such as a hydraulic manifold, into a production-ready 3D part design. For the iterative development of an AM part, this approach enables users to automatically create 3D part

geometries to fabricate and test prototypes or conduct simulations and analyze the part performance. Users can generate production-ready part designs for different layout designs (e.g., design variants of hydraulic manifolds with varying pathways of channels) or production scenarios (e.g., part designs generated for several part orientations to the build direction). This automated design approach allows for rapid design changes, and the pursuit of design alternatives helps reduce uncertainties at an early stage of a development process [109]. Moreover, it makes it possible to individualize AM parts cost-efficiently for custom requirements (e.g., automated design of hydraulic manifolds for customer-specific layout design of flow channels and valve bodies). The automated CAD procedures are described in the context of hydraulic manifolds. However, users can apply the procedures also to other AM parts with fluid flow channels, such as valves, parts with conformal cooling, heat exchangers, and process engineering devices [14]. Depending on the examined application, the presented procedures can be reused, or it is necessary to implement additional features.

5.4.2 Consideration of overhang restriction

This work implements procedures that automatically create CAD features and modify their shape to comply with the AM overhang constraint. For this purpose, users specify the part orientation to the build direction and values for the minimum build angle α_{min} and maximum diameter D_{max} of horizontal circular cross-sections. It is important to note that the specific values for α_{min} and D_{max} are set by users and vary depending on the AM process, material, machine, and process parameters used to fabricate the part [1][4][98][99]. Given the user inputs, the procedures generate design features such as support-free flow channels and support structures and adapt their shape depending on the geometric parameters of the features and the user-specified AM restrictions. Therefore, the work contributes to the concept of “manufacturing elements”, which connect geometric features with manufacturing information and constraints of the examined AM process, material, machine, and process parameters [48][214][215][216].

Although the procedures enable users through an automated design approach, users still need to consider essential aspects of DFAM. Firstly, the generated part designs only avoid fabrication defects coming from the part design, but process-related defects can still occur during fabrication [1][217][218]. Secondly, process defects can lead to an increased surface roughness at the inner surface of flow channels [219], which can be reduced using post-processing methods such as abrasive flow machining [220]. Thirdly, selecting the orientation of a part to the build direction plays an important role [109]. It influences if and to what extent design features need to be modified for manufacturability. For instance, to avoid the adaptation of circular cross-sections for channels, boreholes, and valves, one possible solution is to orient the axis of such design features along the build direction accordingly.

5.4.3 Possible enhancements of presented procedures

The presented procedures only generate and adapt CAD features for manufacturability but do not optimize them for improved part performance. Therefore, this work can be categorized as a restrictive DFAM approach [108], which mainly aims to simplify and automate the consideration of AM restrictions in the CAD-based design of parts. For this purpose, the work provides a set of automated CAD procedures to synthesize production-ready 3D part designs. The use of such automated and knowledge-based CAD procedures has the advantage that they can be (re-)used and shared as building blocks by novice users for various fluid flow applications [14]. However, predefined building blocks and features such as a library of channel cross-sections restrict the attainable design space. This aspect is a disadvantage compared to design methods such as TO, which can generate functionally optimized and manufacturable part designs without predefined design features.

Future works can combine the described procedures with design optimization methods to leverage the design freedom and opportunistic aspect of DFAM [108]. A parametric optimization can be conducted to iteratively generate 3D part designs using the procedures of this work and analyze and optimize the part performance (e.g., minimization of pressure losses) through numerical CFD and FEA simulations [26][188][191][209][210].

Possible design variables of a parametric, simulation-driven design optimization include the diameter, cross-section shape, and pathways of channels or production variables such as the part orientation to the build direction. Future works can use routing and path planning algorithms to generate the pathways of flow channels automatically. For parts such as hydraulic manifolds, the generated flow channels should lie in proximity to achieve a compact part design. However, flow channels should not intersect after their creation and adaptation for AM. In this work, flow channel paths are defined manually, and therefore overlaps may occur between different flow channels. Future work can automate the correction of overlaps by automatically modifying paths of flow channels to avoid overlaps.

5.5 Conclusion

This work focused on the design of AM parts with fluid flow channels such as hydraulic manifolds and presented automated CAD procedures to generate design features such that they automatically comply with the AM overhang constraint. Especially for novice users, this approach significantly reduces the required CAD work by avoiding manual loops of evaluating and modifying design features for manufacturability. A case study demonstrated the automated procedures by revisiting a hydraulic manifold fabricated using L-PBF of stainless steel. The study applied the procedures to generate production-ready 3D part designs for different orientations to the build direction and modified pathways of flow channels. One of the design variants was fabricated to show the manufacturability of the automatically generated part designs. Finally, the work discussed the benefits and transferability of the procedures and possible enhancements to generate manufacturable and functionally optimized part designs.

5.6 Acknowledgment

The authors would like to thank the anonymous reviewers for their valuable feedback and comments. The work was supported by the initiative “*ETH Strategic Focus Area: Advanced Manufacturing.*”

5.7 Appendix

5.7.1 Derivation of formula for the minimum required profile angle β

This section derives a formula for the minimum profile angle β of an adapted cross-section required to fulfill the overhang constraint and avoid supports inside a flow channel. Fig. 55 (A) displays a channel segment with a droplet-shaped cross-section. The derivation is identical for other cross-section shapes such as triangular or diamond profiles, which also possess a hat-like form at the upper part of the cross-section.

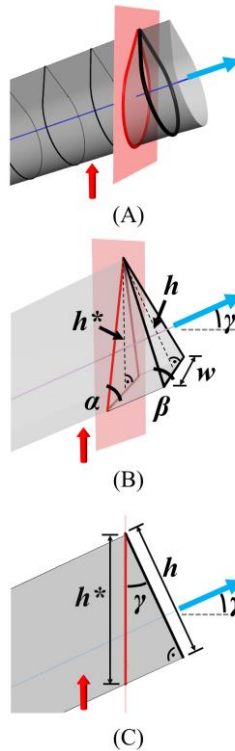


Fig. 55. (A) Cut view of flow channel segment using a plane with vertical orientation to build plane; (B) Cross-section inclination γ , profile angle β , build angle α , width w , and height h and h^* ; (C) Side view.

Fig. 55 (B) shows a cut of the channel segment utilizing a plane that is aligned vertically to the build plate. The plane is defined using the build direction and tangent of the channel path. The intersection between the plane and channel leads to an intersection curve colored red. The variable α marks the build angle measured in the intersection plane. The intersection curve shows if a particular value of the profile angle β leads to a critical overhang to a minimum build angle α_{min} . Parameters h and h^* denote the height of the cross-section and intersection curve. The value w specifies their width, which is equal for both curves.

In the first step, the profile angle β of the cross-section is related to the build angle α . Based on Fig. 55 (B), the following two equations are stated:

$$\tan(\beta) = h / w \quad (\text{Eq. 3})$$

$$\tan(\alpha) = h^* / w \quad (\text{Eq. 4})$$

Dividing (Eq. 3) by (Eq. 4) cancels out the width w and leads to:

$$\tan(\beta) / \tan(\alpha) = h / h^* \quad (\text{Eq. 5})$$

In a second step, the side view in Fig. 55 (C) is used to relate the height h of the cross-section and h^* of the intersection curve. Both are connected through the inclination angle γ :

$$\cos(\gamma) = h / h^* \quad (\text{Eq. 6})$$

Combining (Eq. 5) and (Eq. 6) leads to:

$$\tan(\beta) / \tan(\alpha) = \cos(\gamma) \quad (\text{Eq. 7})$$

Reordering (Eq. 7) yields:

$$\beta = \arctan(\tan(\alpha) \cdot \cos(\gamma)) \quad (\text{Eq. 8})$$

5 Study II: Automated consideration of overhang constraint

This equation relates the profile angle β of the cross-section to the inclination angle γ and the build angle α . The build angle α must be greater than or equal to the minimum build angle α_{min} to avoid a critical overhang at the inner surface of the channel:

$$\alpha \geq \alpha_{min} \quad (\text{Eq. 9})$$

Inserting this expression into (Eq. 8) leads to:

$$\beta_{min} \geq \arctan(\tan(\alpha_{min}) \cdot \cos(\gamma)) \quad (\text{Eq. 10})$$

This equation describes the minimum required profile angle β_{min} of an adapted cross-section with inclination angle γ to fulfill the overhang constraint and avoid supports inside a flow channel.

6 Study III: Automated routing of multiple flow channels

The content of this chapter has been published in the journal of *Additive Manufacturing* [150] under the title “*Routing multiple flow channels for additive manufactured parts using iterative cable simulation.*”

Abstract

Many prior works highlight the potential of additive manufacturing (AM) for flow components. Examples include hydraulic manifolds with multiple crossing flow channels that guide separate fluid flows in a single part. Creating the 3D geometry of such complex parts can be challenging. Designers must consider functional requirements, such as minimizing the channels' length, creating smooth channel paths, and preventing overlaps between channels for different fluid flows. Furthermore, designers must adhere to manufacturing restrictions specific to the chosen AM technology. Critical overhangs inside channels must be avoided for processes such as laser powder bed fusion by adapting the shape of channel cross-sections. However, such production-related design changes can cause overlaps between different channels and require re-adjusting the channel paths. Consequently, routing several flow channels is often challenging when manually designing parts for AM. This work aims to automate the routing of multiple channels considering the AM overhang restriction. The presented approach models flow channels as virtual cables defined by a chain of particles (connected by line segments) and collision spheres (located at the cable particles). The cable line segments describe the path or centerline of channels, while the cable collision spheres approximate the required space of each channel. The cables are initialized as straight lines between the channel inlets and outlets and iteratively subjected to geometric-based constraints, e.g., to minimize the cables' length and smoothen their paths. The collision spheres are used to detect overlaps between channels for different flows and repel the affected cables from each other. The radii of the collision spheres are iteratively updated to consider the adaption of cross-sections for AM. After the iterative cable simulation convergences, the cable paths

are used to generate a detailed 3D part design. A case study applies the approach to a hydraulic manifold fabricated using laser powder bed fusion of stainless steel. The study demonstrates the automated design and production of customized design variants.

6.1 Introduction

Many prior works demonstrate the potential of additive manufacturing (AM) for parts with fluid flow channels [14]. Applications include nozzles, hydraulic manifolds, tooling, heat exchangers, and reactors [10][15][16][18][26][27][28][30][148][149][210][221].

Fig. 56 provides one example of a hydraulic manifold fabricated using laser powder bed fusion (L-PBF) of stainless steel [149]. The use of AM offers many advantages for flow components compared to conventional manufacturing methods such as milling and drilling. The design freedom of AM allows integrating multiple, freeform-shaped channels that guide separate fluid flows with multiple crossings in a single part. AM makes it possible to reduce the mass and size of parts and reduce pressure losses [27][210][221]. Moreover, AM enables the production of individualized parts tailored for customer and application-specific requirements.

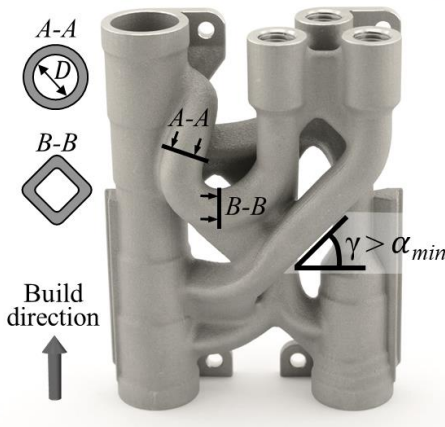


Fig. 56. Hydraulic manifold fabricated using L-PBF of stainless steel [149] (initially redesigned by [26]).

Despite this potential, creating the 3D geometry of complex-shaped parts for AM can be challenging [4][43][55][98][99]. Designers must consider the functional requirements of a part and adhere to manufacturing restrictions that depend on the chosen AM production technology, material, machine, and process parameters [1][3][48][49][50][51]. For example, critical overhangs need to be avoided for processes such as L-PBF. As shown in Fig. 56, the inclination angle γ between the build plate and overhangs should be larger than the minimum build angle α_{min} . Otherwise, support structures must be attached to these overhangs, which often have to be removed during post-processing, leading to additional effort and costs [1][3]. Critical overhangs for internal features such as channels can be prevented by changing circular cross-sections to adapted shapes (e.g., droplet, diamond). The adaption of a circular cross-section is required if it is oriented horizontally to the build plate and its diameter D exceeds D_{max} . The threshold D_{max} marks the maximum diameter of horizontal circular channels that can be fabricated as self-supporting geometries without supports.

It requires advanced skills with computer-aided design (CAD) tools to create organic-shaped part geometries and ensure their manufacturability for AM, which can demand multiple manual loops for analyzing and modifying CAD features. Therefore, the manual creation of part designs is often a tedious and challenging task, especially for complex parts enabled by AM. However, the availability of a detailed 3D part geometry is the basis for fabricating prototypes and experimental tests [209][210][221] or conducting simulations using computational fluid dynamics (CFD) and finite element analysis (FEA) [26][188][190][191][222]. Therefore, the automated creation of part designs for AM is seen as a promising approach [4][43][55][98][99] to lowering the barrier for novice designers and allowing CAD users to explore an increased number of design variants, make quick design changes during the iterative development of parts, and tailor part designs to custom requirements.

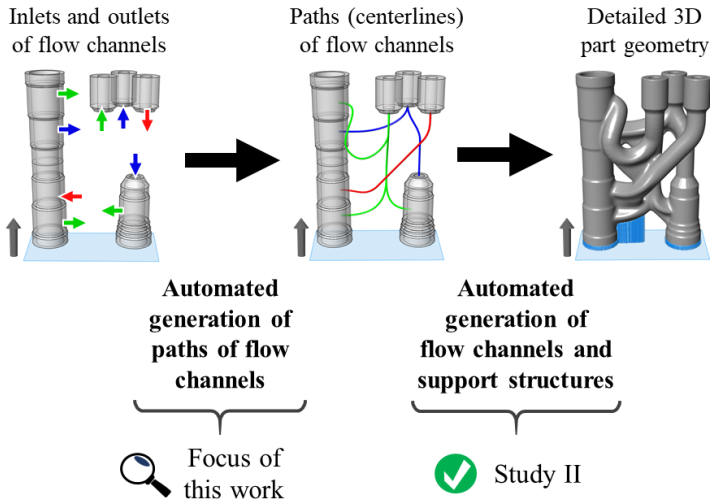


Fig. 57. Process chain for automated design generation of hydraulic manifolds.

Study II [149] in Chapter 5 presents CAD procedures that automatically create the 3D geometry of flow channels considering the AM overhang constraint, as shown in Fig. 57. The procedures also generate integrated supports and sacrificial supports for critical overhangs at outer channel surfaces. The output is a detailed and production-ready 3D part geometry. Different colors distinguish paths that represent channels for separate fluid flows. Study II assumes that CAD users manually define the paths (meaning the centerlines) of the flow channels along with other user inputs (e.g., channel diameter D , wall thickness t , build direction, α_{min} and D_{max}). Based on these inputs, the procedures generate the channels and automatically modify circular cross-sections to adapted shapes along the channel path where the AM overhang restriction is violated.

In contrast to Study II [149], this work aims to avoid the manual definition of flow channel paths. As depicted in Fig. 57, the basic idea is that CAD users just specify the position and normal vectors of inlets and outlets of flow channels along with other inputs (e.g., connectivity between inlets and outlets, channel dimensions, build direction, α_{min} and

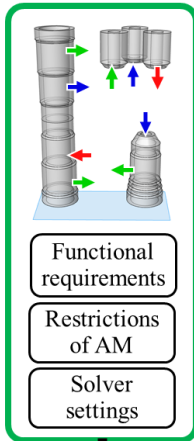
D_{max}). Given these inputs, this work aims to automatically create the channel paths to further advance the workflow and achieve a higher level of automation in the design process.

Automating the design and routing of multiple flow channels for AM parts is challenging for several reasons. It is necessary to consider functional requirements such as reducing pressure losses by minimizing the length of channel paths, avoiding sharp bends, and aligning the paths to the normal vectors at the inlets and outlets. In addition, different channels for separate fluid flows are never allowed to intersect. This requirement can be challenging to meet, especially for complex-shaped flow components that integrate many intertwined and branched channels with multiple crossings in a densely packed part. Besides functional requirements, it is also necessary to consider manufacturing restrictions for AM. The AM overhang restriction can demand adapting the shape of channel cross-sections as described above. However, such production-related design changes can cause new overlaps between different channels and require several re-adjustments of the channel paths.

Current literature offers different techniques to automate the design and routing of flow channels. One approach is fluid-based topology optimization (TO) [73][223]. Several studies use TO to generate optimized flow structures under the AM overhang restriction [74][129][224]. However, most works on TO consider only one or two fluid flows [77]. Another potential approach is to use common path search algorithms to find the shortest path between points [225][226], but such algorithms only find the shortest path between two points. Yet another approach is to re-use algorithms applied to route wires, cables, and pipes [227][228][229][230][231][232][233][234][235][236][237][238]. However, they are mainly developed for other fields (e.g., aircraft, vehicles) and do not consider the AM overhang restriction.

This work addresses this research gap and presents a computational approach to automatically create the paths of multiple flow channels guiding separate fluid flows while considering the AM overhang restriction. Fig. 58 provides an overview of this work.

User inputs (Sec. 6.2.1)



Output

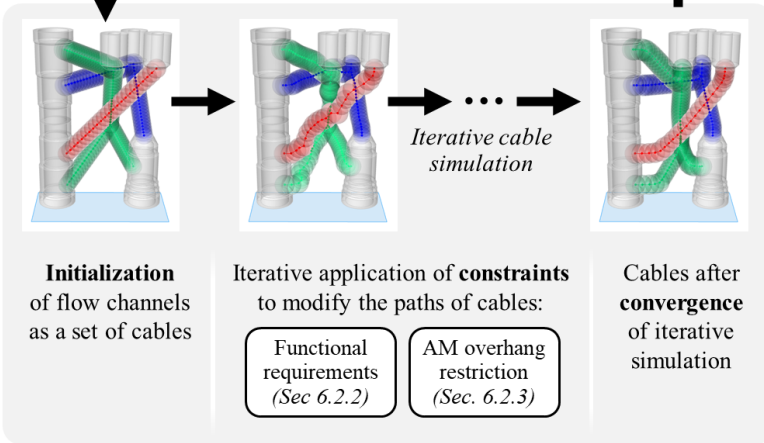
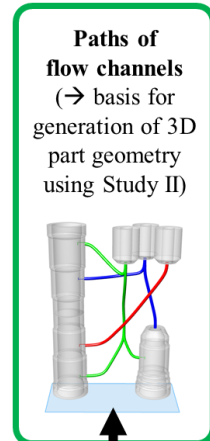


Fig. 58. Overview of approach showing automated generation of flow channel paths.

The main user inputs (see Sec. 6.2.1) include functional requirements (e.g., inlets, outlets, connectivity), restrictions for AM (e.g., build direction, α_{min} and D_{max}), and solver settings. Based on the inputs, the flow channels are represented and initialized as virtual cables. In the initialization step, the cables are created as straight lines between the

inlets and outlets based on the user-defined connectivity. The cables consist of particles connected by line segments and collision spheres located at the particle positions. The line segments approximate the paths (centerlines) of the flow channel. The cable collision spheres approximate the required space of each flow channel and are used to detect and correct overlaps between channels for separate fluid flows.

The different cables are created as straight lines and overlap after the initialization step. Therefore, the cables are iteratively subjected to a set of constraints. These constraints are computed based on geometric calculations and enforce different geometric properties on the cable paths by modifying the position of the cable particles. The constraints minimize the cables' length, smoothen their paths, and align the paths to the normal vectors of inlets and outlets (see Sec. 6.2.2). The constraints also avoid intersections between cables of different colors by checking overlaps between collision spheres and repelling the cables of different fluid flows away from each other. The adaption of channel cross-sections for AM is considered by iteratively updating the radius of each collision sphere depending on the AM restrictions and the local inclination of each cable line segment to the build plane (see Sec. 6.2.3). After the convergence of this iterative cable simulation, the cable paths are extracted and used to generate the corresponding flow channels and detailed 3D part geometry, as shown in Fig. 57.

The work demonstrates the application of this automated design approach using the hydraulic manifold in Fig. 56 as a benchmark example (see Sec. 6.3). The case study assumes that a company offers customers the possibility to individualize the hydraulic manifold for custom specifications. The presented approach is used to automatically create a detailed 3D part geometry of the hydraulic manifold for twelve individual specifications of potential customers. For each custom design variant, the approach automatically solves the routing of multiple crossing flow channels and considers the overhang restriction for L-PBF of stainless steel. The manufacturability of the generated designs is shown by fabricating two design variants as prototypes.

Eventually, the work discusses the benefits and limitations of the presented approach (see Sec. 6.4). Finally, the work finishes with a summary and conclusion (see Sec. 6.5).

6.2 Computational design methods

6.2.1 Overview of iterative cable simulation

6.2.1.1 User inputs and terminology

CAD users need to define various inputs before starting the automated design workflow. These inputs are shown in Fig. 59.

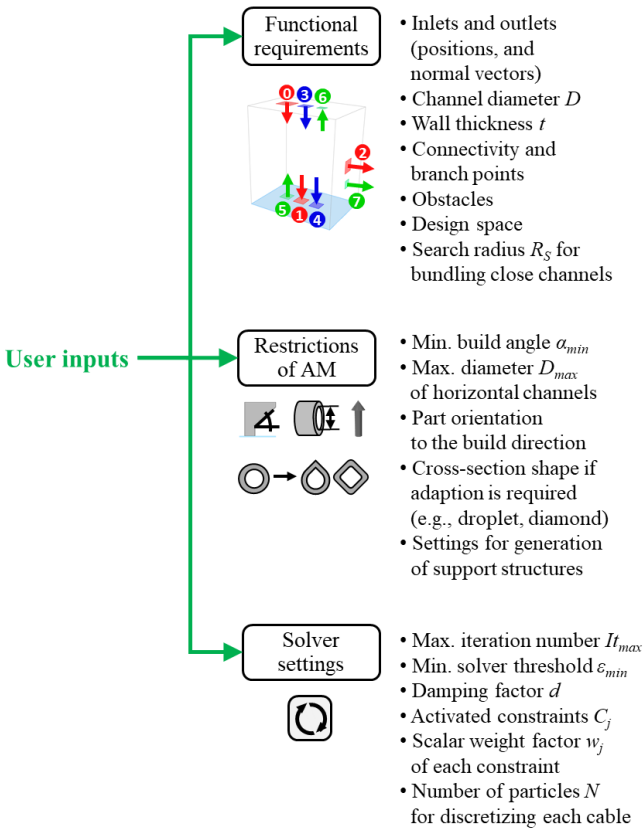


Fig. 59. Overview of user inputs, including functional requirements, AM restrictions, and solver settings.

The first group of user inputs focuses on functional requirements. Users specify the inlets and outlets of all flow channels. At each inlet and outlet, users define the position, normal vector, channel diameter D , and channel wall thickness t . Inlets and outlets are automatically assigned numbers. Based on the numbering, users specify the connectivity between the inlets and outlets, defining how these boundaries need to be connected using channels (e.g., connect inlet ‘0’ with outlet ‘1’). In this work, it is assumed that the connectivity of channels is given by the functional requirements of the part (e.g., 2D hydraulic circuit diagram). If required, users can further modify the connectivity of channels by defining additional branch points between the inlets and outlets. Other user inputs include the geometry of the design space and potential obstacles. The design space defines the allowable space in which the channels can be routed. Obstacles mark geometries that cannot intersect or overlap with the channels. One common goal in designing flow components is to achieve a compact part design and package flow channels densely. For this purpose, users can define a search radius R_S that is used to identify proximate channels and bundle the channels (see Sec. 6.2.2.7).

The second group of inputs concerns the manufacturing restrictions of AM. The specific restrictions depend on the chosen AM process, material, machine, and parameters [1][3]. Users need to provide the minimum build angle α_{min} and the maximum allowable diameter D_{max} of cross-sections that are horizontally oriented to the build plate. Users can define these values based on prior studies [48][49][50][51]. Another input is the orientation of the part to the build direction. Prior works [109][110] provide guidelines to select the part orientation under the consideration of different factors (e.g., the orientation of functional interfaces, manufacturing costs, or the effect on the part strength). The AM overhang restriction can make it necessary to adjust the circular shape of channel cross-sections (see Sec. 6.2.3.1). Users need to select the desired shape of the adapted channel cross-section (e.g., droplet, diamond, triangle, house). Additional inputs include parameters for the generation of support structures that support critical overhangs at the outer surfaces of channels [149].

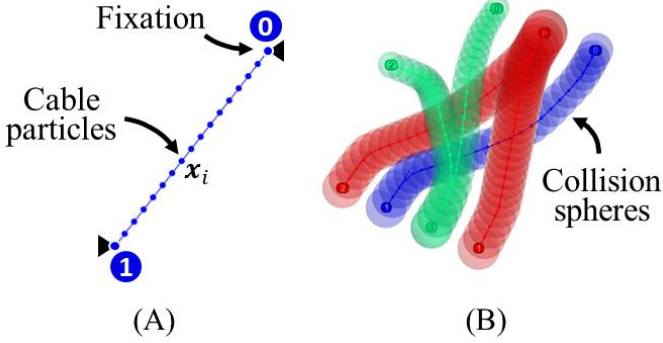


Fig. 60. (A) Cable discretized using particles at positions x_i ; (B) Visualization of cables with collision spheres.

The final group of inputs is related to the settings of the cable simulation. Fig. 60 (A) shows one example of a cable after it is initialized as a straight line between the inlet (0) and outlet (1). The length L^0 marks the initial cable length after the initialization step. The vector x_i defines the location of each particle with index $i = 0 \dots N - 1$. Line segments connect the cable particles and approximate the path of the corresponding flow channel. The number N denotes the number of particles used to discretize the cable and should be chosen high enough to approximate a complex-shaped cable path sufficiently. The parameter N can be specified using

$$N = (4 \cdot L^0 / D) - 1 \quad (\text{Eq. 11})$$

based on the initial cable length L^0 and the channel diameter D . This formula achieves a distance of $D/4$ between the particles of a single cable. (Eq. 11) should be regarded as a rule of thumb, and N may need to be adapted depending on the examined design problem. Based on the user-defined number N , the workflow automatically initializes the cable and places the cable particles at equidistant points along the initial cable path.

As outlined in the introduction (see Sec. 6.1), the cables are iteratively subjected to a set of constraints C_j with index $j = 0 \dots m$. The constraints compute geometric-based calculations and enforce different properties on

the paths by modifying the position of the cable particles (e.g., tangency to normal vectors, bending angle between consecutive cable segments, preventing cables overlap). Users specify a scalar weight w_j to activate each constraint C_j and define its importance relative to the other constraints. Users also define other solver settings, including the maximum number of iterations It_{max} , a minimum solver threshold ϵ_{min} , and a damping factor d to dampen the movement and adjustment of the cable particles during the iterative cable simulation (see Sec. 6.2.1.3).

The position of the particles at the inlet and outlet is fixed, as indicated by the triangles. The remaining particles can freely change their position x_i due to the influence of the constraints C_j . Fig. 60 (B) depicts the cable with collision spheres attached to each particle. The collision spheres with radii R_i are used to detect and correct potential overlaps between the different cables or between cables and the design space and any obstacles.

6.2.1.2 User interface and interaction

The workflow is implemented using the CAD software *Rhinoceros*®. Users define the inputs through the integrated user interface *Grasshopper*®, as shown in Fig. 61 (A). One advantage of *Grasshopper* is its graphical programming interface that is accessible to users without advanced CAD skills. Novice CAD users can define the inputs in a canvas and visually connect them with pre-built workflow modules, as depicted in Fig. 61 (B). The cable objects and constraints are implemented as custom *Grasshopper* modules. Inputs are defined using points, vectors, and number sliders. This work uses the *Kangaroo* plugin developed by Daniel Piker [239][240][241] for conducting the iterative simulation of cables. The 3D cables are visualized in the 3D viewer of *Rhinoceros*.

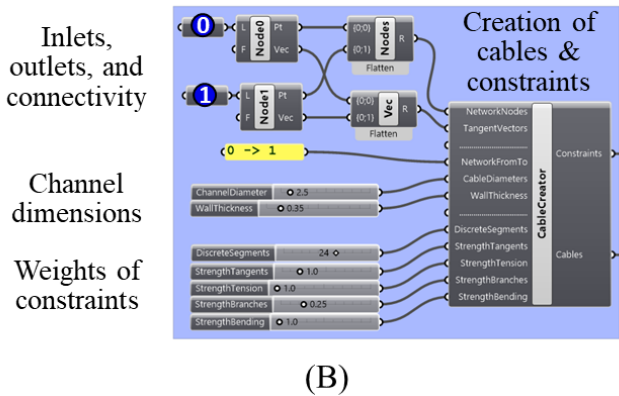
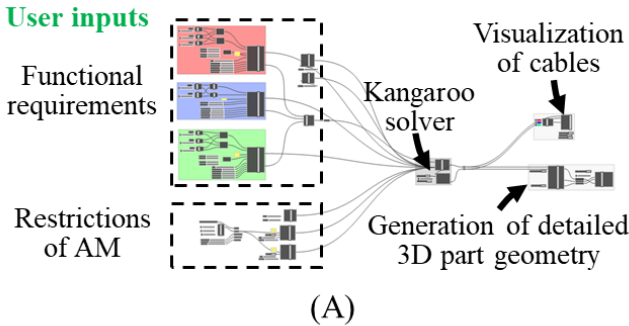


Fig. 61. (A) Definition of inputs using Grasshopper; (B) Detailed view of flow channels (colored in blue).

Fig. 62 illustrates the workflow using an example with two sets of cables colored in red and blue. After defining the user inputs, the workflow starts by initializing cables as straight lines between the inlets and outlets based on the user-defined connectivity and branch points. In this initial state, the cables do not fulfill the constraints. For example, they are not aligned to the normal vectors of the inlets and outlets, and differently colored cables overlap. The iterative application of the constraints C_j leads to the adjustment of the cable paths. During the iterative cable simulation, the radii R_i of the collision spheres are dynamically updated to consider the AM overhang restriction and required adaption of cross-sections (see Sec. 6.2.3.2). The *Kangaroo*

solver allows users to interact with the cables in real-time. Users can pick and drag the cables and change the spatial nesting of the cables. After users release the cables, the *Kangaroo* solver restarts and resolves the constraints based on the modified position of the cables. After the convergence of the cable simulation, the cables' paths are extracted and used to generate the detailed 3D part geometry, including the channels, integrated supports, and sacrificial supports [149].

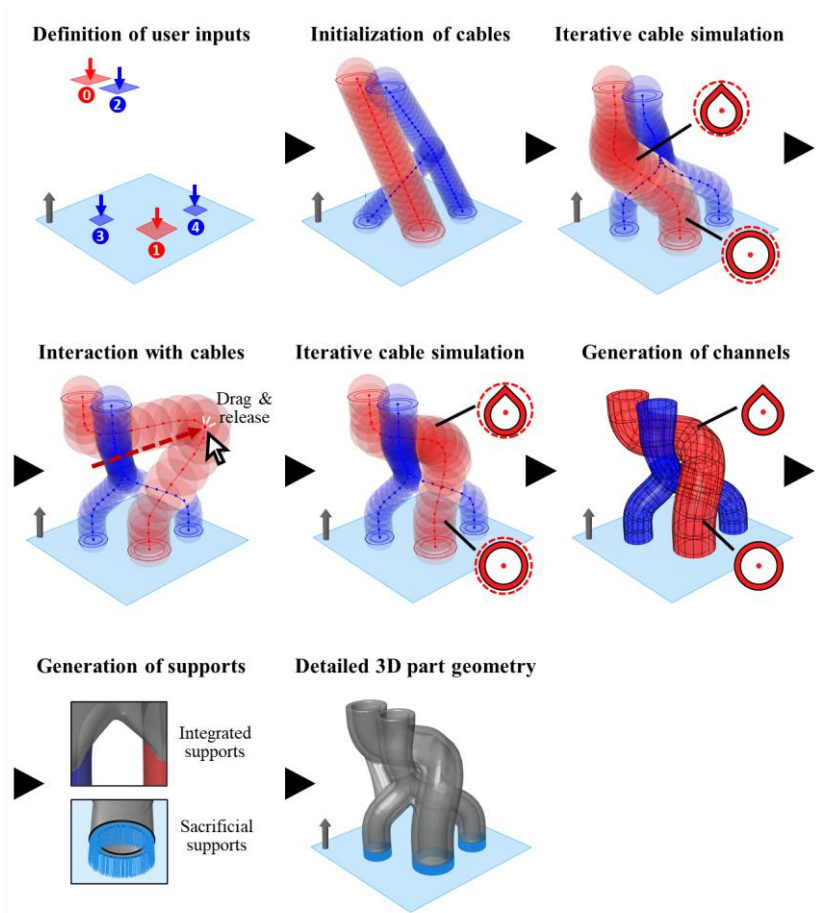


Fig. 62. Main workflow steps showing user interaction with cables and generation of detailed 3D part geometry.

6.2.1.3 Process flow chart of solver

An iterative simulation of cables can be implemented using various methods. In this work, the iterative simulation of cables is implemented based on the paradigm of position-based dynamics (PBD) [242][243][244][245][246][247]. PBD is commonly used for computer animations, game physic engines, and form-finding techniques due to its fast speed, stability, and robustness of the approach, making it highly suitable for interactive, real-time applications.

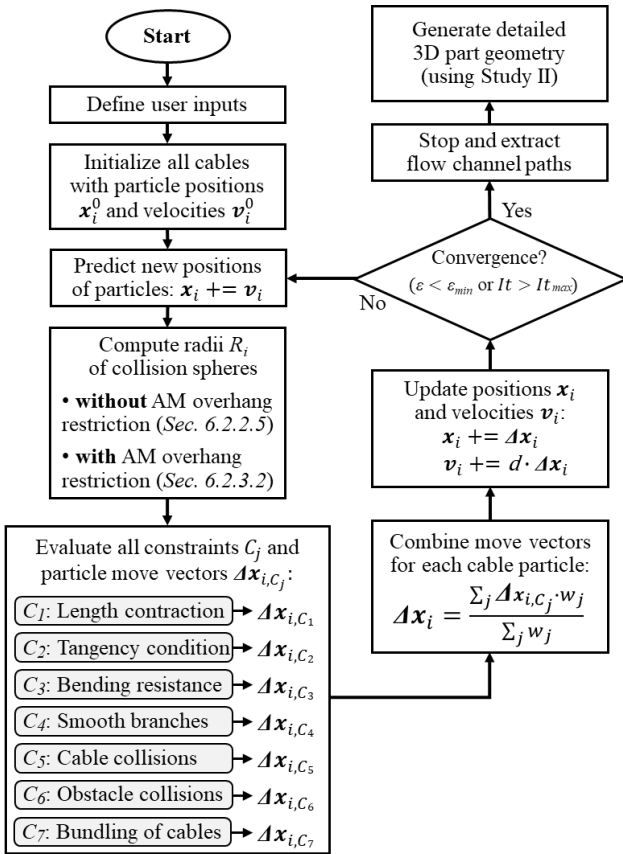


Fig. 63. Flow chart of the iterative cable simulation (modified based on the implementation of DynaShape [248]).

Fig. 63 shows a flow chart for implementing the iterative cable simulation. It is based on the open-source implementation of the tool *DynaShape* by Long Nguyen [248] and is similar to the *Kangaroo* solver.

After defining the user inputs, the process starts by initializing the cable particles with their initial positions \mathbf{x}_i^0 and velocities \mathbf{v}_i^0 . The velocities are zero vectors in the first iteration. In subsequent iterations, the velocities \mathbf{v}_i are non-zero and used to predict the new positions of the cable particles:

$$\mathbf{x}_i += \mathbf{v}_i \quad (\text{Eq. 12})$$

The next step is to calculate the radii R_i of the cable collision spheres. This work presents two approaches for computing the radii R_i either without or with the consideration of the AM overhang restriction and adaption of channel cross-sections (see Secs. 2.2.5 and 2.3.2). Then, the solver evaluates all constraints C_j that are imposed on the cable particles (e.g., length contraction C_1 , tangency to normal vectors C_2 , bending resistance C_3) (see Sec. 6.2.2). The constraints are computed separately. For each particle i , the evaluation of constraint C_j leads to a move vector $\Delta\mathbf{x}_{i,C_j}$ of the particle. These separate move vectors $\Delta\mathbf{x}_{i,C_j}$ are combined into a single vector $\Delta\mathbf{x}_i$ as follows:

$$\Delta\mathbf{x}_i = \left(\sum_j^m \Delta\mathbf{x}_{i,C_j} \cdot w_j \right) / \left(\sum_j^m w_j \right) \quad (\text{Eq. 13})$$

For each particle, the move vectors $\Delta\mathbf{x}_{i,C_j}$ of the constraints C_j are multiplied with the corresponding weights w_j and the expression is divided by the sum of the weights w_j . The weight-averaged move vector $\Delta\mathbf{x}_i$ is used to update the position \mathbf{x}_i and velocity \mathbf{v}_i of each particle:

$$\mathbf{x}_i += \Delta\mathbf{x}_i \quad (\text{Eq. 14})$$

$$\mathbf{v}_i += d \cdot \Delta\mathbf{x}_i \quad (\text{Eq. 15})$$

Before starting the next solver iteration, the solver analyzes two convergence criteria. Firstly, it checks if the iteration number It exceeds

the maximum value It_{max} . Secondly, the solver computes a threshold ε . For the solver of *Kangaroo*, ε is computed as

$$\varepsilon = (\sum_i^{N_{total}} \mathbf{v}_i^2) / N_{total} \quad (\text{Eq. 16})$$

by averaging the squared velocities \mathbf{v}_i of all cable particles using the total number of particles N_{total} . The solver converges if ε falls below the predefined threshold ε_{min} . In this case, the solver converges to a stable state, leading to no further changes in the cable paths. After the convergence of the cable simulation, the process extracts the paths of the cables (and corresponding channels) and generates the 3D part geometry.

6.2.2 Constraints due to functional requirements

6.2.2.1 Length contraction (C_1)

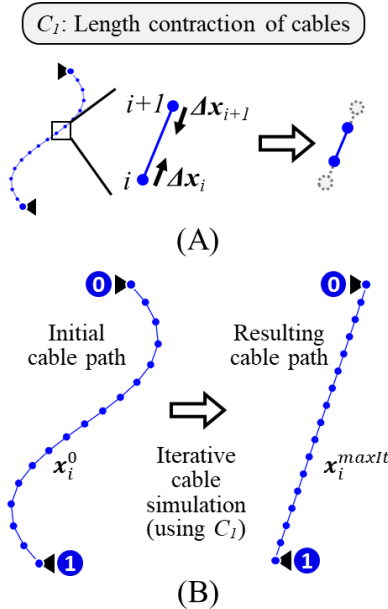


Fig. 64. (A) Discrete cable and constraint C_1 for length contraction; (B) Example to show the effect of C_1 .

The first type of constraint C_1 imposes a length contraction of the cable segments. As depicted in Fig. 64 (A), the constraint pulls the particles of a cable segment with indices i and $i + 1$ towards each other. The attraction of the particles minimizes the length of the segment. Within a single iteration step of the iterative cable simulation, the constraint C_1 imposes the following move vectors $\Delta \mathbf{x}_{i,C_1}$ and $\Delta \mathbf{x}_{i+1,C_1}$ on the two particles of a segment:

$$\Delta \mathbf{x}_{i,C_1} = 0.5 \cdot (\mathbf{x}_{i+1} - \mathbf{x}_i) \quad (\text{Eq. 17})$$

$$\Delta \mathbf{x}_{i+1,C_1} = 0.5 \cdot (\mathbf{x}_i - \mathbf{x}_{i+1}) \quad (\text{Eq. 18})$$

Fig. 64 (B) demonstrates the effect of constraint C_1 using a single cable lying between the inlet (0) and outlet (1). In this sub-section, the initial cable path is initialized as an S-shaped curve to show the effect of the constraint. The cable particles are located at \mathbf{x}_i^0 and the position of the particles is fixed at the inlet and outlet, as indicated by the triangles. Length contraction constraints C_1 are defined for each cable segment, resulting in $N - 1$ constraints.

The constraints are iteratively applied to the particles changing their positions \mathbf{x}_i based on the move vectors. This iterative process reduces the length of each segment and thereby shortens the overall cable length. The resulting cable with particle positions \mathbf{x}_i^{maxIt} resembles a straight path between the inlet and outlet. Please note that the constraints used for the iterative simulation of the cable are based on purely geometric calculations. However, as an analogy, the simulated cable can be viewed as a pre-tensioned rubber band contracting its length.

6.2.2.2 Tangency condition (C_2)

The second constraint C_2 prescribes a tangency condition to cables. This constraint is useful to align the cables (and the corresponding channels) along the normal vectors of inlets and outlets. As shown in Fig. 65 (A), the constraint makes the cable tangent to a vector \mathbf{T} while maintaining a smooth cable path. The constraint C_2 is implemented by pulling a predefined number of cable particles close to an inlet or outlet

towards fixed points located on the tangent vector. The constraint pulls a cable particle with index i towards the associated tangent point with index k by imposing the following move vector on particle i :

$$\Delta \mathbf{x}_{i,C_2} = \mathbf{x}_k - \mathbf{x}_i \quad (\text{Eq. 19})$$

Fig. 65 (B) illustrates the constraint. In the example, tangency constraints C_2 are enforced on particles located close to the inlet (0) and outlet (1). Also, the cable is subjected to length contraction constraints C_1 . The iterative application of the constraints leads to a length-reduced cable with smooth tangency conditions.

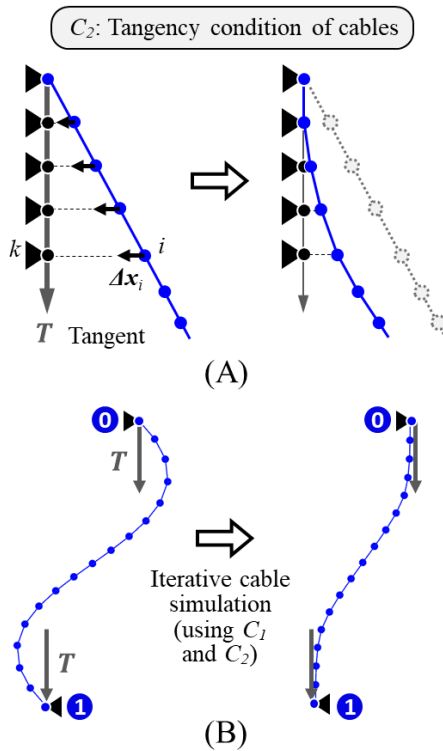


Fig. 65. (A) Constraint C_2 to prescribe tangency conditions on cables; (B) Example to show the effect of C_2 .

6.2.2.3 Bending resistance (C_3)

The third constraint C_3 aims to smoothen the path of cables (and the resulting channels) by modifying the angle between subsequent cable segments. As an analogy, the constraint can be regarded as a cable bending resistance.

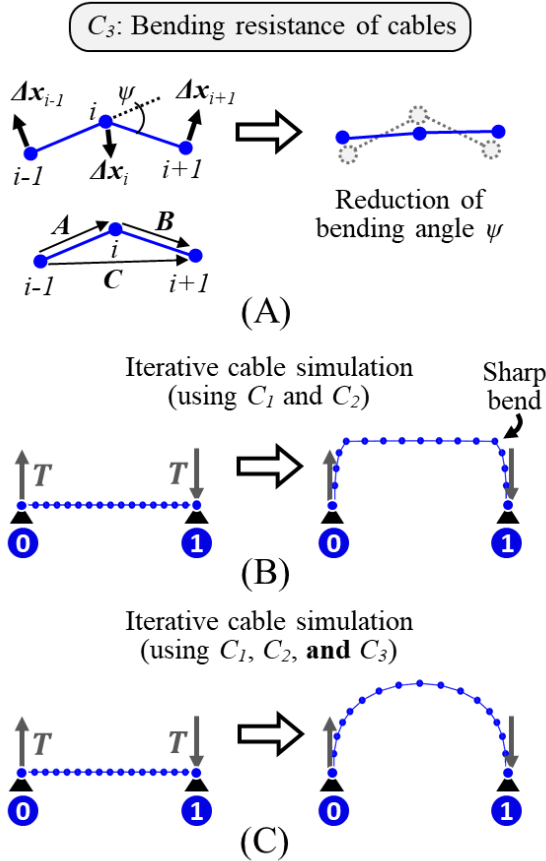


Fig. 66. (A) Constraint C_3 for bending resistance; (B) Example without C_3 ; (C) Example to show the effect of C_3 .

Fig. 66 (A) visualizes the constraint. It shows two subsequent segments defined by particles with indices $i - 1$, i , and $i + 1$. The bending angle ψ marks the angle between the two segments. The vectors \mathbf{A} , \mathbf{B} , and \mathbf{C} denote vectors between the particles and are unitized. The constraint imposes move vectors on the particles such that ψ decreases and sharp bends are avoided along the cable path. Based on prior works [239][249], the move vectors are:

$$\Delta \mathbf{x}_{i-1, C_3} = \frac{2 \cdot \sin \psi}{\|\mathbf{A}\| \cdot \|\mathbf{C}\|} \cdot (\mathbf{A} \times (\mathbf{A} \times \mathbf{B}))_{Unitized} \quad (\text{Eq. 20})$$

$$\Delta \mathbf{x}_{i+1, C_3} = \frac{2 \cdot \sin \psi}{\|\mathbf{B}\| \cdot \|\mathbf{C}\|} \cdot (\mathbf{B} \times (\mathbf{A} \times \mathbf{B}))_{Unitized} \quad (\text{Eq. 21})$$

$$\mathbf{x}_{i, C_3} = -(\Delta \mathbf{x}_{i-1, C_3} + \Delta \mathbf{x}_{i+1, C_3}) \quad (\text{Eq. 22})$$

Fig. 66 (B) and (C) illustrate the effect of constraint C_3 . In Fig. 66 (B), the simulation uses only length contraction constraints C_1 and tangency constraints C_2 . This setup leads to a length-minimized cable tangent to the normal vectors. However, the cable path is not smooth and contains sharp bends. Therefore, bending constraints C_3 are imposed on all segments. Fig. 66 (C) shows that this setup results in a smoother cable path without sharp bends.

6.2.2.4 Smooth branches (C_4)

The fourth constraint C_4 focuses on cable branches. This constraint aims to achieve smooth transitions at cable branches and avoid abrupt changes and sharp bends of the cable paths (and the corresponding flow channels).

Fig. 67 (A) explains the effect of the constraint using a branch with two sub-branches. In the initial state, the sub-branches possess a sharp bend at the branch point. Constraint C_4 smoothens the transition by attracting a predefined number of neighboring particles lying on the cables of the sub-branches. For two sets of neighboring particles with indices i and k , constraint C_4 imposes move vectors as follows:

6 Study III: Automated routing of multiple flow channels

$$\Delta \mathbf{x}_{i,C_4} = 0.5 \cdot (\mathbf{x}_k - \mathbf{x}_i) \quad (\text{Eq. 23})$$

$$\Delta \mathbf{x}_{k,C_4} = 0.5 \cdot (\mathbf{x}_i - \mathbf{x}_k) \quad (\text{Eq. 24})$$

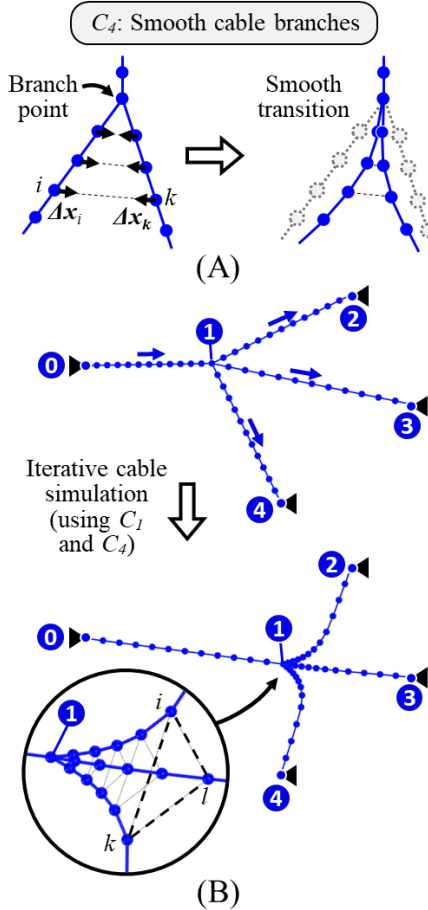


Fig. 67. (A) Constraint C_4 for smooth cable branches; (B) Example to show the effect of C_4 .

As a more complex example, Fig. 67 (B) visualizes a cable network consisting of four cables connected at the branch point (1). The position of the branch point is free to move, whereas the inlet (0) and outlets (2), (3), and (4) are fixed. Constraint C_4 is applied to sets of particles that lie on the sub-branches (in this case, denoted with indices i , k , and l). Also, length contraction constraints C_1 are imposed on all cable segments. The iterative application of all constraints leads to a cable network with a smooth transition between the main branch and the sub-branches. Importantly, a branch point may combine multiple in- and outgoing sub-branches. In this case, the constraint C_4 uses the connectivity of channels to determine sets of sub-branches that are attracted to each other at a branch.

6.2.2.5 Cable collisions (C_5)

The fifth constraint C_5 detects and corrects potential collisions between differently colored cables representing channels for separate fluid flows. Cables of the same color are allowed to overlap, for instance, in the case of multiple sub-branches (see Sec. 6.2.2.4). Fig. 68 (A) depicts the approach for implementing the collision constraint C_5 between different cables. This sub-section does not consider the adaption of cross-sections for AM. The integration of the AM overhang restriction is explained later in the work (see Sec. 6.2.3).

The approach is to assign collision spheres to all particles of a cable. Each particle i possesses a collision sphere with a radius R_i . Suppose a cable represents a flow channel with diameter D and wall thickness t . In this case, the collision radius R_i of each cable particle is defined as:

$$R_i = 0.5 \cdot D + t \quad (\text{Eq. 25})$$

A flow channel can also be specified using a start diameter D_{start} and end diameter D_{end} . In that case, the collision sphere radii R_i of a cable with N particles are interpolated as:

$$R_i = 0.5 \cdot \left(\frac{N-i}{N} D_{start} + \frac{i}{N-1} D_{end} \right) + t \quad (\text{Eq. 26})$$

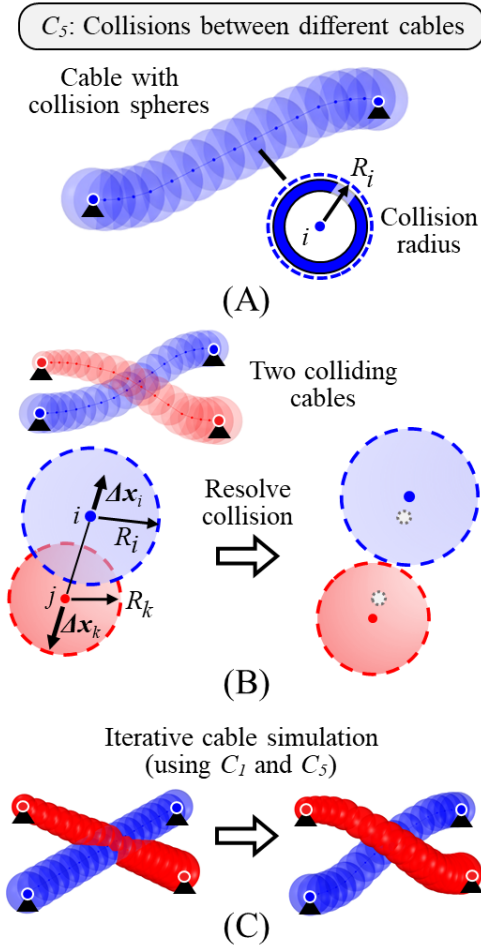


Fig. 68. (A) Cable collision spheres; (B) Constraint C_5 for cable collisions; (C) Example to show the effect of C_5 .

Fig. 68 (B) demonstrates the constraint. It shows two cables colored blue and red. In the initial state, blue and red collision spheres overlap. To resolve an overlap between a pair of a blue collision sphere with index i and a red one with index k , constraint C_5 applies the following move vectors on the particles:

$$\Delta \mathbf{x}_{i,C_5} = 0.5 \cdot \left(1 - \frac{R_i + R_k}{\|\mathbf{x}_i - \mathbf{x}_k\|}\right) \cdot (\mathbf{x}_i - \mathbf{x}_k)_{Unitized} \quad (\text{Eq. 27})$$

$$\Delta \mathbf{x}_{k,C_5} = -\Delta \mathbf{x}_{i,C_5} \quad (\text{Eq. 28})$$

Fig. 68 (C) shows an example and depicts a blue and red cable in the initial state and after the simulation using collision constraints C_5 and length contraction constraints C_1 . Collision constraints C_5 are activated for all possible colliding pairs of blue and red spheres. During each iteration step, the solver checks all collision pairs and, if necessary, resolves occurring overlaps by moving the affected particles apart from each other.

6.2.2.6 Collisions of cables with obstacles and design space (C_6)

The sixth constraint C_6 resolves collisions and overlaps between obstacles and collision spheres of cables, as illustrated in Fig. 69 (A). The obstacles are fixed in their position and represented by a closed surface mesh. Fig. 69 (B) shows the overlap of the collision sphere with radius R_i of the particle i with an obstacle. In case I, the particle position \mathbf{x}_i is outside the obstacle. The point \mathbf{P}_i denotes the point that lies on the obstacle surface and is closest to the particle position \mathbf{x}_i . The constraint resolves the overlap by applying the following move vector:

$$\Delta \mathbf{x}_{i,C_6} = |R_i - \|\mathbf{x}_i - \mathbf{P}_i\|| \cdot (\mathbf{x}_i - \mathbf{P}_i)_{Unitized} \quad (\text{Eq. 29})$$

If the collision sphere penetrates the obstacle even further, the particle \mathbf{x}_i can lie inside the obstacle. In this case II, the constraint C_6 imposes the move vector as follows:

$$\Delta \mathbf{x}_{i,C_6} = |R_i + \|\mathbf{x}_i - \mathbf{P}_i\|| \cdot (\mathbf{P}_i - \mathbf{x}_i)_{Unitized} \quad (\text{Eq. 30})$$

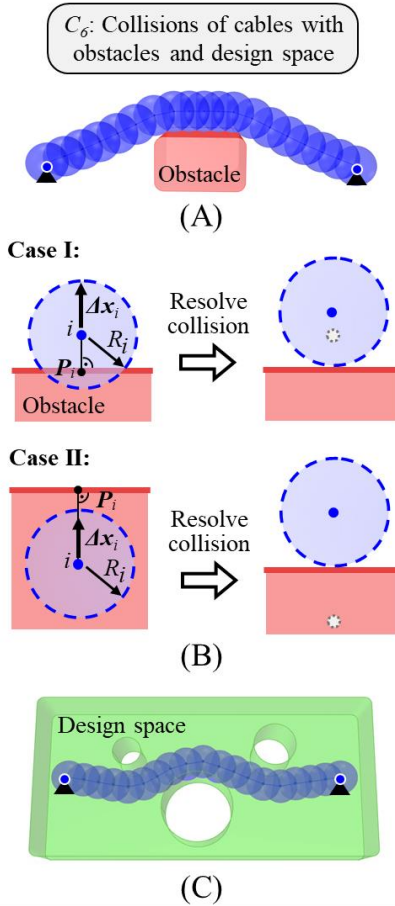


Fig. 69. (A) Constraint C_6 for collisions of cables with obstacles; (B) Overlap between a single particle i with collision sphere radius R_i and an obstacle marked red; (C) Collisions of cable with design space colored green.

The collision constraint C_6 can also be applied to keep a cable inside a closed surface mesh. Fig. 69 (C) shows how a cable is confined in a user-defined design space. For this purpose, Eqs. (19) and (20) are re-used, but the move vectors must be inverted to keep the collision spheres inside the design space.

6.2.2.7 Bundling of cables (C_7)

Constraint C_7 focuses on bundling channels in close proximity. This constraint aims to avoid larger gaps between adjacent flow channels, as depicted in Fig. 70 (A). Such gaps between channels result in unused space and increase the bounding volume occupied by an AM part. As shown in Fig. 70 (B), the goal is to bundle channels to achieve a dense and space-efficient nesting of channels and increase the part's structural integrity. However, the bundling of channels also increases their length. Therefore, constraint C_7 can be activated by users as an optional constraint.

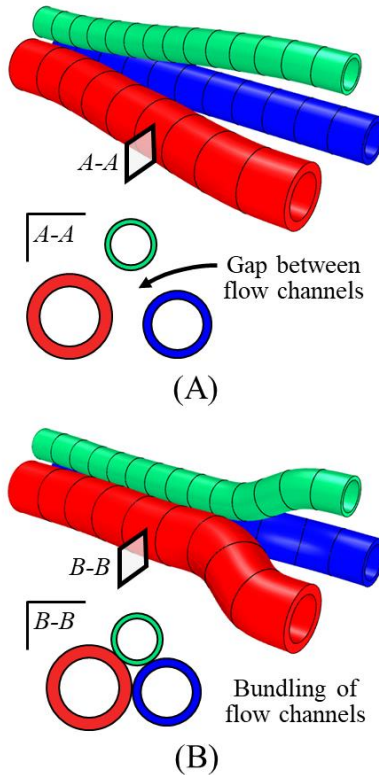


Fig. 70. (A) Gap between flow channels; (B) Bundling of channels to increase the compactness of a part.

Fig. 71 illustrates the basic mechanism of the constraint using two cables colored in blue and red. In each solver iteration, the constraint iterates through all particles of the cables. For each particle, the constraint spans a search sphere using the user-defined radius R_S , as shown in Fig. 71 (A). The procedure identifies particles within the search sphere that belong to other cables. In the example, the blue particle i is associated with three red particles marked with indices $k - 1$, k , $k + 1$. The constraint C_7 imposes the following move vector on particle i :

$$\Delta \mathbf{x}_{i,C_7} = \frac{1}{3} \cdot ((\mathbf{x}_{k-1} - \mathbf{x}_i) + (\mathbf{x}_k - \mathbf{x}_i) + (\mathbf{x}_{k+1} - \mathbf{x}_i)) \quad (\text{Eq. 31})$$

The move vector is constructed by averaging the attraction of the blue particle with index i towards the three red particles with indices $k - 1$, k , $k + 1$. It is important to note that (Eq. 31) depends on the number of particles lying in the search sphere of the examined particle i and can change accordingly through the solver iterations.

Fig. 71 visualizes the effect of constraint C_7 . It is applied to all blue and red cable particles during the simulation and pulls the two cables towards each other. The use of collision constraints C_5 prevents overlaps between the cables. Length contraction constraints C_1 are applied to keep the cables under a minimized length.

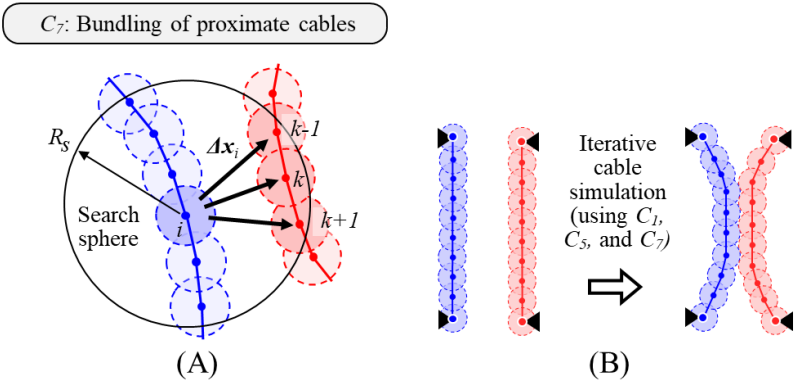


Fig. 71. (A) Constraint C_7 for bundling of proximate channels; (B) Example to show the effect of C_7 .

6.2.3 Consideration of overhang restriction for AM

6.2.3.1 Designing flow channels for AM

Fig. 72 shows basic rules for designing flow channels considering the AM overhang restriction. The diameter D marks the diameter of the channel. The angle γ denotes the inclination angle of the channel to the build plate. The angle α_{min} defines the minimum build angle of geometric features that can be fabricated without additional supports. The diameter D_{max} corresponds to the maximum diameter of circular cross-sections that are horizontally oriented to the build plate and can be produced without additional supports or an adaptation of the circular cross-section shape (e.g., droplet shape).

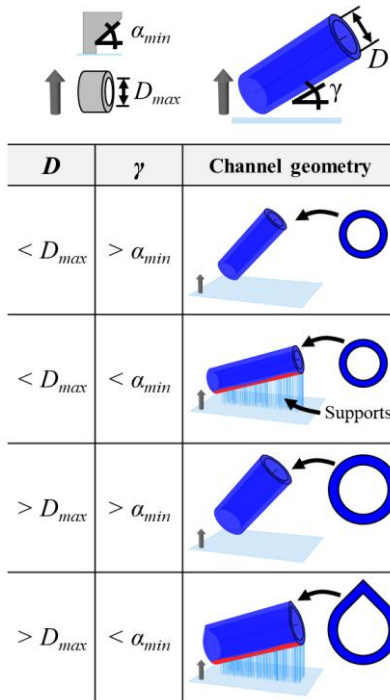


Fig. 72. Design of flow channels considering the AM overhang restriction.

If $D < D_{max}$, the channel cross-section can remain circular and does not need to be adapted. However, it is crucial to also analyze the channel inclination γ to the build plate. Depending on γ , critical overhangs can occur at the outer channel surface and need to be supported using additional supports. This is true if $D < D_{max}$ and $\gamma < \alpha_{min}$.

If $D > D_{max}$, it can be necessary to modify the circular cross-section to an adapted shape (e.g., droplet, diamond) to prevent critical overhangs inside the channel. The decision depends on the channel inclination γ to the build plate. If $\gamma > \alpha_{min}$, the channel can be produced as a self-supporting, circular-shaped channel without additional support. However, if $\gamma < \alpha_{min}$, it is necessary to adapt the cross-section and use additional supports to support critical overhangs at the outer channel surface.

6.2.3.2 Consideration of cross-section adaption

As outlined above, it can be necessary to change the shape of circular cross-sections to avoid critical overhangs inside channels. A circular cross-section needs to be adapted if the following two conditions are met: $D > D_{max}$ and $\gamma < \alpha_{min}$. This sub-section focuses on this aspect and describes how the radii R_i of the cable collision spheres are dynamically updated during the cable simulation to consider the adaption of channel cross-sections for AM.

Fig. 73 depicts a flow chart that outlines the computation of the radii R_i of the cable collision spheres. This procedure is executed in each solver iteration before evaluating the constraints C_j and calculating the move vectors $\Delta \mathbf{x}_i$ (see Fig. 63). In a particular solver iteration, the procedure begins by loading the current path of a cable, which is defined by a chain of particles connected by line segments. Furthermore, the procedure loads the diameter D and wall thickness t of the channel corresponding to the examined cable. Other inputs related to the AM overhang restriction (e.g., build direction, α_{min} , D_{max}) are given based on the user inputs.

In the next step, the procedure compares D with the threshold D_{max} . If $D < D_{max}$, all cross-sections along the channel path can remain circular and do not have to be adapted. In this case I, the procedure uses regular cable collision spheres with radii R_i that are computed based on D and t using Eqs. (9) and (10) (see Sec. 6.2.2.5).

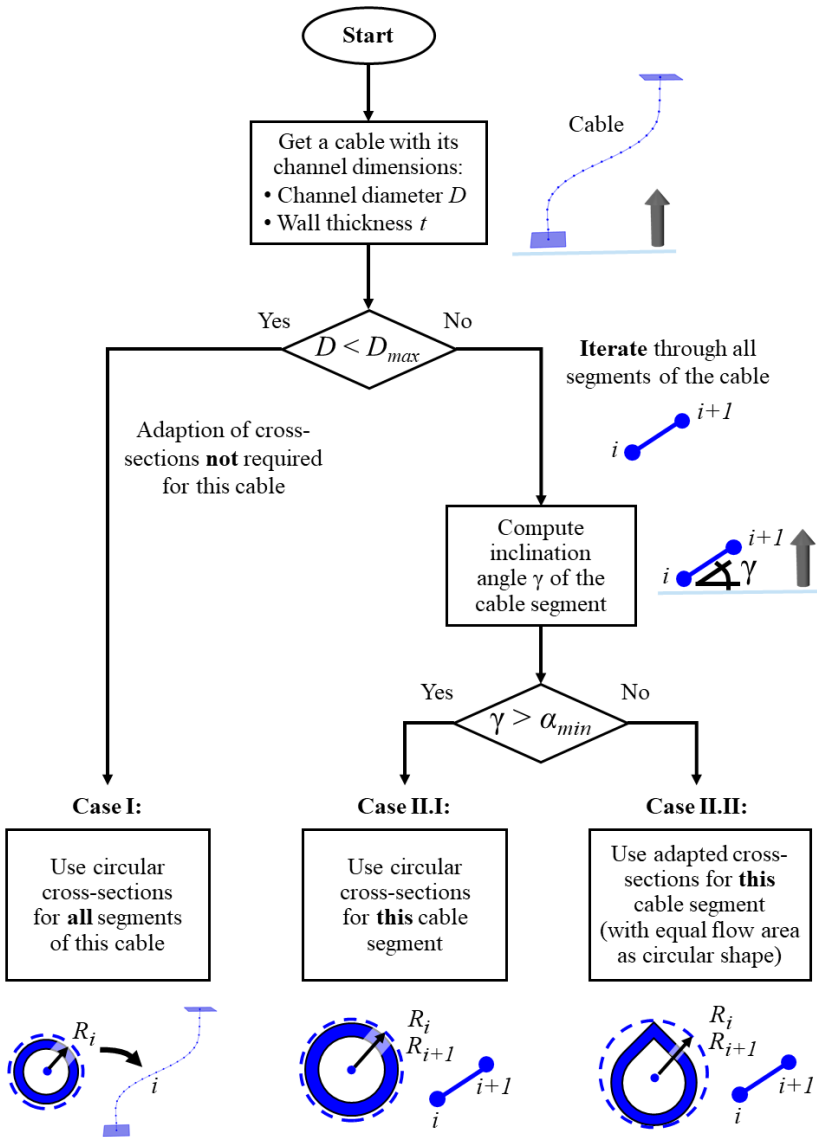


Fig. 73. Flow chart for computing radii R_i of collision spheres considering cross-section adaption for AM.

If $D > D_{max}$, it can be necessary to use adapted cross-section shapes to avoid critical overhangs inside the channel. The decision depends on the local inclination γ of the cable path to the build plate. For this purpose, the procedure iterates through all segments of the cable. For each cable segment, denoted by indices i and $i + 1$, the procedure computes the inclination γ of the examined cable segment to the build plate.

If the segment inclination γ is larger than α_{min} , it is possible to apply circular cross-sections at this segment of the cable path. In this case II.I, the procedure assigns the segment particles i and $i + 1$ regular collision spheres with radii R_i and R_{i+1} using circular cross-sections based on D and t (see Sec. 6.2.2.5).

However, if the segment inclination γ is below α_{min} , it is necessary to adapt the cross-sections at this segment of the cable path to avoid critical overhangs inside the channel.

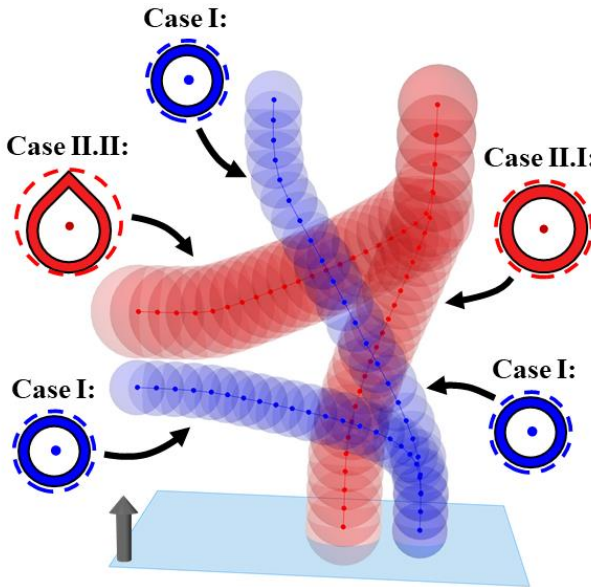


Fig. 74. Example with two cables (with $D_{red} > D_{max}$ and $D_{blue} < D_{max}$) visualizing how cable collision spheres are updated during the iterative cable simulation to consider the adaptation of channel cross-sections for AM.

Therefore, in this case II.II, the procedure generates the user-defined adapted cross-section shape (e.g., droplet) with the same cross-sectional area as a circular cross-section with a diameter D . The procedure creates a bounding circle around the adapted cross-section (including the flow area and channel wall). Based on the bounding circle, the procedure determines the required radii R_i and R_{i+1} of the collision spheres, which are used for the two segment particles i and $i + 1$.

As an example, Fig. 74 shows two cables. The red cable corresponds to a channel with a diameter $D_{red} > D_{max}$. The blue cable represents a channel with $D_{blue} < D_{max}$. The cable collision spheres are dynamically computed and updated to consider the adaptation of channel cross-sections for AM. The different cases (I, II.I, and II.II) are marked accordingly at different positions of the cables.

6.3 Case study

This case study demonstrates the presented approach using the hydraulic manifold introduced in Fig. 56 as a benchmark example. The study assumes that a company wants to offer the hydraulic manifold as a customized part to customers. Customers can choose a design configuration that defines the basic layout of the valves and connectors of the hydraulic manifold. As an example, Fig. 75 shows three possible design configurations. More configurations are possible but omitted in the scope of this study. Based on the chosen design configuration, customers can further customize the part by modifying the position and orientation of the valves and connectors. Customers may choose a custom design variant based on several criteria. For example, customers may prefer a particular design variant that allows access to the connectors and valves from a single side, thus simplifying the installation of the part. The size and shape of the installation space may also limit the part's dimensions and lead to the decision in favor of a design variant. Other possible criteria are the total length L of the flow channels [27] as an indicator for pressure losses, the build height H as an indicator for the build time and manufacturing costs [87], or a reduced part mass m_p , which can be advantageous for mobile applications [28].

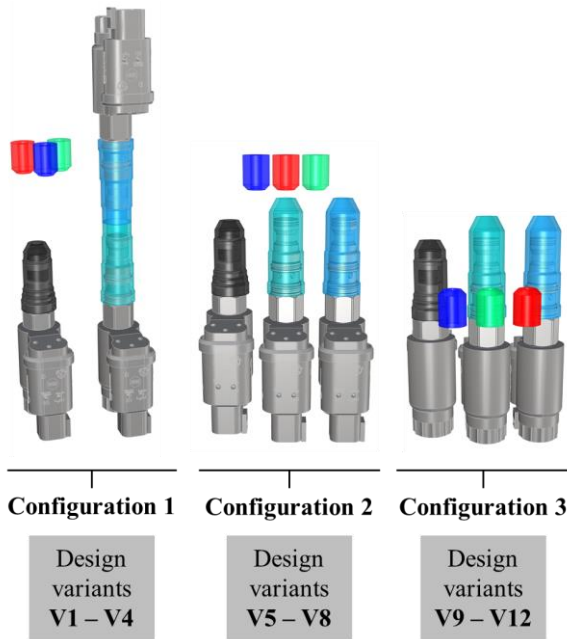


Fig. 75. Three possible design configurations of the hydraulic manifold.

Using a manual CAD process would require an increased manual effort to create a detailed part geometry of the hydraulic manifold for individual customer specifications. For each custom design variant, it would be necessary to manually design the paths of multiple interlaced flow channels based on the specific layout of the valves and connectors while considering the AM overhang restriction and potential adaption of channel cross-sections. The case study addresses this challenge by applying the presented approach to automatically route the flow channels and create the part design for custom specifications. The case study aims to demonstrate the functionality of such an automated design approach by generating the detailed 3D part geometry for twelve custom design variants (V1-V12) of the hydraulic manifold. In addition, the study aims to fabricate some design variants to show the manufacturability of the generated part designs.

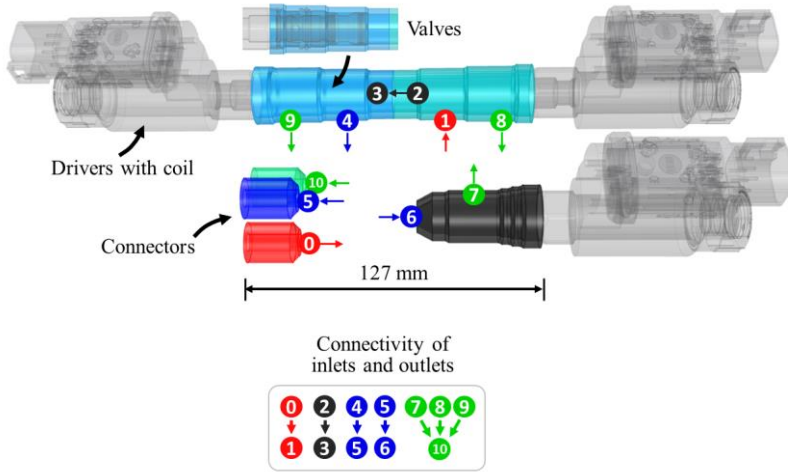


Fig. 76. Boundary conditions of hydraulic manifold (based on [26]).

As a starting point, Fig. 76 depicts the boundary conditions of the hydraulic manifold [26]. Table 5 lists the main parameters and chosen values for this case study. The part consists of three connectors and three valves. The connectors use ISO-M12 threads. The valves have an inner diameter D_{Valves} between 15 and 21 mm and a wall thickness of $t_{Valves} = 3$ mm. The differently colored numbers and arrows mark the positions and normal vectors of the inlets and outlets of flow channels. All flow channels are defined with a diameter of $D = 8$ mm and a wall thickness of $t = 2.5$ mm. The connectivity defines how the inlets and outlets need to be connected using flow channels. The connectivity of channels is the same for all generated design variants (V1-V12).

The hydraulic manifold part shall be fabricated using L-PBF of stainless steel with a density of $\rho = 7.9$ g/cm³. The design restrictions are chosen for this material-process combination based on prior work [49]. The minimum build angle is defined as $\alpha_{min} = 45^\circ$. A value of $D_{max} = 7$ mm is set as the maximum allowable diameter of circular cross-sections with horizontal orientation to the build plate. The specific values for α_{min} and D_{max} are selected to demonstrate the automated design approach. However, these values may be different depending on the chosen AM process, material, machine, and parameters [1][3].

Table 5. Parameters and chosen values for case study

Parameter	Description	Unit	Value
D	Diameter of flow channels	mm	8.0
t	Wall thickness of flow channels	mm	2.5
ρ	Density of material (stainless steel 316L)	g/cm^3	7.9
α_{min}	Minimum build angle	$^\circ$	45.0
D_{max}	Maximum diameter of horizontal cross-sections	mm	7.0
N	Number of particles for discretizing each cable	-	22
d	Damping factor for solver of cable simulation	-	0.95
ε_{min}	Minimum threshold for solver of cable simulation	-	0.0001
w_1	Weight for length contraction (C_1)	-	1.00
w_2	Weight for tangency condition (C_2)	-	1.00
w_3	Weight for bending resistance (C_3)	-	10.00
w_4	Weight for smooth branches (C_4)	-	0.25
w_5	Weight for collisions between cables (C_5)	-	30.00
w_6	Weight for collisions with obstacles (C_6)	-	30.00
w_7	Weight for bundling of cables (C_7) (deactivated in this study)	-	0.00

It may be necessary to adjust circular cross-sections to avoid critical overhangs in the flow channels (see Sec. 2.3.1). In this case study, the setting is defined to use diamond-shaped cross-sections with a fillet radius of $r = 0.5$ mm if it is required to change the shape of circular cross-sections. The distance between the part and build plate is set as 3 mm. The required volume of sacrificial support structures V_f is estimated using block type supports with a volume fraction of 15% [80][212].

A number of parameters must be defined to set up the iterative cable simulation for routing the flow channels. Each flow channel is discretized using a cable with $N = 22$ particles. The damping factor for the solver is specified with $d = 0.95$. The value $\varepsilon_{min} = 0.0001$ serves as a minimum threshold for the convergence of the cable simulation (see (Eq. 16)). The maximum number of solver iterations is tracked for each design variant. The cable simulation considers the adaption of channel cross-section for AM by automatically updating the radii of the cable collision sphere in each solver iteration to consider the required space of the corresponding flow channel (see Sec. 6.2.3.2). Table 5 lists the weights for all constraints. The iterative cable simulation is set up using the constraints (C_1 - C_6). The specific values of the weights were fine-tuned during the development of the design tool and may need to be adjusted for other

cases (see Sec. 6.4.2). The weights of the collision constraints (C_5 and C_6) are chosen with an increased value (compared to the other constraints) to prevent any overlaps between the cables or overlaps between cables and obstacles (e.g., connectors and valves). In this case study, the goal is to demonstrate the fully automated creation of part designs. Therefore, the case study does not make use of the drag and release feature of *Kangaroo* to modify the paths of cables by users (see Sec. 6.2.1.2).

After preparing the workflow, it is applied to generate twelve custom design variants of the hydraulic manifold. Each design variant is created for a custom layout of the connectors and valves and requires a different channel routing. Fig. 77 shows four variants (V1-V4) generated for configuration 1, whereas Fig. 78 depicts four variants (V5-V8) for configuration 2, and Fig. 79 displays four variants (V9-V12) for configuration 3. For each design variant, the workflow uses an iterative cable simulation to create the paths of the flow channels. After generating the paths of the cables, the workflow automatically creates the detailed 3D part geometry of the hydraulic manifold.

Fig. 80 (A) visualizes the progress of the cable simulation for design variant V1. In the first iteration (state I), the initialized cables overlap and do not fulfill the constraints (C_1 - C_6). The solver resolves the overlaps by repelling the cables from each other (state II). The repulsion of the cables leads to an increase in the total length L of the cables. After resolving the overlaps, the cables contract in their length due to the length contraction constraints C_1 . The solver also adapts the cable paths based on the other constraints (e.g., tangency conditions C_2 , bending resistance C_3 , smooth branches C_4) while fulfilling the collision constraints (C_5 and C_6). The solver converges to a stable state with no further changes in the cable paths, which indicates the fulfillment of the imposed constraints (state III). In Fig. 80 (B), the threshold ε is plotted over the iterations. The solver stops and converges if ε (see (Eq. 16)) falls below ε_{min} . In the case of V1, the cable simulation converges after 221 iterations and requires a total time of $t_{cables} = 33.0$ s using a consumer-grade computer (Intel Core i5-7300U CPU @ 2.60 GHz, 8GB of RAM). The computational costs and convergence behavior are similar for all design variants. Table 7 in appendix Sec. 6.7.2 lists the time t_{cables} and the number of iterations. Appendix Sec. 6.7.3 provides the corresponding convergence plots.

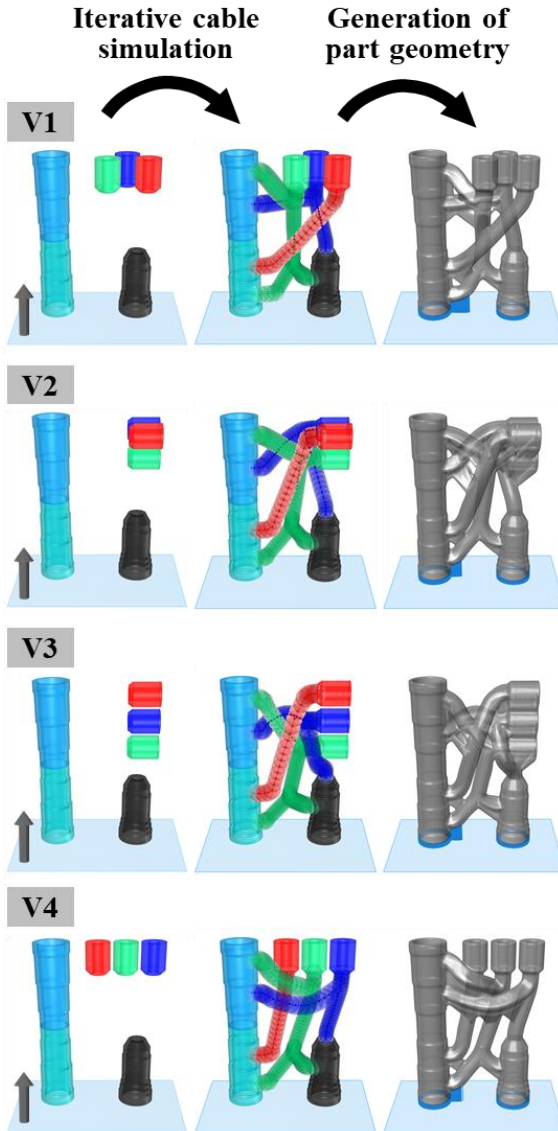


Fig. 77. Automated generation of custom design variants (V1-V4) for configuration I.

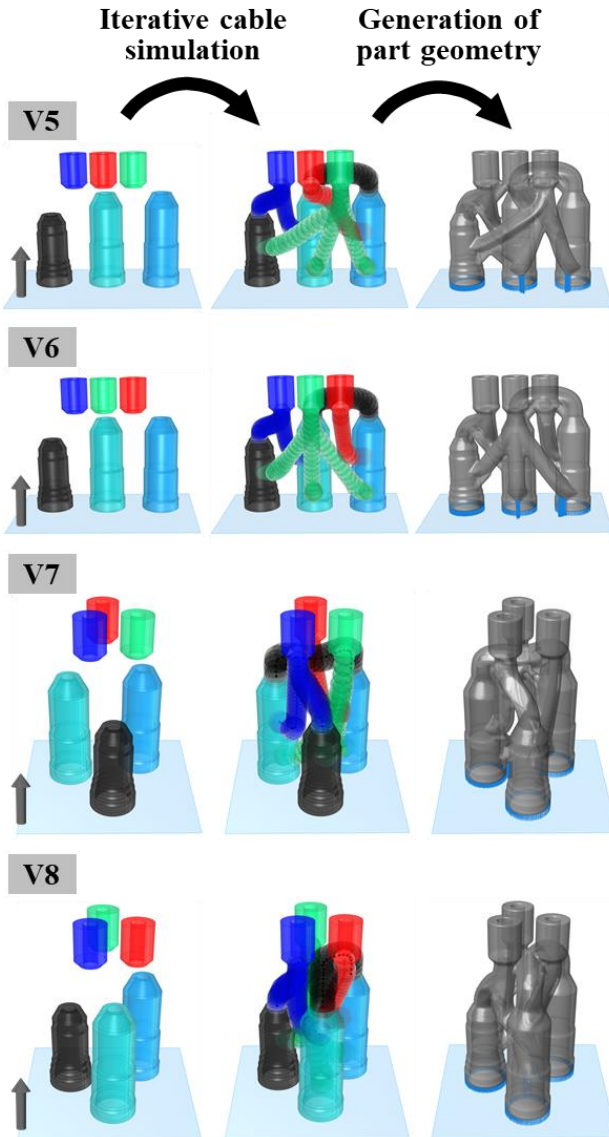


Fig. 78. Automated generation of custom design variants (V5-V8) for configuration 2.

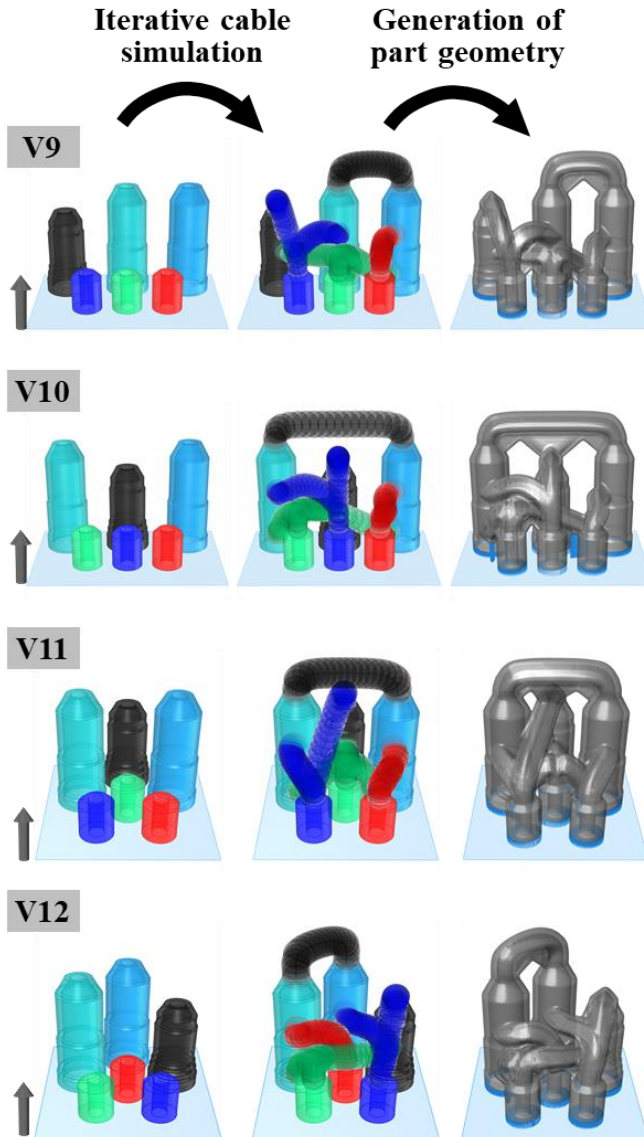


Fig. 79. Automated generation of custom design variants (V9-V12) for configuration 3.

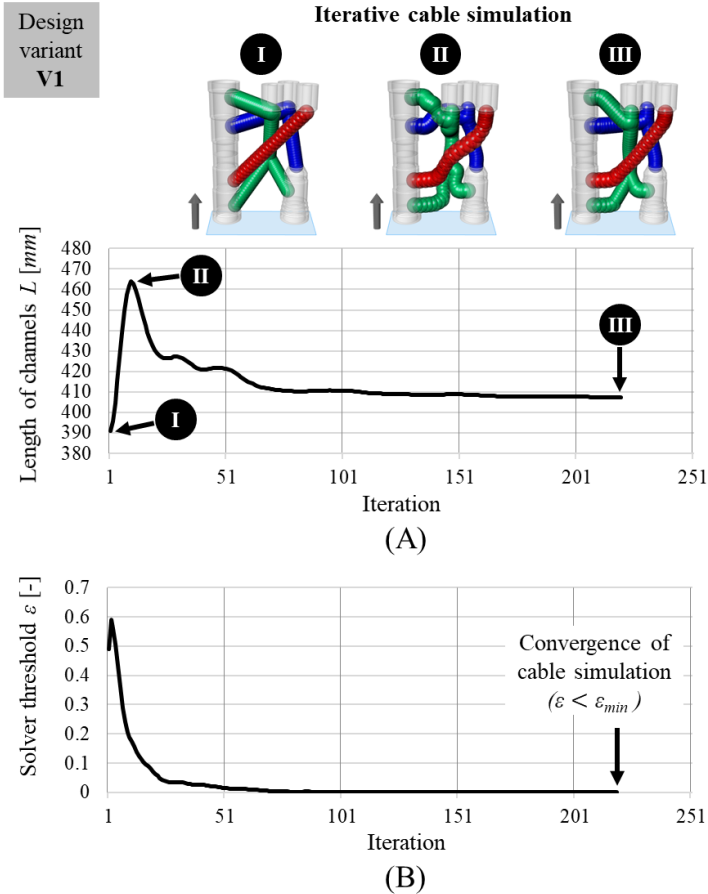


Fig. 80. (A) Cable simulation of design variant V1 showing total length of flow channels L plotted over solver iterations; (B) Solver threshold ε plotted over iterations showing convergence ($\varepsilon < \varepsilon_{min}$) after 221 iterations.

Based on the extracted cable paths, the workflow generates the detailed 3D part geometry of the hydraulic manifold design. This step includes generating the 3D flow channels, integrated supports, and sacrificial supports. For design variant V1, this step takes $t_{Geometry} = 42$ s. Again, Table 7 in appendix Sec. 6.7.2 lists the time

$t_{Geometry}$ for all design variants. The final output is a production-ready 3D geometry of the customized hydraulic manifold.

Table 6 lists quantitative criteria to compare the different design variants. Depending on the chosen design variant, the part requires access from one, two, or three sides to install and access the valves and connectors. The total length L of the flow channels (also known as *Manhattan distance*) [27] is used as an indicator for pressure losses. The table also lists the build height H of the part, its dimensions X and Y , part volume V_P , part mass m_P , and volume of required sacrificial supports V_S . The selected criteria have the advantage that they are based on analytical formulas and can be quickly extracted from the generated 3D part geometries. However, also other criteria may be used to evaluate the design variants. The use of CFD and FEA simulations, for example, is shown in many prior works to compute pressure losses and stress peaks [26][188][190][191][209][210][221][222]. The reader is referred to these works given the limited scope of this case study, which focuses on the automated routing of flow channels.

Table 6. Evaluation criteria for comparison of design variants

Design variant	Access to valves and connectors required from ...	Total length of flow channels L [mm]	Build height of part H [mm]	Part dimensions projected on build plate $X \times Y$ [mm]	Volume of 3D part geometry V_P [mm ³]	Mass of part ($= \rho * V_P$) m_P [g]	Sacrificial support volume V_S [mm ³]
V1	2 sides	404	130	91 x 37	79774	630	735
V2	3 sides	429	130	92 x 38	87454	691	630
V3	3 sides	410	130	92 x 41	84513	668	635
V4	2 sides	427	130	96 x 32	83262	658	620
V5	2 sides	439	101	107 x 44	84740	669	970
V6	2 sides	417	101	107 x 44	80198	634	981
V7	2 sides	462	112	71 x 69	79160	625	825
V8	2 sides	457	112	71 x 69	77061	609	884
V9	1 side	361	90	103 x 50	74681	590	1573
V10	1 side	423	90	103 x 50	82010	648	1603
V11	1 side	345	90	77 x 74	77828	615	1642
V12	1 side	413	90	77 x 74	79824	631	1583

In the following, it is assumed that a customer requires a compact part design. When comparing all design variants, V11 and V12 have the advantage that they possess small part sizes based on their reduced build height H and part dimensions X and Y . The reduced build height H also

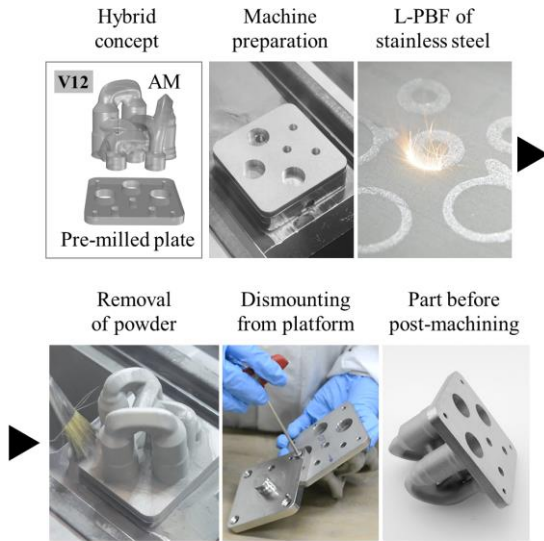
reduces the manufacturing costs for AM. Furthermore, the two design variants allow accessing the connectors and valves from a single side, which is beneficial for post-machining all functional interfaces after AM and installing the part in the application. Variant V11 also offers the advantage of a reduced total length L of the flow channels. Based on these advantages, V11 and V12 are selected for further examination. They are produced as prototypes to show the manufacturability of the generated part designs. However, other design variants may also be chosen for fabrication but are omitted in this case study.

Fig. 81 (A) shows one possible manufacturing route for fabricating V11 and V12 using a hybrid manufacturing concept [250]. A pre-milled plate made of stainless steel serves as a build plate. The 8 mm thick plate contains the hole pattern for the connectors and valves. It is sandblasted and mounted on the build platform. The build job is prepared, and the boreholes are filled with powder. The part is fabricated on the milled plate using L-PBF. After the fabrication process, the unfused powder is removed, and the part is dismantled from the build platform simply by loosening the screws of the milled plate.

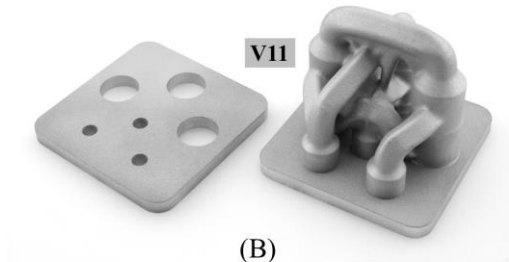
The manufacturing approach avoids using and removing sacrificial supports and thereby reduces costs for post-processing. It also prevents the removal of the part from the build plate using wire electrical discharge machining (EDM), which can increase costs and cause different issues (e.g., increased wire fatigue, release of unfused metallic powder) [26]. As the plate is integrated into the part, it can be used for clamping the part for further post-processing steps. For example, it is necessary to machine threads and interfaces requiring tight tolerances, such as the contact surfaces inside the valves. Also, the plate can serve as an interface for installing the part in the final application.

The manufacturing route is applied to successfully produce the design variants V11 and V12, as shown in Fig. 81 (B) and (C). The pre-milled plate and hole pattern are identical and re-used as a standard part for both variants. The part mass of V11 and V12 is 950 g and 980 g, respectively. For both variants, the plate has a mass of 444 g and takes up a relatively large share of the total part mass (~45-47%). Future studies are expected to reduce the part mass, for example, by reducing the plate wall thickness or removing excess material during post-machining.

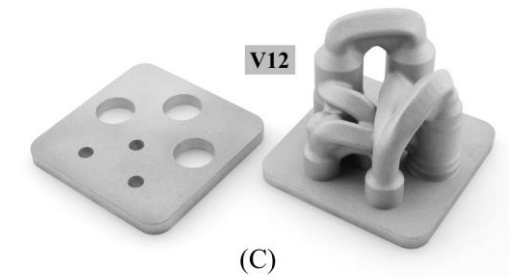
6 Study III: Automated routing of multiple flow channels



(A)



(B)



(C)

Fig. 81. (A) Process chain for fabricating hydraulic manifolds; (B) Prototype of V11; (C) Prototype of V12.

6.4 Discussion

6.4.1 Benefits

The presented approach provides many benefits for developing AM flow components, such as hydraulic manifolds. It automates the collision-free routing of multiple flow channels for separate fluid flows while considering the potential adaption of channel cross-sections to fulfill the AM overhang restriction. Solving this routing problem with a manual CAD approach can be a challenging and tedious design task, especially for novice CAD users. The presented approach enables CAD users to automatically create the paths of flow channels and generate complex part designs for AM that integrate multiple interlaced channels with several crossings in a tightly packed part.

The approach is accessible to novice users without advanced CAD skills. They can simply enter top-level user inputs through the visual interface of *Grasshopper*. Furthermore, users have a high level of control over the generated part geometries as they can prescribe many different inputs (e.g., connectivity between inlets and outlets, shape of adapted cross-sections). Another advantage is that users can interact with the cables in real-time using the drag-and-drop feature of *Kangaroo*. This interaction allows CAD users to quickly modify the spatial arrangement of the cables and the corresponding flow channels.

The case study shows how the approach can be used to automatically create the design of complex AM parts that are tailored for individual customer specifications. The approach generates detailed 3D part designs that do not require further manual editing. The generated 3D part geometries are production-ready and can be directly used for further steps in the development process, for instance, to fabricate and test prototypes or conduct CFD and FEA simulations, as shown in prior works using a simulation-based approach [26][188][190][191][209][210][221][222].

6.4.2 Limitations

While successful, the presented approach does have limitations. Firstly, CAD users still need to consider essential aspects of designing parts for AM. For example, the specified wall thickness of flow channels t should lie above the minimum value allowed by the restrictions of the chosen AM production technology and material. Designers also need to check if the chosen wall thickness of channels mechanically withstands the operating pressure of the fluid, for example, by analyzing the generated 3D part geometry using FEA simulations [26][191][188][222]. Another consideration for AM is the selection of the part orientation to the build plate. The part orientation influences important aspects such as production costs, the required amount of support structures, and the part's mechanical properties [109][110]. Furthermore, designers need to consider the increased surface roughness at the inner walls of flow channels [251] and analyze the part regarding potential defects due to AM [28][219].

The second aspect concerns the accuracy of the approach. The approach employs only a simplified model of flow channels, as channels are abstracted using cable line segments and collision spheres. This simplified representation allows solving the routing of multiple channels at reduced computational costs (see appendix Sec. 6.7.2). However, the approach does not consider the fluid flow inside the channels and only enforces geometric-based constraints on the generated paths of cables (and the corresponding channels). The assumption is that these constraints result in flow channels with smooth paths and minimized length, which is assumed to reduce occurring pressure losses. As a first indicator, users can use the total length of flow channels L for comparing design variants (see case study in Sec. 6.3 and [27]). However, based on the generated 3D part geometry, it is necessary to conduct CFD simulations to analyze the fluid flow in detail and compute pressure losses, as shown in prior works [188][190][191][209][210][221][222].

The third aspect is related to the chosen user inputs. In the case study, the values of the weights w_j of the different constraints are selected based on trials conducted during the development of the design tool. It can be necessary to modify and fine-tune the weights for other case studies.

Future studies should further focus on this aspect and study the influence of the user-defined weights on the generated cable paths. Another limitation is that some settings prescribe certain design features of the generated part geometries. For example, the flow channels are generated based on a library of predefined shapes (e.g., circular, diamond, droplet) [149]. Such predefined settings restrict the design space of possible routing solutions and are a limitation not shared by methods such as fluid-based TO, which can generate optimized flow structures without predefined design features [74][129][224].

6.4.3 Future works

One possible enhancement of the work is further automating the design process of flow components. Future works can let CAD users directly input the 2D hydraulic circuit diagram and automate the selection and placement of modules (e.g., valves, connectors) [252][253]. Another enhancement concerns the initialization of the cables. The approach initializes cables as straight lines between the inlets and outlets. However, such a simple initialization can lead to local optimal routing solutions, especially if many routing solutions are possible and the channels can be arranged in various spatial layouts [231][253]. Future works can initialize cables not as straight lines but define the initial paths using 3D splines constructed by several points. The position of these spline points can be altered to automatically change the initial shape and nesting of cable paths and generate different spatial layouts of the cables. Clustering algorithms may be used to detect and group routing solutions with a similar spatial topology of the cable paths [254]. Future works may also alter the connectivity of channels between inlets and outlets using techniques such as graph grammars [255]. Moreover, future studies may apply different PBD solvers instead of the simple local averaging rule to determine the move vectors of the cable particles [242][243][244][245][246][247].

6.4.4 Practical implications

This work focuses on hydraulic manifolds as an application field. However, the approach may also be utilized for other AM flow components. For example, the approach can be applied to route cooling

channels through injection molds and guide them to critical temperature hot spots [10]. For such applications, it can be necessary to modify the presented constraints or develop new ones based on application-specific requirements. The approach may also be used for AM parts that integrate electrical wires [252]. Such parts can be fabricated using multi-material AM, vacuum casting of conductive materials, or soldering on part surfaces [256][257][258][259]. Again, the presented approach may be applied to route multiple electrical wires without overlaps under a minimized length of wires. A promising research direction is to use the presented approach to simultaneously route flow channels and electrical wires to design multi-functional AM parts that integrate fluidics and electronics.

6.5 Conclusion

AM enables the fabrication of complex-shaped flow components such as hydraulic manifolds. However, the design of multiple crossing flow channels is often a challenging design task for AM [14]. For this purpose, the work presents an approach to automate the routing and design of multiple flow channels considering the AM overhang restriction. The case study illustrates the potential of the presented approach by automatically creating customized hydraulic manifold designs that are generated for individual customer specifications. The discussion highlights the benefits and limitations and describes future research directions for advancing the presented approach further.

6.6 Acknowledgment

The authors would like to thank the reviewers for their feedback and comments. The authors also would like to thank Daniel Piker and Long Nguyen for their contributions in the area of physically-based form-finding and their freely-available design tools *Kangaroo* and *DynaShape*.

6.7 Appendix

6.7.1 Algorithm

Fig. 82 shows the algorithm of one possible implementation of a PBD solver that can be used to implement an iterative cable simulation. The algorithm is modified based on the implementation of the open-source tool *DynaShape* [60]. Please note that prior works also present other implementations of a PBD solver [242][243][244][245][246][247].

Algorithm 1:

```
1: for each Particle  $i$  do
2:    $\mathbf{x}_i = \mathbf{x}_i^0$ 
3:    $\mathbf{v}_i = \mathbf{v}_i^0$ 
4: end
5: for  $It = 0$  to  $It_{max}$ 
6:   for each Particle  $i$  do
7:      $\mathbf{x}_i += \mathbf{v}_i$ 
8:     calculate  $R_i$ 
9:      $\Delta \mathbf{x}_{i,sum} = 0$ 
10:     $w_{i,sum} = 0$ 
11:   end
12:   for each Constraint  $j$  do
13:     for each Particle  $i$  affected by  $C_j$  do
14:       calculate  $\Delta \mathbf{x}_{i,C_j}$ 
15:        $\Delta \mathbf{x}_{i,sum} += \Delta \mathbf{x}_{i,C_j} \cdot w_j$ 
16:        $w_{i,sum} += w_j$ 
17:     end
18:   end
19:   for each Particle  $i$  do
20:      $\Delta \mathbf{x}_i = \Delta \mathbf{x}_{i,sum} / w_{i,sum}$ 
21:      $\mathbf{x}_i += \Delta \mathbf{x}_i$ 
22:      $\mathbf{v}_i += d \cdot \Delta \mathbf{x}_i$ 
23:   end
24:   break if  $\varepsilon < \varepsilon_{min}$ 
25: end
```

Fig. 82. Algorithm modified based on the implementation of the open-source tool *DynaShape* [60].

6.7.2 Computational costs

The case study is conducted using a consumer-grade computer (Intel Core i5-7300U CPU @ 2.60 GHz, 8GB of RAM). Table 7 quantifies the computational costs for generating the design variants. For each design variant (V1-V12), the table lists the time t_{Cables} needed to perform the cable simulation and generate the cable paths. The table also provides the number of iterations until the solver threshold ε falls below the predefined minimum value ε_{min} and converges (see (Eq. 16)). After the cable simulation, the automated design workflow extracts the cable paths and generates the 3D part geometry, which in total requires the time $t_{Geometry}$.

Table 7. Computational costs for design variants

Design variant	Time for convergence of cable simulation t_{Cables} [s]	Number of iterations for convergence of cable simulation	Time for generation of 3D part geometry $t_{Geometry}$ [s]
V1	33.0	221	24.7
V2	34.8	227	38.6
V3	38.0	262	31.5
V4	38.8	271	24.3
V5	30.0	205	41.7
V6	33.0	218	32.9
V7	31.8	207	24.4
V8	27.0	178	23.9
V9	34.0	224	30.3
V10	34.4	231	37.0
V11	36.0	255	40.2
V12	42.3	278	36.3

6.7.3 Convergence plots

Fig. 83, Fig. 84, and Fig. 85 show convergence plots for all design variants (V1-V12) of the case study (see Sec. 6.3). The figures plot the total length of the flow channels L throughout the iterations of the cable simulation.

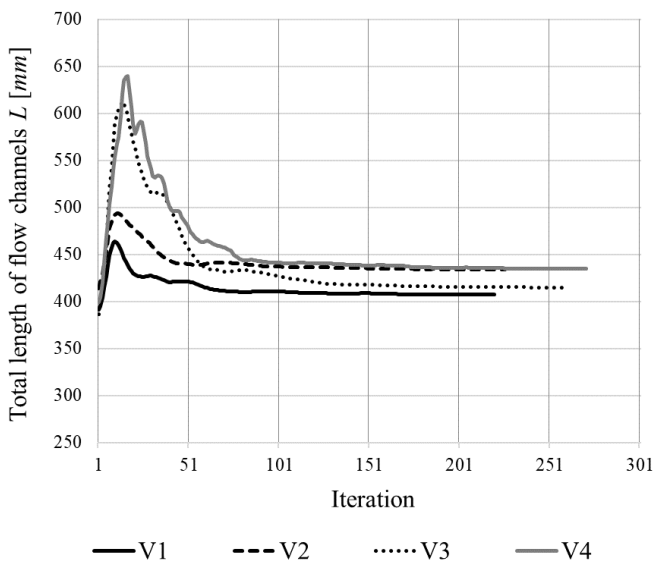


Fig. 83. Convergence plot for design variants V1-V4.

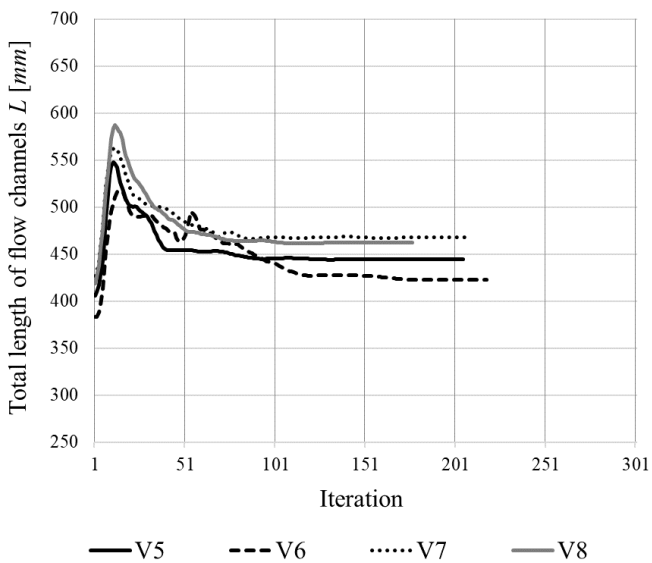


Fig. 84. Convergence plot for design variants V5-V8.

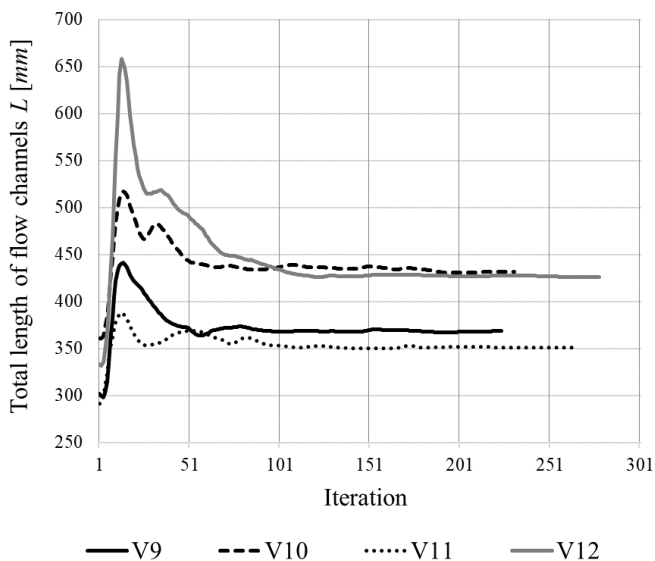


Fig. 85. Convergence plot for design variants V9-V12.

7 Conclusion and outlook

AM offers a large potential for rethinking the design of conventionally manufactured parts. However, in today's practice, the 3D geometry of AM parts is often still created using a manual design process with CAD tools. Such a manual design process can be tedious and time-consuming for expert designers and can be a critical barrier for novice designers to implement AM parts and leverage the potential benefits of AM. This work aims to contribute novel algorithms to automate the design of complex-shaped AM flow components. In particular, this work focuses on multi-flow nozzles and hydraulic manifolds produced using the AM process of L-PBF. This chapter concludes by reflecting on the main findings and providing an outlook for potential future research directions.

7.1 Conclusion

This work focuses on three specific design challenges that are relevant and frequently recurring in the design of AM flow components, such as multi-flow nozzles and hydraulic manifolds. Specifically, this work addresses the following questions:

- **RQ I:** What framework can be used to automatically generate the design of complex AM multi-flow nozzles, considering the creation and nesting of multiple flow channels?
- **RQ II:** What procedures can be used to consider the overhang constraint of AM when generating the geometry of flow channels for AM parts such as hydraulic manifolds?
- **RQ III:** What approach can be used to automate the routing of multiple flow channels guiding separate fluid flows, as required for AM parts such as hydraulic manifolds?

This work presents three studies (I-III) to answer these questions. Table 8 lists the proposed solutions and techniques used in each study.

Table 8. Overview of the studies and the proposed solutions and techniques

Study	Research question (RQ)	Proposed solutions and techniques
Study I	RQ I – What framework can be used to automatically generate the design of complex AM multi-flow nozzles, considering the creation and nesting of multiple flow channels?	<ul style="list-style-type: none"> • Rule- and knowledge-based design approach • Composition of nozzle designs using a set of application-specific design elements (e.g., cross-sections, channels, branches, guiding vanes) • Organization of design elements through a hierarchical architecture for nozzles • Implementation of design elements using object-oriented programming • Optimization of the performance of nozzles using parametric, CFD-driven optimization • Automated detection and exclusion of non-manufacturable design variants
Study II	RQ II – What procedures can be used to consider the overhang constraint of AM when generating the geometry of flow channels for AM parts such as hydraulic manifolds?	<ul style="list-style-type: none"> • Rule- and knowledge-based design approach • Consideration of AM overhang constraint directly in the automated design generation • Generation of flow channels by adapting the shape of cross-sections locally to avoid critical overhangs inside the channels • Generation of integrated and sacrificial supports to support critical overhangs located at the outer walls of flow channels • Generation of detailed features considering the AM overhang constraint (e.g., boreholes, interfaces, ribs, channel branches) • Voxel-based modeling for the computationally efficient generation of complex part designs
Study III	RQ III – What approach can be used to automate the routing of multiple flow channels guiding separate fluid flows, as required for AM parts such as hydraulic manifolds?	<ul style="list-style-type: none"> • Rule- and knowledge-based design approach • Modeling of flow channels as virtual cables defined by a chain of particles (= channel centerline) and collision spheres (= required space of each channel) • Routing of flow channels by iteratively imposing geometric-based constraints on the cables • Enforcement of different constraints to impose functional part requirements (e.g., minimizing the channels' length, preventing overlaps between channels for different flows) • Consideration of the potential adaption of cross-sections for AM by updating the radii of the collision spheres during the routing of channels

Study I automates the design of complex AM multi-flow nozzles. The basic modeling idea is to decompose nozzles into a set of design elements that are used as the basic building blocks of nozzles and include recurring features, such as different cross-section shapes, flow channels, channel branches, guiding vanes, and reinforcement ribs. These design elements are organized using a hierarchical structure. This modeling approach allows to capture the hierarchical nature of complex nozzles and automate the design creation and nesting of multiple flow channels.

Study II focuses on the automated consideration of the AM overhang constraint during the design generation of AM parts, such as hydraulic manifolds. For this purpose, the study models the dependency between geometric parameters (e.g., inclination of flow channel cross-sections) and process-related parameters of AM (e.g., build direction, minimal build angle, and maximum diameter of horizontal cross-sections). Based on these relations, this study demonstrates how to automatically create flow channels without critical overhangs inside the channels by locally modifying the shape of circular cross-sections to adapted shapes (e.g., droplet). In addition, this study shows how to generate integrated and sacrificial supports. The result is a production-ready 3D part design that can be used to fabricate prototypes or conduct simulations.

Study III automates the routing of multiple flow channels for AM flow components, such as hydraulic manifolds. For this purpose, the study models flow channels as virtual cables defined by a chain of particles (= centerline of flow channels) and collision spheres (= required space of each flow channel). These cables are iteratively subjected to geometric-based constraints in order to impose different functional part requirements (e.g., minimizing the length of flow channels and preventing overlaps between different channels). In addition, the adaption of channel cross-sections for AM is taken into account by iteratively updating the radii of the collision spheres during the automated routing of flow channels.

The overall contribution of this work is that it models the specific design and production knowledge required to automate the design of AM flow components, such as multi-flow nozzles and hydraulic manifolds. Based on this knowledge, this work shows the detailed implementation of rule- and knowledge-based design algorithms and demonstrates their benefits using illustrative case studies.

In the following, this section draws the main conclusions by analyzing the results of the studies. In particular, this section reflects on

- using a rule- and knowledge-based approach to automate the design of AM flow components,
- considering restrictions for AM in the automated design of parts (e.g., overhang constraint), and
- utilizing different computational techniques to implement an automated design process for AM parts.

Rule- and knowledge-based approach

All three studies follow a rule- and knowledge-based approach to develop automated design algorithms for AM. The results show that this approach can be successfully applied to automate the design of complex-shaped AM flow components. The approach can be used for automating design tasks, such as creating and nesting multiple flow channels for multi-flow nozzles (see Study I) or generating production-ready 3D part designs of hydraulic manifolds considering the AM overhang constraint (see Study II). In addition, the work shows that the approach can be applied successfully to automate very challenging design tasks. In particular, the simultaneous arrangement of several flow channels remained a challenge for AM parts, as outlined in the research gap described in Sec. 2.5. This work shows that a rule- and knowledge-based approach can be used to solve this design task and automatically route multiple flow channels guiding separate fluid flows (see Study III).

Therefore, one key conclusion of this work is that a rule- and knowledge-based approach can be used to automate the design of complex-shaped AM flow components. However, it is important to be aware of the potential limitations of such an approach (see the detailed discussions in each study). One limitation of all the studies is that the presented algorithms are developed for specific applications, such as multi-flow nozzles and hydraulic manifolds. Therefore, it is necessary to modify these algorithms before they can be used in other applications. Additionally, it is necessary to capture and model further knowledge related to the specific application and chosen AM production technology.

Automated consideration of AM restrictions

The presented studies demonstrate two possible methods to consider the restrictions of AM in an automated design process.

In Study I, algorithms are used to generate the 3D geometry of nozzles. This design generation step can lead to design variants that do not fulfill the restrictions of AM. For this purpose, algorithms are applied to analyze the manufacturability of the generated nozzle designs. In particular, these algorithms check the minimal wall thickness of a part and identify regions with critical overhangs. If a particular design variant of a nozzle does not fulfill these restrictions, it is detected and excluded during a parametric design optimization. Hence, Study I implements the enforcement of restrictions for AM by excluding (or filtering out) non-manufacturable design variants after the design generation step.

In Studies II and III, algorithms consider AM restrictions directly in the design generation step. For example, the algorithms in Study II directly create and modify the shape of cross-sections in the generation of flow channels to avoid critical overhangs inside channels. Similarly, the algorithms in Study III consider the overhang constraint and potential adaption of channel cross-sections in the routing of flow channels. Hence, the algorithms in Studies II and III generate and modify design features to automatically comply with the AM overhang constraint.

In summary, two methods can be used to consider AM restrictions, such as the overhang constraint. Automated design algorithms can either 1) automatically identify and exclude non-manufacturable design variants or 2) automatically create and modify design features for AM directly in the design generation step. The studies show that a rule- and knowledge-based approach enables the implementation of both methods.

Use of different computational design techniques

The presented studies apply different computational design techniques to implement automated design algorithms for AM parts.

For example, Study I uses object-oriented programming to program the basic building blocks and design elements of multi-flow nozzles. These design elements are defined as different classes and objects and are assigned various functions and properties. This object-oriented approach

makes it possible to capture the hierarchical structure of complex AM nozzles that may be composed of several flow channels.

Another technique is voxel-based modeling. Compared to classical CAD kernels, such as solid-based or surface-based modeling, voxels (or 3D pixels) enable the computationally efficient handling of complex geometry operations. For example, Study II applies voxel-based modeling to generate support structures to support critical overhangs located at the outer walls of flow channels. Using voxels makes it possible to generate integrated support structures and computationally efficiently unite them with the flow channels.

The presented studies show that different techniques can be used to evaluate the performance of the generated part designs. Study I uses CFD simulations to evaluate and optimize the performance of the generated nozzle designs. Such a simulation-based approach may lead to increased computational costs for generating a large number of design variants, as required for a parametric design optimization. Therefore, another possible technique is to apply analytical or geometric-based criteria to evaluate and compare different design variants at reduced computational costs. For example, Studies II and III use criteria, such as the mass of parts, total length of flow channels (as an indicator of pressure losses) or build height (as an indicator of AM costs).

Another technique applied in all studies is to use a visual, node-based CAD editor, such as *Grasshopper*. Such a visual user interface enables CAD users to build procedural design workflows by visually creating and combining prebuilt logic blocks and connecting them using wires in a visual canvas. Such a visual editor can help novice designers without CAD knowledge access the developed automated design algorithms and (re-)combine them for specific workflows.

In summary, a key conclusion is that various techniques can be used to implement an automated design approach for AM parts (e.g., visual editor, object-oriented programming, voxel-based modeling, particle systems, parametric optimization, topology optimization). Developers should be aware of these techniques when implementing an automated design process for AM parts. In addition, educators can try to incorporate these different techniques into DFAM courses to make novice designers aware of the possibilities for automating the design of AM parts.

7.2 Outlook

This section outlines potential future research directions. These include transferring the results to different application areas, further simplifying the design process, and using machine learning techniques.

Transfer of results to different applications

The focus of this work is on multi-flow nozzles and hydraulic manifolds. Future works can transfer the presented results to other applications, as shown in Fig. 86. For example, automatically generated multi-flow nozzles can be applied to extrude different materials, such as food products, polymer materials, and hydrogels. In this regard, a recent study by the author and co-authors [260] demonstrates an automated and simulation-based design approach to design AM nozzles used for the co-extrusion of polymer profiles. In addition to nozzles and hydraulic manifolds, the results may also be transferred to other flow components. Possible applications in fluid and process engineering include heat exchangers, static mixers, injection molding molds, reactors, and other devices. Another promising research direction is to extend the presented techniques to domains other than fluidics. For example, multi-material AM offers the possibility of fabricating parts with integrated electrical wires. For such parts, the routing approach presented in Study III can be used to route multiple wires that are integrated into an AM part. In this regard, future works can use the presented routing technique to simultaneously route flow channels and electrical wires to design multi-functional parts that integrate fluidics and electronics.



Multi-flow nozzles for the extrusion of different materials (e.g., food, polymers, hydrogels)



Various devices of **fluidic and process engineering** (e.g., heat exchangers, static mixers, molds, reactors)



Multi-functional AM parts requiring routing of flow channels and electric wires (e.g., robotics, actuators)

Fig. 86. Transfer of results presented in this work to different application areas.

Simplification of user inputs and design process

The presented studies allow CAD users to automatically generate the design of AM parts based on top-level user inputs. For example, in Study III, users just define the inlets and outlets, dimensions, and connectivity of flow channels. In addition, users specify restrictions of AM, such as the build direction and the minimum build angle. Then, design algorithms generate the detailed 3D geometry of the AM parts, such as hydraulic manifolds. Future studies can aim to further advance this automated design process. As shown in Fig. 87, future works can enable CAD users to define even higher-level inputs, such as the 2D circuit diagram of a hydraulic manifold. Algorithms may automatically interpret such a 2D diagram, select the corresponding subcomponents from a feature library, arrange them in a pre-defined 3D design space, perform the routing of flow channels, and generate a 3D detailed part geometry. In doing so, the design algorithms can automatically generate and compare different arrangements of components and optimize their layout based on different constraints and objectives (e.g., maximized packing efficiency and minimized total length of flow channels). Such a workflow makes it possible to raise the level of automation, reduce the manual effort required to define various user inputs, and further simplify the design process, particularly for novice designers. The figure illustrates this approach using an example of a hydraulic manifold. However, a similar process chain can also be used for other AM parts and applications.

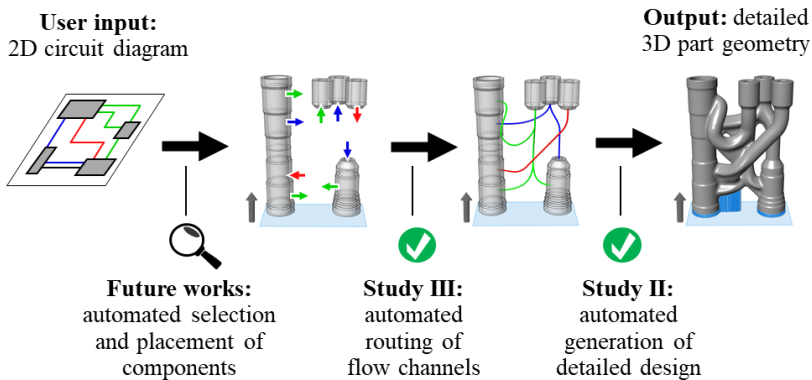


Fig. 87. Automated design of hydraulic manifolds based on a 2D circuit diagram.

Integration of machine learning techniques

An automated design approach for AM enables the generation of detailed 3D part designs with reduced manual effort. Such an automated design approach can lead to an increased amount of data. For example, the evaluation of many design variants using simulations can result in an increased amount of data. Likewise, the AM-based digital production and experimental testing of many different prototypes can generate a large amount of data. As shown in Fig. 88, future works can use machine learning techniques [261][262][263][264][265][266] to automatically structure and analyze these datasets and feed knowledge derived from the data back into an automated design process. For example, future studies can apply supervised learning methods such as artificial neural networks to "learn" the relationship between the geometry of an AM part and its performance. For example, suppose that the studied part is an AM nozzle used for the extrusion of protein-based textured meat substitutes [267][268]. In this case, a neural network may be trained to "learn" the relationship between different input variables (e.g., 3D nozzle geometry, process parameters of extrusion, composition of raw materials) and experimental test data (e.g., quality and texture of extrudate, data from sensors, temperature and velocity profile of extrudate). Such relations are often difficult to simulate due to the complex multi-physics nature of the extrusion process and formation of the fibrous structure [267][268]. Machine learning techniques may offer the possibility of discovering such relations and suggesting to users the fabrication and testing of specific nozzle designs, thereby enabling a fully closed digital design loop.

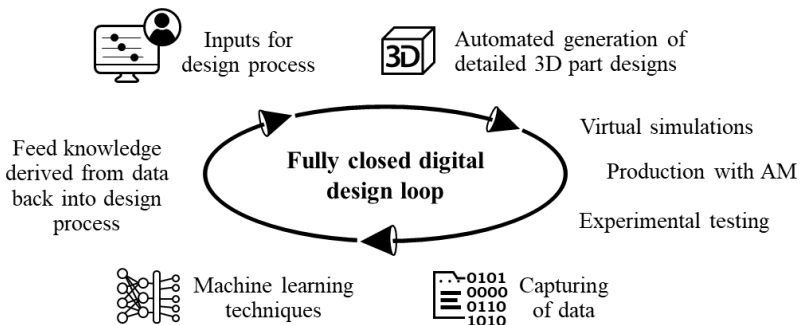


Fig. 88. Use of machine learning techniques for closing the digital design loop.

Bibliography

- [1] I. Gibson, D. Rosen, B. Stucker, M. Khorasani, Additive Manufacturing Technologies, Springer International Publishing, 2021. <https://doi.org/10.1007/978-3-030-56127-7>.
- [2] M. Leary, Design for Additive Manufacturing - Additive Manufacturing Materials and Technologies, Elsevier, 2020. <https://doi.org/https://doi.org/10.1016/C2017-0-04238-6>.
- [3] I. Yadroitsev, A. Du Plessis, E. Macdonald, Fundamentals of Laser Powder Bed Fusion of Metals, Elsevier, 2021. <https://doi.org/https://doi.org/10.1016/C2020-0-01200-4>.
- [4] M.K. Thompson, G. Moroni, T. Vaneker, G. Fadel, R.I. Campbell, I. Gibson, A. Bernard, J. Schulz, P. Graf, B. Ahuja, F. Martina, Design for Additive Manufacturing: Trends, opportunities, considerations, and constraints, CIRP Ann. - Manuf. Technol. 65 (2016) 737–760. <https://doi.org/10.1016/j.cirp.2016.05.004>.
- [5] S.J. Hu, Evolving Paradigms of Manufacturing: From Mass Production to Mass Customization and Personalization, Procedia CIRP. 7 (2013) 3–8. <https://doi.org/10.1016/J.PROCIR.2013.05.002>.
- [6] R. Lachmayer, P.C. Gembarski, P. Gottwald, R.B. Lippert, The Potential of Product Customization Using Technologies of Additive Manufacturing, in: Springer, Cham, 2017: pp. 71–81. https://doi.org/10.1007/978-3-319-29058-4_6.
- [7] J. Spallek, D. Krause, Process Types of Customisation and Personalisation in Design for Additive Manufacturing Applied to Vascular Models, Procedia CIRP. 50 (2016) 281–286. <https://doi.org/10.1016/J.PROCIR.2016.05.022>.
- [8] B. Blakey-Milner, P. Gradl, G. Snedden, M. Brooks, J. Pitot, E. Lopez, M. Leary, F. Berto, A. du Plessis, Metal additive manufacturing in aerospace: A review, Mater. Des. 209 (2021) 110008. <https://doi.org/10.1016/J.MATDES.2021.110008>.
- [9] M. Wiese, S. Thiede, C. Herrmann, Rapid manufacturing of automotive polymer series parts: A systematic review of processes, materials and challenges, Addit. Manuf. 36 (2020) 101582. <https://doi.org/10.1016/J.ADDMA.2020.101582>.
- [10] N. Asnafi, Application of Laser-Based Powder Bed Fusion for Direct Metal Tooling, Metals (Basel). 11 (2021) 458. <https://doi.org/10.3390/met11030458>.
- [11] R. Wrobel, B. Mecrow, Additive manufacturing in construction of electrical machines-a review, Proc. - 2019 IEEE Work. Electr. Mach.

- Des. Control Diagnosis, WEMDCD 2019. (2019) 15–22. <https://doi.org/10.1109/WEMDCD.2019.8887765>.
- [12] C. Culmone, G. Smit, P. Breedveld, Additive manufacturing of medical instruments: A state-of-the-art review, *Addit. Manuf.* 27 (2019) 461–473. <https://doi.org/10.1016/J.ADDMA.2019.03.015>.
- [13] T. Wangler, E. Lloret, L. Reiter, N. Hack, F. Gramazio, M. Kohler, M. Bernhard, B. Dillenburger, J. Buchli, N. Roussel, R. Flatt, Digital Concrete: Opportunities and Challenges, *RILEM Tech. Lett.* 1 (2016) 67. <https://doi.org/10.21809/rilemtechlett.2016.16>.
- [14] C. Zhang, S. Wang, J. Li, Y. Zhu, T. Peng, H. Yang, Additive manufacturing of products with functional fluid channels: A review, *Addit. Manuf.* (2020) 101490. <https://doi.org/10.1016/j.addma.2020.101490>.
- [15] T. Femmer, I. Flack, M. Wessling, Additive Manufacturing in Fluid Process Engineering, *Chemie-Ingenieur-Technik.* 88 (2016) 535–552. <https://doi.org/10.1002/cite.201500086>.
- [16] J.R. McDonough, A perspective on the current and future roles of additive manufacturing in process engineering, with an emphasis on heat transfer, *Therm. Sci. Eng. Prog.* (2020) 100594. <https://doi.org/10.1016/j.tsep.2020.100594>.
- [17] O.H. Laguna, P.F. Lietor, F.J.I. Godino, F.A. Corpas-Iglesias, A review on additive manufacturing and materials for catalytic applications: Milestones, key concepts, advances and perspectives, *Mater. Des.* 208 (2021) 109927. <https://doi.org/10.1016/j.matdes.2021.109927>.
- [18] C. Sun, Y. Wang, M.D. McMurtrey, N.D. Jerred, F. Liou, J. Li, Additive manufacturing for energy: A review, *Appl. Energy.* 282 (2021) 116041. <https://doi.org/10.1016/j.apenergy.2020.116041>.
- [19] A.K. Stark, Manufactured chemistry: Rethinking unit operation design in the age of additive manufacturing, *AIChE J.* 64 (2018) 1162–1173. <https://doi.org/10.1002/aic.16118>.
- [20] C. Kiener, S. Boschert, Y. Küsters, A. Nicolai, R. Otto, Hochdruckgeeignete AM-Konstruktionselemente mit hierarchisch-funktionalen Metallstrukturen, *Chemie Ing. Tech.* 94 (2022) 1040–1045. <https://doi.org/10.1002/CITE.202200050>.
- [21] J. Meißner, S. Weiske, D. Faidel, A. Tschauer, R.C. Samsun, J. Pasel, R. Peters, D. Stolten, Highly integrated catalytic burner with laser-additive manufactured manifolds, *React. Chem. Eng.* 2 (2017) 437–445. <https://doi.org/10.1039/C6RE00223D>.
- [22] A. Maiorova, A. Sviridenkov, V. Tretyakov, A. Vasilev, V. Yagodki, The Development of the Multi - Fuel Burner, in: *Econ. Eff. Biofuel*

Bibliography

- Prod., InTech, 2011. <https://doi.org/10.5772/20287>.
- [23] R. Rajasegar, C.M. Mitsingas, E.K. Mayhew, Q. Liu, T. Lee, J. Yoo, Development and Characterization of Additive-Manufactured Mesoscale Combustor Array, *J. Energy Eng.* 144 (2018) 04018013. [https://doi.org/10.1061/\(ASCE\)EY.1943-7897.0000527](https://doi.org/10.1061/(ASCE)EY.1943-7897.0000527).
- [24] M. Mazur, T. Bhatelia, B. Kuan, J. Patel, P.A. Webley, M. Brandt, V. Pareek, R. Utikar, Additively manufactured, highly-uniform flow distributor for process intensification, *Chem. Eng. Process. - Process Intensif.* 143 (2019) 107595. <https://doi.org/10.1016/j.cep.2019.107595>.
- [25] Y.J. Park, T. Yu, S.J. Yim, D. You, D.P. Kim, A 3D-printed flow distributor with uniform flow rate control for multi-stacked microfluidic systems, *Lab Chip.* 18 (2018) 1250–1258. <https://doi.org/10.1039/c8lc00004b>.
- [26] J. Schmelzle, E. V. Kline, C.J. Dickman, E.W. Reutzler, G. Jones, T.W. Simpson, (Re)Designing for Part Consolidation: Understanding the Challenges of Metal Additive Manufacturing, *J. Mech. Des. Trans. ASME.* 137 (2015) 1–12. <https://doi.org/10.1115/1.4031156>.
- [27] O. Diegel, J. Schutte, A. Ferreira, Y.L. Chan, Design for additive manufacturing process for a lightweight hydraulic manifold, *Addit. Manuf.* 36 (2020) 101446. <https://doi.org/10.1016/j.addma.2020.101446>.
- [28] J.T. Geating, M.C. Wiese, M.F. Osborn, Design, Fabrication, and Qualification of a 3D Printed Metal Quadruped Body: Combination Hydraulic Manifold, Structure and Mechanical Interface, *Solid Free. Fabr. Symp.* (2017) 2447–2466.
- [29] R. Neugebauer, B. Mller, M. Gebauer, T. Tppel, Additive manufacturing boosts efficiency of heat transfer components, *Assem. Autom.* 31 (2011) 344–347. <https://doi.org/10.1108/01445151111172925>.
- [30] S.A. Niknam, M. Mortazavi, D. Li, Additively manufactured heat exchangers: a review on opportunities and challenges, *Int. J. Adv. Manuf. Technol.* 112 (2020) 1–18. <https://doi.org/10.1007/s00170-020-06372-w>.
- [31] I. Kaur, P. Singh, State-of-the-art in heat exchanger additive manufacturing, *Int. J. Heat Mass Transf.* 178 (2021) 121600. <https://doi.org/10.1016/j.ijheatmasstransfer.2021.121600>.
- [32] K.M. Zentel, M. Fassbender, W. Pauer, G.A. Luinstra, 3D printing as chemical reaction engineering booster, in: *Adv. Chem. Eng., Academic Press Inc., 2020: pp. 97–137.* <https://doi.org/10.1016/bs.ache.2020.08.002>.

- [33] M.J. Harding, S. Brady, H. O'Connor, R. Lopez-Rodriguez, M.D. Edwards, S. Tracy, D. Dowling, G. Gibson, K.P. Girard, S. Ferguson, 3D printing of PEEK reactors for flow chemistry and continuous chemical processing, *React. Chem. Eng.* (2020). <https://doi.org/10.1039/C9RE00408D>.
- [34] C. Spille, A. Lyberis, M.I. Maiwald, D. Herzog, M. Hoffmann, C. Emmelmann, M. Schlüter, SMART-Reactors: Tailoring Gas Holdup Distribution by Additively Manufactured Lattice Structures, *Chem. Eng. Technol.* (2020) ceat.202000211. <https://doi.org/10.1002/ceat.202000211>.
- [35] S. Bettermann, F. Kandelhard, H.-U. Moritz, W. Pauer, Digital and lean development method for 3D-printed reactors based on CAD modeling and CFD simulation, *Chem. Eng. Res. Des.* 152 (2019) 71–84. <https://doi.org/10.1016/J.CHERD.2019.09.024>.
- [36] F. Grinschek, S. Ren Dü Bal, C. Klahn, R. Dittmeyer, Einfluss des additiven Fertigungsverfahrens auf die Gestalt einer Mikrorektifikationsapparatur, *Chemie Ing. Tech.* (2022). <https://doi.org/10.1002/CITE.202200011>.
- [37] A. Jastram, S. Schaack, C. Kiener, Simulation-Driven Design of an Additively Manufactured Reactor for Exothermic Liquid-Liquid Reactions, *Chemie Ing. Tech.* 94 (2022) 948–957. <https://doi.org/10.1002/CITE.202200049>.
- [38] I.R. Woodward, L. Attia, P. Patel, C.A. Fromen, Scalable 3D-printed lattices for pressure control in fluid applications, *AIChE J.* (2021) e17452. <https://doi.org/10.1002/aic.17452>.
- [39] F. Grinschek, D. Xie, M. Klumpp, M. Kraut, E. Hansjosten, R. Dittmeyer, Regular Microstructured Elements for Intensification of Gas-Liquid Contacting Made by Selective Laser Melting, *Ind. Eng. Chem. Res.* 59 (2020) 3736–3743. <https://doi.org/10.1021/acs.iecr.9b04548>.
- [40] D. Xie, R. Dittmeyer, Correlations of laser scanning parameters and porous structure properties of permeable materials made by laser-beam powder-bed fusion, *Addit. Manuf.* 47 (2021) 102261. <https://doi.org/10.1016/j.addma.2021.102261>.
- [41] M. Biedermann, T. Kamps, C. Kiener, Redesign of a Burner Tip with Multiple Integrated Flow Distributors: Presentation held at Fraunhofer Direct Digital Manufacturing, DDMC 2018, Berlin, March 14-15, 2018.
- [42] C. Higman, M. van der Burgt, *Gasification*, Gulf Professional Publishing, 2008. <https://doi.org/10.1016/B978-0-7506-8528-3.X0001-6>.

Bibliography

- [43] R.F. Riesenfeld, R. Haimes, E. Cohen, Initiating a CAD renaissance: Multidisciplinary analysis driven design: Framework for a new generation of advanced computational design, engineering and manufacturing environments, *Comput. Methods Appl. Mech. Eng.* 284 (2015) 1054–1072. <https://doi.org/10.1016/J.CMA.2014.11.024>.
- [44] Y.-S.S. Leung, T.H. Kwok, X. Li, Y. Yang, C.C.L. Wang, Y. Chen, Challenges and status on design and computation for emerging additive manufacturing technologies, *J. Comput. Inf. Sci. Eng.* 19 (2019). <https://doi.org/10.1115/1.4041913>.
- [45] N. Letov, P.T. Velivela, S. Sun, Y.F. Zhao, Challenges and Opportunities in Geometric Modelling of Complex Bio-Inspired 3D Objects Designed for Additive Manufacturing, *J. Mech. Des.* (2021) 1–27. <https://doi.org/10.1115/1.4051720>.
- [46] D. Fuchs, R. Bartz, S. Kuschmitz, T. Vietor, Necessary advances in computer-aided design to leverage on additive manufacturing design freedom, *Int. J. Interact. Des. Manuf.* (2022) 1–19. <https://doi.org/10.1007/s12008-022-00888-z>.
- [47] T. Reiher, S. Vogelsang, R. Koch, Computer integration for geometry generation for product optimization with Additive Manufacturing, *Solid Free. Fabr. 2017 Proc. 28th Annu. Int. Solid Free. Fabr. Symp. - An Addit. Manuf. Conf. SFF 2017.* (2020) 903–921.
- [48] G.A.O. Adam, D. Zimmer, On design for additive manufacturing: evaluating geometrical limitations, *Rapid Prototyp. J.* 21 (2015) 662–670. <https://doi.org/10.1108/RPJ-06-2013-0060>.
- [49] D. Thomas, The development of design rules for selective laser melting, University of Wales Institute, PhD Thesis, 2009. <https://repository.cardiffmet.ac.uk/handle/10369/913> (accessed April 21, 2017).
- [50] Q. Han, H. Gu, S. Soe, R. Setchi, F. Lacan, J. Hill, Manufacturability of AlSi10Mg overhang structures fabricated by laser powder bed fusion, *Mater. Des.* 160 (2018) 1080–1095. <https://doi.org/10.1016/j.matdes.2018.10.043>.
- [51] J. Kranz, D. Herzog, C. Emmelmann, Design guidelines for laser additive manufacturing of lightweight structures in TiAl6V4, *J. Laser Appl.* 27 (2015) S14001. <https://doi.org/10.2351/1.4885235>.
- [52] D. Omidvarkarjan, R. Rosenbauer, D. Kirschenbaum, D. Cipriano, D. Ochsner, H. Woodfin, C. Klahn, M. Meboldt, Prototyping strategies for the agile development of additive manufactured products: A case study from the COVID-19 pandemic, *Proc. 31st Symp. Des. X, DFX 2020.* (2020) 161–168. <https://doi.org/10.35199/DFX2020.17>.

- [53] P. Pradel, R.I. Campbell, R. Bibb, When Design Never Ends - A Future Scenario for Product Development, *Proc. Des. Soc. Int. Conf. Eng. Des.* 1 (2019) 829–838. <https://doi.org/10.1017/dsi.2019.87>.
- [54] D.W. Rosen, A review of synthesis methods for additive manufacturing, *Virtual Phys. Prototyp.* 11 (2016) 1–13. <https://doi.org/10.1080/17452759.2016.1240208>.
- [55] A. Wiberg, J. Persson, J. Ölvander, Design for additive manufacturing – a review of available design methods and software, *Rapid Prototyp. J.* 25 (2019) 1080–1094. <https://doi.org/10.1108/RPJ-10-2018-0262>.
- [56] T. Zegard, G.H. Paulino, Bridging topology optimization and additive manufacturing, *Struct. Multidiscip. Optim.* 53 (2016) 175–192. <https://doi.org/10.1007/s00158-015-1274-4>.
- [57] J. Liu, A.T. Gaynor, S. Chen, Z. Kang, K. Suresh, A. Takezawa, L. Li, J. Kato, J. Tang, C.C.L. Wang, L. Cheng, X. Liang, A.C. To, Current and future trends in topology optimization for additive manufacturing, *Struct. Multidiscip. Optim.* 57 (2018) 2457–2483. <https://doi.org/10.1007/s00158-018-1994-3>.
- [58] S.N. Reddy, I. Ferguson, M. Frecker, T.W. Simpson, C.J. Dickman, Topology optimization software for additive manufacturing: A review of current capabilities and a real-world example, in: *Proc. ASME Des. Eng. Tech. Conf., American Society of Mechanical Engineers (ASME)*, 2016. <https://doi.org/10.1115/DETC2016-59718>.
- [59] G. La Rocca, Knowledge based engineering: Between AI and CAD. Review of a language based technology to support engineering design, *Adv. Eng. Informatics.* 26 (2012) 159–179. <https://doi.org/10.1016/j.aei.2012.02.002>.
- [60] E.J. Reddy, C.N. V. Sridhar, V.P. Rangadu, Knowledge Based Engineering: Notion, Approaches and Future Trends, *Am. J. Intell. Syst.* (2015). <https://doi.org/10.5923/j.ajis.20150501.01>.
- [61] F. Dworschak, P. Kügler, B. Schleich, S. Wartzack, Model and Knowledge Representation for the Reuse of Design Process Knowledge Supporting Design Automation in Mass Customization, *Appl. Sci.* 11 (2021) 9825. <https://doi.org/10.3390/app11219825>.
- [62] A. Wiberg, Towards Design Automation for Additive Manufacturing Optimization approach, Linköping University, PhD Thesis, 2019. <https://doi.org/10.3384/lic.diva-160888>.
- [63] S. Vajna, C. Weber, K. Zeman, P. Hehenberger, D. Gerhard, S. Wartzack, *CAX für Ingenieure*, Springer Berlin Heidelberg, 2018. <https://doi.org/10.1007/978-3-662-54624-6>.

Bibliography

- [64] A. Wiberg, J. Persson, J. Ölvander, Design for additive manufacturing using a master model approach, in: Proc. ASME Des. Eng. Tech. Conf., American Society of Mechanical Engineers (ASME), 2019: pp. 1–11. <https://doi.org/10.1115/DETC2019-97915>.
- [65] S. Bin Maidin, I. Campbell, E. Pei, Development of a design feature database to support design for additive manufacturing, *Assem. Autom.* 32 (2012) 235–244. <https://doi.org/10.1108/01445151211244375>.
- [66] D. Omidvarkarjan, D. Cipriano, R. Rosenbauer, M. Biedermann, M. Meboldt, Implementation of a design support tool for additive manufacturing using a feature database: an industrial case study, *Prog. Addit. Manuf.* (2020). <https://doi.org/10.1007/s40964-020-00119-5>.
- [67] H. Li, R. Lachmayer, Automated Exploration of Design Solution Space Applying the Generative Design Approach, *Proc. Des. Soc. Int. Conf. Eng. Des.* 1 (2019) 1085–1094. <https://doi.org/10.1017/dsi.2019.114>.
- [68] M. Fuge, G. Carmean, J. Cornelius, R. Elder, The MechProcessor: Helping Novices Design Printable Mechanisms Across Different Printers, *J. Mech. Des.* 137 (2015) 111415. <https://doi.org/10.1115/1.4031089>.
- [69] A.N. Danun, P. Dalla Palma, C. Klahn, M. Meboldt, Building Block Synthesis of Self Supported 3D Compliant Elements for Metallic Additive Manufacturing, *J. Mech. Des.* (2020) 1–20. <https://doi.org/10.1115/1.4048220>.
- [70] S. Detzel, N. Besch, B.L. Soballa, R. Bazan, T.C. Lueth, Automated Design of Snap-Fit Joints for the Additive Manufacturing of Robot Links, 2021 IEEE Int. Conf. Robot. Biomimetics, ROBIO 2021. (2021) 643–649. <https://doi.org/10.1109/ROBIO54168.2021.9739617>.
- [71] D. Wang, S. Park, D.W. Rosen, Data-Driven Design Space Exploration and Exploitation for Design for Additive Manufacturing, 141 (2019) 1–12. <https://doi.org/10.1115/1.4043587>.
- [72] J. Plocher, A. Panesar, Review on design and structural optimisation in additive manufacturing: Towards next-generation lightweight structures, *Mater. Des.* 183 (2019) 108164. <https://doi.org/10.1016/J.MATDES.2019.108164>.
- [73] J. Alexandersen, C.S. Andreasen, A review of topology optimisation for fluid-based problems, *Fluids.* 5 (2020) 1–32. <https://doi.org/10.3390/fluids5010029>.
- [74] J. Verboom, Design and Additive Manufacturing of Manifolds for

- Navier-Stokes Flow: A Topology Optimisation Approach. Master thesis. TU Delft., (2017). <https://repository.tudelft.nl/islandora/object/uuid:c843e8a0-3041-40db-a6b0-d4558a5fd1dd> (accessed January 15, 2019).
- [75] E. Ven, C. Ayas, M. Langelaar, Computational Design of Complex 3D Printed Objects, in: 3D Print. Energy Appl., Wiley, 2021: pp. 91–108. <https://doi.org/10.1002/9781119560807.ch4>.
- [76] M. Yu, S. Ruan, J. Gu, M. Ren, Z. Li, X. Wang, C. Shen, Three-dimensional topology optimization of thermal-fluid-structural problems for cooling system design, *Struct. Multidiscip. Optim.* 62 (2020) 3347–3366. <https://doi.org/10.1007/s00158-020-02731-z>.
- [77] L.C. Høghøj, D.R. Nørhave, J. Alexandersen, O. Sigmund, C.S. Andreasen, Topology optimization of two fluid heat exchangers, *Int. J. Heat Mass Transf.* 163 (2020) 120543. <https://doi.org/10.1016/j.ijheatmasstransfer.2020.120543>.
- [78] ISO - ISO/ASTM 52900:2021, Additive manufacturing — General principles — Fundamentals and vocabulary, (2021). <https://www.iso.org/standard/74514.html> (accessed July 13, 2022).
- [79] W.E. Frazier, Metal additive manufacturing: A review, *J. Mater. Eng. Perform.* 23 (2014) 1917–1928. <https://doi.org/10.1007/s11665-014-0958-z>.
- [80] J. Jiang, X. Xu, J. Stringer, Support Structures for Additive Manufacturing: A Review, *J. Manuf. Mater. Process.* 2 (2018) 64. <https://doi.org/10.3390/jmmp2040064>.
- [81] A.M. Kamat, Y. Pei, An analytical method to predict and compensate for residual stress-induced deformation in overhanging regions of internal channels fabricated using powder bed fusion, *Addit. Manuf.* 29 (2019) 100796. <https://doi.org/10.1016/j.addma.2019.100796>.
- [82] J. Ferchow, Additive Manufacturing towards Industrial Series Production: Post-Processing Strategies and Design, ETH Zurich, PhD Thesis, 2021. <https://doi.org/10.3929/ethz-b-000514979>.
- [83] C. Klahn, M. Meboldt, F. Fontana, B. Leutenecker-Twelsiek, D. Omidvarkarjan, J. Jansen, Entwicklung und Konstruktion für die Additive Fertigung, Vogel Business Media, Würzburg, 2021.
- [84] M. Leary, AM production economics, in: *Des. Addit. Manuf.*, Elsevier, 2020: pp. 7–31. <https://doi.org/10.1016/b978-0-12-816721-2.00002-6>.
- [85] D. Thomas, S. Gilbert, Costs and Cost Effectiveness of Additive Manufacturing - A Literature Review and Discussion, *NIST Spec. Publ.* 1176 (2014) 1–77. <https://doi.org/10.6028/NIST.SP.1176>.
- [86] M. Baumers, P. Dickens, C. Tuck, R. Hague, The cost of additive

- manufacturing: machine productivity, economies of scale and technology-push, *Technol. Forecast. Soc. Change.* 102 (2016) 193–201. <https://doi.org/10.1016/j.techfore.2015.02.015>.
- [87] A.Z.A. Kadir, Y. Yusof, M.S. Wahab, Additive manufacturing cost estimation models—a classification review, *Int. J. Adv. Manuf. Technol.* 107 (2020) 4033–4053. <https://doi.org/10.1007/s00170-020-05262-5>.
- [88] F. Fontana, C. Klahn, M. Meboldt, Value-driven clustering of industrial additive manufacturing applications, *J. Manuf. Technol. Manag.* 30 (2019) 366–390. <https://doi.org/10.1108/JMTM-06-2018-0167>.
- [89] F.J. Keil, Process intensification, *Rev. Chem. Eng.* 34 (2018) 135–200. <https://doi.org/10.1515/revce-2017-0085>.
- [90] A.K. Tula, M.R. Eden, R. Gani, Computer-aided process intensification: Challenges, trends and opportunities, *AIChE J.* 66 (2020) 1–12. <https://doi.org/10.1002/aic.16819>.
- [91] S. Bettermann, R. Stuhr, H.U. Moritz, W. Pauer, Customizable 3D-printed stirrers for investigation, optimization and scale-up processes of batch emulsion copolymerizations, *Chem. Eng. Sci.* 206 (2019) 50–62. <https://doi.org/10.1016/j.ces.2019.05.026>.
- [92] M. Biedermann, M. Meboldt, Swiss AM Guide 2018 - Exploring new applications in additive manufacturing Swiss AM Guide 2018, pdf/z, ETH Zurich, AM Network Switzerland, 2018. <https://doi.org/http://hdl.handle.net/20.500.11850/314330>.
- [93] J.Y. Ho, K.K. Wong, K.C. Leong, T.N. Wong, S.B. Tor, Customised design of a water-cooled cold plate fabricated by selective laser melting, *Proc. Int. Conf. Prog. Addit. Manuf.* 2018-May (2018) 101–108. <https://doi.org/10.25341/D4KG65>.
- [94] F. Walachowicz, I. Bernsdorf, U. Papenfuss, C. Zeller, A. Graichen, V. Navrotsky, N. Rajvanshi, C. Kiener, Comparative Energy, Resource and Recycling Lifecycle Analysis of the Industrial Repair Process of Gas Turbine Burners Using Conventional Machining and Additive Manufacturing, *J. Ind. Ecol.* 21 (2017) S203–S215. <https://doi.org/10.1111/JIEC.12637>.
- [95] N. Asnafi, Tool and Die Making, Surface Treatment, and Repair by Laser-based Additive Processes, *BHM Berg- Und Hüttenmännische Monatshefte.* 166 (2021) 225–236. <https://doi.org/10.1007/s00501-021-01113-2>.
- [96] N. V. Ganter, L. V. Hoppe, J. Dünte, P.C. Gembariski, R. Lachmayer, Knowledge-Based Assistance System for Part Preparation in Additive Repair by Laser Powder Bed Fusion, *Proc. Des. Soc.* 2

- (2022) 1381–1390. <https://doi.org/10.1017/PDS.2022.140>.
- [97] G. Schuh, M. Behr, C. Brecher, A. Bührig-Polaczek, W. Michaeli, R. Schmitt, J. Arnoscht, A. Bohl, D. Buchbinder, J. Bültmann, A. Diatlov, S. Elgeti, W. Herfs, C. Hinke, A. Karlberger, D. Kupke, M. Lenders, C. Nußbaum, M. Probst, Y. Queudeville, J. Quick, H. Schleifenbaum, M. Vorspel-Rüter, C. Windeck, Individualised Production, in: *Integr. Prod. Technol. High-Wage Ctries.*, Springer Berlin Heidelberg, 2012: pp. 77–239. https://doi.org/10.1007/978-3-642-21067-9_3.
- [98] N. Guo, M.C. Leu, Additive manufacturing: Technology, applications and research needs, *Front. Mech. Eng.* 8 (2013) 215–243. <https://doi.org/10.1007/s11465-013-0248-8>.
- [99] S. Yang, Y.F. Zhao, Additive manufacturing-enabled design theory and methodology: a critical review, *Int. J. Adv. Manuf. Technol.* 80 (2015) 327–342. <https://doi.org/10.1007/s00170-015-6994-5>.
- [100] D.W. Rosen, Research supporting principles for design for additive manufacturing: This paper provides a comprehensive review on current design principles and strategies for AM, *Virtual Phys. Prototyp.* 9 (2014) 225–232. <https://doi.org/10.1080/17452759.2014.951530>.
- [101] L.L. Lopez Taborda, H. Maury, J. Pacheco, Design for additive manufacturing: a comprehensive review of the tendencies and limitations of methodologies, *Rapid Prototyp. J.* (2021). <https://doi.org/10.1108/RPJ-11-2019-0296>.
- [102] M.U. Obi, P. Pradel, M. Sinclair, R. Bibb, A bibliometric analysis of research in design for additive manufacturing, *Rapid Prototyp. J.* 28 (2022) 967–987. <https://doi.org/10.1108/RPJ-11-2020-0291/FULL/PDF>.
- [103] A. Alfaify, M. Saleh, F.M. Abdullah, A.M. Al-Ahmari, Design for additive manufacturing: A systematic review, *Sustain.* 12 (2020) 7936. <https://doi.org/10.3390/SU12197936>.
- [104] A. du Plessis, C. Broeckhoven, I. Yadroitsava, I. Yadroitsev, C.H. Hands, R. Kunju, D. Bhate, Beautiful and Functional: A Review of Biomimetic Design in Additive Manufacturing, *Addit. Manuf.* 27 (2019) 408–427. <https://doi.org/10.1016/J.ADDMA.2019.03.033>.
- [105] P. Pradel, Z. Zhu, R. Bibb, J. Moultrie, A framework for mapping design for additive manufacturing knowledge for industrial and product design, *J. Eng. Des.* 29 (2018) 291–326. <https://doi.org/10.1080/09544828.2018.1483011>.
- [106] M. Kumke, H. Watschke, T. Vietor, A new methodological framework for design for additive manufacturing, *Addit. Manuf.*

- Handb. Prod. Dev. Def. Ind. 11 (2017) 3.
<https://doi.org/10.1201/9781315119106>.
- [107] T. Kamps, M. Gralow, G. Schlick, G. Reinhart, Systematic Biomimetic Part Design for Additive Manufacturing, *Procedia CIRP*. 65 (2017) 259–266. <https://doi.org/10.1016/J.PROCIR.2017.04.054>.
- [108] F. Laverne, F. Segonds, N. Anwer, M. Le Coq, Assembly Based Methods to Support Product Innovation in Design for Additive Manufacturing: An Exploratory Case Study, *J. Mech. Des.* 137 (2015) 121701. <https://doi.org/10.1115/1.4031589>.
- [109] B. Leutenecker-Twelsiek, C. Klahn, M. Meboldt, Considering Part Orientation in Design for Additive Manufacturing, *Procedia CIRP*. 50 (2016) 408–413. <https://doi.org/10.1016/j.procir.2016.05.016>.
- [110] O. Diegel, A. Nordin, D. Motte, *A Practical Guide to Design for Additive Manufacturing*, Springer Singapore, 2019. <https://doi.org/10.1007/978-981-13-8281-9>.
- [111] L. Di Angelo, P. Di Stefano, E. Guardiani, Search for the Optimal Build Direction in Additive Manufacturing Technologies: A Review, *J. Manuf. Mater. Process.* 4 (2020) 71. <https://doi.org/10.3390/jmmp4030071>.
- [112] A. Bloesch-Paidosh, K. Shea, Enhancing Creative Redesign through Multi-Modal Design Heuristics for Additive Manufacturing, *J. Mech. Des.* (2021) 1–52. <https://doi.org/10.1115/1.4050656>.
- [113] F. Valjak, A. Lindwall, REVIEW OF DESIGN HEURISTICS AND DESIGN PRINCIPLES IN DESIGN FOR ADDITIVE MANUFACTURING, *Proc. Des. Soc.* 1 (2021) 2571–2580. <https://doi.org/10.1017/PDS.2021.518>.
- [114] J.W. Booth, J. Alperovich, T.N. Reid, K. Raman, The design for additive manufacturing worksheet, *Proc. ASME 2016 Int. Des. Eng. Tech. Conf. Comput. Inf. Eng. Conf. IDETC/CIE 2016.* 1 (2016) 15. <https://doi.org/10.1115/DETC201660407>.
- [115] J. Bracken, T. Pomorski, C. Armstrong, R. Prabhu, T.W. Simpson, K. Jablowski, W. Cleary, N.A. Meisel, Design for Metal Powder Bed Fusion: The Geometry for Additive Part Selection (GAPS) Worksheet, *Addit. Manuf.* 35 (2020) 101163. <https://doi.org/10.1016/j.addma.2020.101163>.
- [116] S. Kim, D.W. Rosen, P. Witherell, H. Ko, A Design for Additive Manufacturing Ontology to Support Manufacturability Analysis, in: *Vol. 2A 44th Des. Autom. Conf., ASME, 2018:* p. V02AT03A036. <https://doi.org/10.1115/DETC2018-85848>.
- [117] E.M. Sanfilippo, F. Belkadi, A. Bernard, Ontology-based knowledge representation for additive manufacturing, *Comput. Ind.* 109 (2019)

- 182–194. <https://doi.org/10.1016/J.COMPIND.2019.03.006>.
- [118] G. Formentini, C. Favi, M. Mandolini, M. Germani, A Framework to Collect and Reuse Engineering Knowledge in the Context of Design for Additive Manufacturing, *Proc. Des. Soc.* 2 (2022) 1371–1380. <https://doi.org/10.1017/PDS.2022.139>.
- [119] Y. Tang, Y.F. Zhao, A survey of the design methods for additive manufacturing to improve functional performance, *Rapid Prototyp. J.* 22 (2016) 569–590. <https://doi.org/10.1108/RPJ-01-2015-0011>.
- [120] Y. Oh, C. Zhou, S. Behdad, Part decomposition and assembly-based (Re) design for additive manufacturing: A review, *Addit. Manuf.* 22 (2018) 230–242. <https://doi.org/10.1016/j.addma.2018.04.018>.
- [121] F. Grinschek, B. Ladewig, A. Navarrete Munoz, C. Klahn, R. Dittmeyer, D.-I. habil Roland Dittmeyer, Getting Chemical and Biochemical Engineers Excited about Additive Manufacturing, *Chemie Ing. Tech.* 2022 (2022) 1–9. <https://doi.org/10.1002/CITE.202200010>.
- [122] J. Spallek, D. Krause, Decision-Making in Additive Manufacturing – Survey on AM Experience and Expertise of Designers, *Ind. Addit. Manuf. - Proc. Addit. Manuf. Prod. Appl. - AMPA2017.* (2018) 347–360. https://doi.org/10.1007/978-3-319-66866-6_33.
- [123] J. Pakkanen, F. Calignano, F. Trevisan, M. Lorusso, E.P. Ambrosio, D. Manfredi, P. Fino, Study of Internal Channel Surface Roughnesses Manufactured by Selective Laser Melting in Aluminum and Titanium Alloys, *Metall. Mater. Trans. A Phys. Metall. Mater. Sci.* 47 (2016) 3837–3844. <https://doi.org/10.1007/s11661-016-3478-7>.
- [124] B. Leutenecker-Twelsiek, Additive Fertigung in der industriellen Serienproduktion: Bauteilidentifikation und Gestaltung, *ETH Zurich*, PhD Thesis, 2019. <https://doi.org/10.3929/ethz-b-000347164>.
- [125] Siemens Simcenter, *STAR-CCM+ user guide*, version 2022.1, (2022).
- [126] A.T. Gaynor, J.K. Guest, Topology optimization considering overhang constraints: Eliminating sacrificial support material in additive manufacturing through design, *Struct. Multidiscip. Optim.* 54 (2016) 1157–1172. <https://doi.org/10.1007/s00158-016-1551-x>.
- [127] M. Langelaar, Topology optimization of 3D self-supporting structures for additive manufacturing, *Addit. Manuf.* 12 (2016) 60–70. <https://doi.org/10.1016/j.addma.2016.06.010>.
- [128] G. Allaire, C. Dapogny, R. Estevez, A. Faure, G. Michailidis, Structural optimization under overhang constraints imposed by additive manufacturing technologies, *J. Comput. Phys.* 351 (2017) 295–328. <https://doi.org/10.1016/j.jcp.2017.09.041>.

Bibliography

- [129] R. Behrou, K. Kirsch, R. Ranjan, J.K. Guest, Topology optimization of additively manufactured fluidic components free of internal support structures, *Comput. Methods Appl. Mech. Eng.* (2021) 114270. <https://doi.org/10.1016/j.cma.2021.114270>.
- [130] VDI 5610 Blatt 2 - Wissensmanagement im Ingenieurwesen - Wissensbasierte Konstruktion (KBE), VDI-Verlag, Düsseldorf. (2017). <https://www.vdi.de/richtlinien/details/vdi-5610-blatt-2-wissensmanagement-im-ingenieurwesen-wissensbasierte-konstruktion-kbe>.
- [131] M. Stokes, MOKA Consortium., *Managing engineering knowledge : MOKA: methodology for knowledge based engineering applications*, Professional Engineering Pub, 2001.
- [132] R. Curran, W.J.C. Verhagen, M.J.L. van Tooren, T.H. van der Laan, A multidisciplinary implementation methodology for knowledge based engineering: KNOMAD, *Expert Syst. Appl.* 37 (2010) 7336–7350. <https://doi.org/10.1016/J.ESWA.2010.04.027>.
- [133] A.T. Schreiber, G. Schreiber, H. Akkermans, A. Anjewierden, N. Shadbolt, R. de Hoog, W. de Velde, B. Wielinga, R. Nigel, others, *Knowledge engineering and management: the CommonKADS methodology*, MIT press, 2000.
- [134] K. Amadori, M. Tarkian, J. Ölvander, P. Krus, Flexible and robust CAD models for design automation, *Adv. Eng. Informatics.* 26 (2012) 180–195. <https://doi.org/10.1016/J.AEI.2012.01.004>.
- [135] M. Tarkian, *Design Automation for Multidisciplinary Optimization : A High Level CAD Template Approach*, Linköping University, The Institute of Technology, 2012.
- [136] T. Schumacher, Multipoint Adjoint Optimization | ENGYS Blog, (2019). <https://blog.engys.com/multipoint-adjoint-optimisation/> (accessed July 13, 2022).
- [137] T. Schumacher, Multipoint Adjoint Optimization II | ENGYS Blog, (2019). <https://blog.engys.com/multipoint-adjoint-optimisation-ii/> (accessed July 13, 2022).
- [138] T. Stangl, S. Wartzack, Feature based interpretation and reconstruction of structural topology optimization results, *Int. Conf. Eng. Des.* 6 (2015) 235–244.
- [139] J. Mayer, S. Wartzack, A Concept Towards Automated Reconstruction of Topology Optimized Structures Using Medial Axis Skeletons, *Proc. Munich Symp. Light. Des.* 2020. (2021) 28–35. https://doi.org/10.1007/978-3-662-63143-0_3.
- [140] A. Amroune, J.C. Cuillière, V. François, Automated Lofting-Based Reconstruction of CAD Models from 3D Topology Optimization

- Results, *CAD Comput. Aided Des.* 145 (2022). <https://doi.org/10.1016/J.CAD.2021.103183>.
- [141] P.-T. Doutré, E. Morretton, T.H. Vo, P. Marin, F. Pourroay, G. Prudhomme, F. Vignat, Comparison of some approaches to define a CAD model from topological optimization in design for additive manufacturing, in: Springer, Cham, 2017: pp. 233–240. https://doi.org/10.1007/978-3-319-45781-9_24.
- [142] E. Dalpadulo, F. Pini, F. Leali, Assessment of Design for Additive Manufacturing Based on CAD Platforms, *Lect. Notes Mech. Eng.* (2020) 970–981. https://link.springer.com/chapter/10.1007/978-3-030-31154-4_83 (accessed November 9, 2019).
- [143] C. Ledermann, C. Hanske, J. Wenzel, P. Ermanni, R. Kelm, Associative parametric CAE methods in the aircraft pre-design, *Aerosp. Sci. Technol.* 9 (2005) 641–651. <https://doi.org/10.1016/J.AST.2005.05.001>.
- [144] W.J.C. Verhagen, P. Bermell-Garcia, R.E.C. van Dijk, R. Curran, A critical review of Knowledge-Based Engineering: An identification of research challenges, *Adv. Eng. Informatics.* 26 (2012) 5–15. <https://doi.org/10.1016/J.AEI.2011.06.004>.
- [145] S. Maidin, I. Campbell, I. Drstvensek, P. Sever, Design for Rapid Manufacturing – Capturing Designers Knowledge, in: Proc. 4th Int. Conf. Adv. Res. Virtual Rapid Prototyp., 2009. <https://doi.org/10.1201/9780203859476.ch48>.
- [146] T.J. Hagedorn, S. Krishnamurty, I.R. Grosse, A Knowledge-Based Method for Innovative Design for Additive Manufacturing Supported by Modular Ontologies, *J. Comput. Inf. Sci. Eng.* 18 (2018) 021009. <https://doi.org/10.1115/1.4039455>.
- [147] M. Mayerhofer, W. Lepuschitz, T. Hoebert, M. Merdan, M. Schwentenwein, T.I. Strasser, Knowledge-driven Manufacturability Analysis for Additive Manufacturing, *IEEE Open J. Ind. Electron. Soc.* (2021) 1–1. <https://doi.org/10.1109/OJIES.2021.3061610>.
- [148] M. Biedermann, M. Meboldt, Computational design synthesis of additive manufactured multi-flow nozzles, *Addit. Manuf.* 35 (2020) 101231. <https://doi.org/10.1016/j.addma.2020.101231>.
- [149] M. Biedermann, P. Beutler, M. Meboldt, Automated design of additive manufactured flow components with consideration of overhang constraint, *Addit. Manuf.* 46 (2021) 102119. <https://doi.org/10.1016/j.addma.2021.102119>.
- [150] M. Biedermann, P. Beutler, M. Meboldt, Routing multiple flow channels for additive manufactured parts using iterative cable simulation, *Addit. Manuf.* 56 (2022) 102891.

- <https://doi.org/10.1016/J.ADDMA.2022.102891>.
- [151] J. Alexandersen, O. Sigmund, N. Aage, Large scale three-dimensional topology optimisation of heat sinks cooled by natural convection, *Int. J. Heat Mass Transf.* 100 (2016) 876–891. <https://doi.org/10.1016/J.IJHEATMASSSTRANSFER.2016.05.013>.
- [152] E.M. Dede, S.N. Joshi, F. Zhou, Topology Optimization, Additive Layer Manufacturing, and Experimental Testing of an Air-Cooled Heat Sink, *J. Mech. Des.* 137 (2015) 1–9. <https://doi.org/10.1115/1.4030989>.
- [153] A. Pereira, C. Talischi, G.H. Paulino, I.F. M. Menezes, M.S. Carvalho, Fluid flow topology optimization in PolyTop: stability and computational implementation, *Struct. Multidiscip. Optim.* 54 (2016) 1345–1364. <https://doi.org/10.1007/s00158-014-1182-z>.
- [154] E.M. Papoutsis-Kiachagias, K.C. Giannakoglou, Continuous Adjoint Methods for Turbulent Flows, Applied to Shape and Topology Optimization: Industrial Applications, *Arch. Comput. Methods Eng.* 23 (2016) 255–299. <https://doi.org/10.1007/s11831-014-9141-9>.
- [155] C.S. Andreasen, A.R. Gersborg, O. Sigmund, Topology optimization of microfluidic mixers, *Int. J. Numer. Methods Fluids.* 61 (2009) 498–513. <https://doi.org/10.1002/flid.1964>.
- [156] C. Emmelmann, P. Sander, J. Kranz, E. Wycisk, Laser additive manufacturing and bionics: Redefining lightweight design, *Phys. Procedia.* 12 (2011) 364–368. <https://doi.org/10.1016/j.phpro.2011.03.046>.
- [157] M. Marinov, M. Amagliani, T. Barback, J. Flower, S. Barley, S. Furuta, P. Charrot, I. Henley, N. Santhanam, G.T. Finnigan, S. Meshkat, J. Hallet, M. Sapun, P. Wolski, Generative Design Conversion to Editable and Watertight Boundary Representation, *Comput. Des.* 115 (2019) 194–205. <https://doi.org/10.1016/J.CAD.2019.05.016>.
- [158] J.-C. Cuillière, V. François, A. Nana, Automatic construction of structural CAD models from 3D topology optimization, *Comput. Aided. Des. Appl.* 15 (2018) 107–121. <https://doi.org/10.1080/16864360.2017.1353726>.
- [159] N. Boyard, M. Rivette, O. Christmann, S. Richir, A design methodology for parts using additive manufacturing, in: *High Value Manuf. Adv. Res. Virtual Rapid Prototyp. - Proc. 6th Int. Conf. Adv. Res. Rapid Prototyping, VR@P 2013, Leiria, Portugal, 2013*: pp. 0–6. <https://doi.org/10.1201/b15961-74>.
- [160] P.C. Gembarski, H. Li, R. Lachmayer, Template-Based Modelling of Structural Components, *Int. J. Mech. Eng. Robot. Res.* (2017) 336–

342. <https://doi.org/10.18178/ijmerr.6.5.336-342>.
- [161] J. Cagan, M.I. Campbell, S. Finger, T. Tomiyama, A Framework for Computational Design Synthesis: Model and Applications, *J. Comput. Inf. Sci. Eng.* 5 (2005) 171. <https://doi.org/10.1115/1.2013289>.
- [162] A. Chakrabarti, K. Shea, J. Stone, J. Cagan, M. Campbell, N.V. Hernandez, K.L. Wood, Computer-Based Design Synthesis Research: An Overview, *J. Comput. Inf. Sci. Eng.* 11 (2011) 021003. <https://doi.org/10.1115/1.3593409>.
- [163] E. Rigger, K. Shea, T. Stankovic, Task categorisation for identification of design automation opportunities, *J. Eng. Des.* 29 (2018) 131–159. <https://doi.org/10.1080/09544828.2018.1448927>.
- [164] L. Li, Y. Zheng, M. Yang, J. Leng, Z. Cheng, Y. Xie, P. Jiang, Y. Ma, A survey of feature modeling methods: Historical evolution and new development, *Robot. Comput. Integr. Manuf.* 61 (2020) 101851. <https://doi.org/10.1016/J.RCIM.2019.101851>.
- [165] J.R. Wagner, E.M. Mount, H.F. Giles, J.R. Wagner, E.M. Mount, H.F. Giles, Coextrusion Applications, *Extrusion.* (2014) 449–466. <https://doi.org/10.1016/b978-1-4377-3481-2.00040-5>.
- [166] J. Lipton, D. Arnold, F. Nigl, N. Lopez, D. Cohen, N. Norén, H. Lipson, Multi-Material Food printing with Complex Internal Structure Suitable for Conventional Post-Processing, *J. Chem. Inf. Model.* (2013). <https://doi.org/10.1017/CBO9781107415324.004>.
- [167] F.C. Godoi, S. Prakash, B.R. Bhandari, 3d printing technologies applied for food design: Status and prospects, *J. Food Eng.* 179 (2016) 44–54. <https://doi.org/10.1016/j.jfoodeng.2016.01.025>.
- [168] S. Bodkhe, C. Noonan, F.P. Gosselin, D. Therriault, Coextrusion of Multifunctional Smart Sensors, *Adv. Eng. Mater.* 20 (2018) 1800206. <https://doi.org/10.1002/adem.201800206>.
- [169] J. Mueller, J.R. Raney, K. Shea, J.A. Lewis, Architected Lattices with High Stiffness and Toughness via Multicore-Shell 3D Printing, *Adv. Mater.* 30 (2018) 1705001. <https://doi.org/10.1002/adma.201705001>.
- [170] M.A.H. Khondoker, A. Ostashek, D. Sameoto, Direct 3D Printing of Stretchable Circuits via Liquid Metal Co-Extrusion Within Thermoplastic Filaments, *Adv. Eng. Mater.* 1900060 (2019) 1–8. <https://doi.org/10.1002/adem.201900060>.
- [171] B. Mani, H.A. Tavakolinia, R. Babaie Moghadam, A new design for co-extrusion dies: Fabrication of multi-layer tubes to be used as solid oxide fuel cell, *J. Sci. Adv. Mater. Devices.* 2 (2017) 425–431. <https://doi.org/10.1016/J.JSAM.2017.10.003>.
- [172] Y. Morimoto, M. Kiyosawa, S. Takeuchi, Three-dimensional printed

- microfluidic modules for design changeable coaxial microfluidic devices, *Sensors Actuators, B Chem.* 274 (2018) 491–500. <https://doi.org/10.1016/j.snb.2018.07.151>.
- [173] M.A. Skylar-Scott, J. Mueller, C.W. Visser, J.A. Lewis, Voxellated soft matter via multimaterial multinozzle 3D printing, *Nature*. 575 (2019) 330–335. <https://doi.org/10.1038/s41586-019-1736-8>.
- [174] T. Wortmann, Opossum, CAADRIA 2017 - 22nd Int. Conf. Comput. Archit. Des. Res. Asia Protoc. Flows Glitches. (2017) 283–292. <https://doi.org/10.2307/j.ctv4g1rch.43>.
- [175] J.D. Camba, M. Contero, P. Company, Parametric CAD modeling: An analysis of strategies for design reusability, *Comput. Des.* 74 (2016) 18–31. <https://doi.org/10.1016/J.CAD.2016.01.003>.
- [176] R. Jiang, R. Kleer, F.T. Piller, Predicting the future of additive manufacturing: A Delphi study on economic and societal implications of 3D printing for 2030, *Technol. Forecast. Soc. Change.* 117 (2017) 84–97. <https://doi.org/10.1016/J.TECHFORE.2017.01.006>.
- [177] X. Guo, W. Zhang, W. Zhong, Doing Topology Optimization Explicitly and Geometrically—A New Moving Morphable Components Based Framework, *J. Appl. Mech.* 81 (2014). <https://doi.org/10.1115/1.4027609>.
- [178] J. Bai, W. Zuo, Hollow structural design in topology optimization via moving morphable component method, *Struct. Multidiscip. Optim.* (2019) 1–19. <https://doi.org/10.1007/s00158-019-02353-0>.
- [179] B. Zhang, A. Goel, O. Ghalsasi, S. Anand, CAD-based design and pre-processing tools for additive manufacturing, *J. Manuf. Syst.* 52 (2019) 227–241. <https://doi.org/10.1016/J.JMSY.2019.03.005>.
- [180] B. Schoinochoritis, D. Chantzis, K. Salonitis, Simulation of metallic powder bed additive manufacturing processes with the finite element method: A critical review, *Proc. Inst. Mech. Eng. Part B J. Eng. Manuf.* 231 (2017) 96–117. <https://doi.org/10.1177/0954405414567522>.
- [181] E.G. Merriam, J.E. Jones, S.P. Magleby, L.L. Howell, Monolithic 2 DOF fully compliant space pointing mechanism, *Mech. Sci.* 4 (2013) 381–390. <https://doi.org/10.5194/ms-4-381-2013>.
- [182] S.S. Gill, H. Arora, Jidesh, V. Sheth, On the development of Antenna feed array for space applications by additive manufacturing technique, *Addit. Manuf.* 17 (2017) 39–46. <https://doi.org/10.1016/J.ADDMA.2017.06.010>.
- [183] C. Bader, D. Kolb, J.C. Weaver, S. Sharma, A. Hosny, J. Costa, N. Oxman, Making data matter: Voxel printing for the digital fabrication

- of data across scales and domains, *Sci. Adv.* 4 (2018) eaas8652. <https://doi.org/10.1126/sciadv.aas8652>.
- [184] A.S. Sabau, A. Bejan, D. Brownell, K. Gluesenkamp, B. Murphy, F. List, K. Carver, C.R. Schaich, J.W. Klett, Design, additive manufacturing, and performance of heat exchanger with a novel flow-path architecture, *Appl. Therm. Eng.* 180 (2020) 115775. <https://doi.org/10.1016/j.applthermaleng.2020.115775>.
- [185] T.B. Cao, S. Kedziora, S. Sellen, C. Repplinger, Optimization assisted redesigning a structure of a hydrogen valve: the redesign process and numerical evaluations, *Int. J. Interact. Des. Manuf.* (2020). <https://doi.org/10.1007/s12008-020-00648-x>.
- [186] B.S. Richardson, R.F. Lind, P.D. Lloyd, M.W. Noakes, L.J. Love, B.K. Post, The design of an additive manufactured dual arm manipulator system, *Addit. Manuf.* 24 (2018) 467–478. <https://doi.org/10.1016/j.addma.2018.10.030>.
- [187] C. Semini, J. Goldsmith, D. Manfredi, F. Calignano, E.P. Ambrosio, J. Pakkanen, D.G. Caldwell, Additive manufacturing for agile legged robots with hydraulic actuation, in: *Proc. 17th Int. Conf. Adv. Robot. ICAR 2015*, Institute of Electrical and Electronics Engineers Inc., 2015: pp. 123–129. <https://doi.org/10.1109/ICAR.2015.7251444>.
- [188] G. Xie, Y. Dong, J. Zhou, Z. Sheng, Topology optimization design of hydraulic valve blocks for additive manufacturing, *Proc. Inst. Mech. Eng. Part C J. Mech. Eng. Sci.* (2020) 0954440622090216. <https://doi.org/10.1177/09544406220902166>.
- [189] V. Barasuol, O.A. Villarreal-Magaña, D. Sangiah, M. Frigerio, M. Baker, R. Morgan, G.A. Medrano-Cerda, D.G. Caldwell, C. Semini, Highly-integrated hydraulic smart actuators and smart manifolds for high-bandwidth force control, *Front. Robot. AI.* 5 (2018). <https://doi.org/10.3389/frobt.2018.00051>.
- [190] S. Chekurov, T. Lantela, Selective Laser Melted Digital Hydraulic Valve System, *3D Print. Addit. Manuf.* 4 (2017) 215–221. <https://doi.org/10.1089/3dp.2017.0014>.
- [191] A.A. Alshare, F. Calzone, M. Muzzupappa, Hydraulic manifold design via additive manufacturing optimized with CFD and fluid-structure interaction simulations, *Rapid Prototyp. J.* 25 (2019) 1516–1524. <https://doi.org/10.1108/RPJ-03-2018-0064>.
- [192] S. Feng, S. Chen, A.M. Kamat, R. Zhang, M. Huang, L. Hu, Investigation on shape deviation of horizontal interior circular channels fabricated by laser powder bed fusion, *Addit. Manuf.* (2020) 101585. <https://doi.org/10.1016/j.addma.2020.101585>.
- [193] Y. Zhang, S. Yang, Y.F. Zhao, Manufacturability analysis of metal

- laser-based powder bed fusion additive manufacturing—a survey, *Int. J. Adv. Manuf. Technol.* (2020) 1–22. <https://doi.org/10.1007/s00170-020-05825-6>.
- [194] F. Ning, Y. Zhou, Build Orientation Effect on Geometric Performance of Curved-Surface 316L Stainless Steel Parts Fabricated by Selective Laser Melting, *J. Manuf. Sci. Eng.* (2020) 1–37. <https://doi.org/10.1115/1.4047624>.
- [195] A. Charles, A. Elkaseer, L. Thijs, S.G. Scholz, Dimensional Errors Due to Overhanging Features in Laser Powder Bed Fusion Parts Made of Ti-6Al-4V, *Appl. Sci.* 10 (2020) 2416. <https://doi.org/10.3390/app10072416>.
- [196] D. Wang, S. Mai, D. Xiao, Y. Yang, Surface quality of the curved overhanging structure manufactured from 316-L stainless steel by SLM, *Int. J. Adv. Manuf. Technol.* 86 (2016) 781–792. <https://doi.org/10.1007/s00170-015-8216-6>.
- [197] R. Mertens, S. Clijsters, K. Kempen, J.P. Kruth, Optimization of Scan Strategies in Selective Laser Melting of Aluminum Parts with Downfacing Areas, *J. Manuf. Sci. Eng. Trans. ASME.* 136 (2014) 1–7. <https://doi.org/10.1115/1.4028620>.
- [198] K. Kempen, F. Welkenhuyzen, J. Qian, J.P. Kruth, Dimensional accuracy of internal channels in SLM produced parts, *Proc. - ASPE 2014 Spring Top. Meet. Dimens. Accuracy Surf. Finish Addit. Manuf.* (2014) 76–79.
- [199] M. Cloots, L. Zumofen, A.B. Spierings, A. Kirchheim, K. Wegener, Approaches to minimize overhang angles of SLM parts, *Rapid Prototyp. J.* 23 (2017) 362–369. <https://doi.org/10.1108/RPJ-05-2015-0061>.
- [200] X. Guo, J. Zhou, W. Zhang, Z. Du, C. Liu, Y. Liu, Self-supporting structure design in additive manufacturing through explicit topology optimization, *Comput. Methods Appl. Mech. Eng.* 323 (2017) 27–63. <https://doi.org/10.1016/j.cma.2017.05.003>.
- [201] M. Langelaar, Combined optimization of part topology, support structure layout and build orientation for additive manufacturing, *Struct. Multidiscip. Optim.* 57 (2018) 1985–2004. <https://doi.org/10.1007/s00158-017-1877-z>.
- [202] T.E. Johnson, A.T. Gaynor, Three-dimensional projection-based topology optimization for prescribed-angle self-supporting additively manufactured structures, *Addit. Manuf.* 24 (2018) 667–686. <https://doi.org/10.1016/j.addma.2018.06.011>.
- [203] M. Bi, P. Tran, Y.M. Xie, Topology optimization of 3D continuum structures under geometric self-supporting constraint, *Addit. Manuf.*

- (2020) 101422. <https://doi.org/10.1016/j.addma.2020.101422>.
- [204] E. van de Ven, R. Maas, C. Ayas, M. Langelaar, F. van Keulen, Overhang control based on front propagation in 3D topology optimization for additive manufacturing, *Comput. Methods Appl. Mech. Eng.* 369 (2020) 113169. <https://doi.org/10.1016/j.cma.2020.113169>.
- [205] M. Pietropaoli, F. Montomoli, A. Gaymann, Three-dimensional fluid topology optimization for heat transfer, *Struct. Multidiscip. Optim.* 59 (2019) 801–812. <https://doi.org/10.1007/s00158-018-2102-4>.
- [206] F. Feppon, G. Allaire, C. Dapogny, P. Jolivet, Body-fitted topology optimization of 2D and 3D fluid-to-fluid heat exchangers, *Comput. Methods Appl. Mech. Eng.* 376 (2021) 113638. <https://doi.org/10.1016/j.cma.2020.113638>.
- [207] L. He, H. Peng, M. Lin, R. Konjeti, F. Guimbretière, J.E. Froehlich, *Ondulé : Designing and Controlling 3D Printable Springs*, (2019).
- [208] G. Pahl, K. Wallace, *Engineering design applications*, 2005. [https://doi.org/10.1016/0166-3615\(83\)90041-6](https://doi.org/10.1016/0166-3615(83)90041-6).
- [209] B. Zardin, G. Cillo, C.A. Rinaldini, E. Mattarelli, M. Borghi, Pressure losses in hydraulic manifolds, *Energies*. 10 (2017). <https://doi.org/10.3390/en10030310>.
- [210] J.H. Zhang, G. Liu, R. Ding, K. Zhang, M. Pan, S. Liu, 3D printing for energy-saving: Evidence from hydraulic manifolds design, *Energies*. 12 (2019) 2462. <https://doi.org/10.3390/en12132462>.
- [211] K. Museth, VDB: High-resolution sparse volumes with dynamic topology, *ACM Trans. Graph.* (2013). <https://doi.org/10.1145/2487228.2487235>.
- [212] C. Yan, L. Hao, A. Hussein, P. Young, D. Raymont, Advanced lightweight 316L stainless steel cellular lattice structures fabricated via selective laser melting, *Mater. Des.* 55 (2014) 533–541. <https://doi.org/10.1016/j.matdes.2013.10.027>.
- [213] M. Barclift, A. Armstrong, T.W. Simpson, S.B. Joshi, CAD-Integrated cost estimation and build orientation optimization to support design for metal additive manufacturing, in: *Proc. ASME Des. Eng. Tech. Conf., American Society of Mechanical Engineers (ASME)*, 2017. <https://doi.org/10.1115/DETC2017-68376>.
- [214] D.W. Rosen, Manufacturing elements to support design for additive manufacturing, *Proc. Int. Conf. Prog. Addit. Manuf.* 2018-May (2018) 309–314. <https://doi.org/10.25341/D4V88B>.
- [215] Y. Tang, G. Dong, Q. Zhou, Y.F. Zhao, Lattice Structure Design and Optimization with Additive Manufacturing Constraints, *IEEE Trans. Autom. Sci. Eng.* 15 (2018) 1546–1562.

Bibliography

- <https://doi.org/10.1109/TASE.2017.2685643>.
- [216] Y. Xiong, Y. Tang, S.-I. Park, D.W. Rosen, Harnessing Process Variables in Additive Manufacturing for Design Using Manufacturing Elements, *J. Mech. Des.* 142 (2020) 1–18. <https://doi.org/10.1115/1.4046069>.
- [217] J.P. Oliveira, A.D. LaLonde, J. Ma, Processing parameters in laser powder bed fusion metal additive manufacturing, *Mater. Des.* 193 (2020) 108762. <https://doi.org/10.1016/j.matdes.2020.108762>.
- [218] J.P. Oliveira, T.G. Santos, R.M. Miranda, Revisiting fundamental welding concepts to improve additive manufacturing: From theory to practice, *Prog. Mater. Sci.* 107 (2020) 100590. <https://doi.org/10.1016/j.pmatsci.2019.100590>.
- [219] M. Baier, M. Sinico, A. Witvrouw, W. Dewulf, S. Carmignato, A Novel Tomographic Characterisation Approach for Sag and Dross Defects in Metal Additively Manufactured Channels, *Addit. Manuf.* (2021) 101892. <https://doi.org/10.1016/j.addma.2021.101892>.
- [220] N. Dixit, V. Sharma, P. Kumar, Research trends in abrasive flow machining: A systematic review, *J. Manuf. Process.* 64 (2021) 1434–1461. <https://doi.org/10.1016/j.jmapro.2021.03.009>.
- [221] Y. Zhu, S. Wang, C. Zhang, H. Yang, Am-driven design of hydraulic manifolds: enhancing fluid flow and reducing weight, in: 12th Int. Fluid Power Conf. (12. IFK), Dresdner Verein zur Förderung der Fluidtechnik e. V. Dresden, Dresden, 2020: pp. 155–159. <https://doi.org/10.25368/2020.23>.
- [222] T.B. Cao, S. Kedziora, Innovative designs of an in-tank hydrogen valve towards direct metal laser sintering compatibility and fatigue life enhancement, *Struct. Multidiscip. Optim.* 59 (2019) 2319–2340. <https://doi.org/10.1007/s00158-018-2174-1>.
- [223] A. Klarbring, J. Petersson, B. Torstenfelt, M. Karlsson, Topology optimization of flow networks, *Comput. Methods Appl. Mech. Eng.* 192 (2003) 3909–3932. [https://doi.org/10.1016/S0045-7825\(03\)00393-1](https://doi.org/10.1016/S0045-7825(03)00393-1).
- [224] F. Lange, A.S. Shinde, K. Bartsch, C. Emmelmann, A novel approach to avoid internal support structures in fluid flow optimization for additive manufacturing, in: NAFEMS World Congr. 2019, 2019. <http://hdl.handle.net/11420/3503>.
- [225] P. Cao, Z. Fan, R.X. Gao, J. Tang, Design for additive manufacturing: Optimization of piping network in compact system with enhanced path-finding approach, *J. Manuf. Sci. Eng. Trans. ASME.* 140 (2018) 081013. <https://doi.org/10.1115/1.4040320>.
- [226] O. Souissi, R. Benatitallah, D. Duvivier, A. Artiba, N. Belanger, P.

- Feyzeau, Path planning: A 2013 survey, in: Proc. 2013 Int. Conf. Ind. Eng. Syst. Manag. IEEE - IESM 2013, 2013.
- [227] Z. Zhu, G. La Rocca, M.J.L.L. van Tooren, A methodology to enable automatic 3D routing of aircraft Electrical Wiring Interconnection System, *CEAS Aeronaut. J.* 8 (2017) 287–302. <https://doi.org/10.1007/s13272-017-0238-3>.
- [228] G. Belov, W. Du, M.G. De La Banda, D. Harabor, S. Koenig, X. Wei, From multi-agent pathfinding to 3D pipe routing, in: Proc. 13th Int. Symp. Comb. Search, SoCS 2020, Association for the Advancement of Artificial Intelligence (AAAI), 2020: pp. 11–19.
- [229] M. Drumheller, Constraint-based design of optimal transport elements, *J. Comput. Inf. Sci. Eng.* 2 (2002) 302–311. <https://doi.org/10.1115/1.1554698>.
- [230] H. Du, W. Xiong, H. Wang, Z. Wang, A review: virtual assembly of flexible cables based on physical modeling, *Assem. Autom.* 40 (2019) 293–304. <https://doi.org/10.1108/AA-04-2018-056>.
- [231] E. Gustafsson, J. Persson, M. Tarkian, Combinatorial Optimization of Pre-Formed Hose Assemblies, in: Vol. 3B 47th Des. Autom. Conf., American Society of Mechanical Engineers, 2021. <https://doi.org/10.1115/DETC2021-71408>.
- [232] T. Hermansson, E. Åblad, Routing of curves with piecewise constant curvature applied to routing of preformed hoses, *Comput. Des.* 139 (2021) 103067. <https://doi.org/10.1016/j.cad.2021.103067>.
- [233] T. Hermansson, R. Bohlin, J.S. Carlson, R. Söderberg, Automatic routing of flexible 1D components with functional and manufacturing constraints, *CAD Comput. Aided Des.* 79 (2016) 27–35. <https://doi.org/10.1016/j.cad.2016.05.018>.
- [234] N. Lv, J. Liu, H. Xia, J. Ma, X. Yang, A review of techniques for modeling flexible cables, *CAD Comput. Aided Des.* 122 (2020) 102826. <https://doi.org/10.1016/j.cad.2020.102826>.
- [235] W.R. Patterson, M.I. Campbell, PipeSynth: An Algorithm for Automated Topological and Parametric Design and Optimization of Pipe Networks, in: Vol. 5 37th Des. Autom. Conf. Parts A B, ASME, 2011: pp. 13–23. <https://doi.org/10.1115/DETC2011-47906>.
- [236] C. Wang, Q. Liu, Projection and geodesic-based pipe routing algorithm, *IEEE Trans. Autom. Sci. Eng.* 8 (2011) 641–645. <https://doi.org/10.1109/TASE.2010.2099219>.
- [237] C. Wehlin, J.A. Persson, J. Ölvander, Multi-Objective Optimization of Hose Assembly Routing for Vehicles, *Proc. Des. Soc. Des. Conf.* 1 (2020) 471–480. <https://doi.org/10.1017/dsd.2020.267>.
- [238] V. Savage, R. Schmidt, T. Grossman, G. Fitzmaurice, B. Hartmann,

- A Series of tubes: Adding interactivity to 3D prints using internal pipes, in: UIST 2014 - Proc. 27th Annu. ACM Symp. User Interface Softw. Technol., Association for Computing Machinery, Inc, New York, NY, USA, 2014: pp. 3–12. <https://doi.org/10.1145/2642918.2647374>.
- [239] D. Piker, Kangaroo Physics Plugin for Rhino Grasshopper, (n.d.). <https://github.com/Dan-Piker/Kangaroo-Documentation>.
- [240] D. Piker, Kangaroo: Form finding with computational physics, *Archit. Des.* 83 (2013) 136–137. <https://doi.org/10.1002/ad.1569>.
- [241] A.M. Bauer, R. La Magna, J. Lienhard, D. Piker, G. Quinn, C. Gengnagel, K.-U. Bletzinger, Exploring Software Approaches for the Design and Simulation of Bending Active Systems, in: Proc. IASS Symp. 2018, Creat. Struct. Des. July 16-20, 2018, MIT, Boston, USA, 2018.
- [242] J. Bender, M. Müller, M.A. Otaduy, M. Teschner, M. Macklin, A Survey on Position-Based Simulation Methods in Computer Graphics, *Comput. Graph. Forum.* 33 (2014) 228–251. <https://doi.org/10.1111/cgf.12346>.
- [243] M. Müller, B. Heidelberger, M. Hennix, J. Ratcliff, Position based dynamics, *J. Vis. Commun. Image Represent.* 18 (2007) 109–118. <https://doi.org/10.1016/j.jvcir.2007.01.005>.
- [244] J. Stam, Nucleus: Towards a unified dynamics solver for computer graphics, in: Proc. - 2009 11th IEEE Int. Conf. Comput. Des. Comput. Graph. CAD/Graphics 2009, 2009: pp. 1–11. <https://doi.org/10.1109/CADCG.2009.5246818>.
- [245] M. Deuss, A.H. Deleuran, S. Bouaziz, B. Deng, D. Piker, M. Pauly, ShapeOp—A Robust and Extensible Geometric Modelling Paradigm, *Model. Behav.* (2015). https://doi.org/10.1007/978-3-319-24208-8_42.
- [246] M. MacKlin, M. Müller, N. Chentanez, T.Y. Kim, Unified particle physics for real-time applications, *ACM Trans. Graph.* 33 (2014) 1–12. <https://doi.org/10.1145/2601097.2601152>.
- [247] S. Suzuki, Topology-driven form-finding interactive computational modelling of bending-active and textile hybrid structures through active-topology based real-time physics simulations, and its emerging design potentials, Stuttgart: Institut für Tragkonstruktionen und Konstruktives Entwerfen, Universität Stuttgart, 2020.
- [248] L. Nguyen, DynaShape Plugin for Revit Dynamo, (n.d.). <https://github.com/LongNguyenP/DynaShape>.
- [249] S.M.L. Adriaenssens, M.R. Barnes, Tensegrity spline beam and grid

- shell structures, *Eng. Struct.* 23 (2001) 29–36. [https://doi.org/10.1016/S0141-0296\(00\)00019-5](https://doi.org/10.1016/S0141-0296(00)00019-5).
- [250] P. Stoll, A. Spierings, J. Ferchow, C. Klahn, K. Brünger, P. Nägeli, S. Jung, Valve Body Element with Generative Layer-By-Layer Construction (WO 2019/053083 A1. 2019), 2019. <https://doi.org/10.3929/ethz-b-000406594>.
- [251] L. Zhou, Y. Zhu, H. Liu, T. He, C. Zhang, H. Yang, A comprehensive model to predict friction factors of fluid channels fabricated using laser powder bed fusion additive manufacturing, *Addit. Manuf.* 47 (2021) 102212. <https://doi.org/10.1016/j.addma.2021.102212>.
- [252] A. Panesar, D. Brackett, I. Ashcroft, R. Wildman, R. Hague, Design Framework for Multifunctional Additive Manufacturing: Placement and Routing of Three-Dimensional Printed Circuit Volumes, *J. Mech. Des. Trans. ASME.* 137 (2015). <https://doi.org/10.1115/1.4030996>.
- [253] S.R.T. Peddada, L.E. Zeidner, K.A. James, J.T. Allison, An introduction to 3D SPI2 (spatial packaging of interconnected systems with physics interactions) design problems: A review of related work, existing gaps, challenges, and opportunities, in: *Proc. ASME Des. Eng. Tech. Conf., American Society of Mechanical Engineers (ASME)*, 2021. <https://doi.org/10.1115/DETC2021-72106>.
- [254] G. Yuan, P. Sun, J. Zhao, D. Li, C. Wang, A review of moving object trajectory clustering algorithms, *Artif. Intell. Rev.* 47 (2017) 123–144. <https://doi.org/10.1007/s10462-016-9477-7>.
- [255] A. Hooshmand, M.I. Campbell, Layout synthesis of fluid channels using generative graph grammars, *Artif. Intell. Eng. Des. Anal. Manuf. AIEDAM.* 28 (2014) 239–257. <https://doi.org/10.1017/S0890060414000201>.
- [256] G.T. Carranza, U. Robles, C.L. Valle, J.J. Gutierrez, R.C. Rumpf, Design and Hybrid Additive Manufacturing of 3-D/Volumetric Electrical Circuits, *IEEE Trans. Components, Packag. Manuf. Technol.* 9 (2019) 1176–1183. <https://doi.org/10.1109/TCPMT.2019.2892389>.
- [257] E. MacDonald, R. Salas, D. Espalin, M. Perez, E. Aguilera, D. Muse, R.B. Wicker, 3D printing for the rapid prototyping of structural electronics, *IEEE Access.* 2 (2014) 234–242. <https://doi.org/10.1109/ACCESS.2014.2311810>.
- [258] Y. Lin, O. Gordon, M.R. Khan, N. Vasquez, J. Genzer, M.D. Dickey, Vacuum filling of complex microchannels with liquid metal, *Lab Chip.* 17 (2017) 3043–3050. <https://doi.org/10.1039/c7lc00426e>.
- [259] N. Umetani, R. Schmidt, SurfCuit: Surface Mounted Circuits on 3D

Bibliography

- Prints, *IEEE Comput. Graph. Appl.* 38 (2016) 52–60. <http://arxiv.org/abs/1606.09540> (accessed June 22, 2021).
- [260] M. Biedermann, M. Meboldt, S. Walker, D. Schwendemann, Rethinking Co-Extrusion: Additive Manufacturing and Simulation-Based Design as a Duo for Extrusion Dies, *Kunststoffe Int.* 2021 (2021) 26–29.
- [261] F. Chinesta, E. Cueto, Empowering Engineering with Data , *Machine Learning and Artificial Intelligence : A Short Introductory Review*, (n.d.).
- [262] F. Dworschak, S. Dietze, M. Wittmann, B. Schleich, S. Wartzack, Reinforcement Learning for Engineering Design Automation, *Adv. Eng. Informatics.* 52 (2022) 101612. <https://doi.org/10.1016/J.AEI.2022.101612>.
- [263] J. Jiang, Y. Xiong, Z. Zhang, D.W. Rosen, Machine learning integrated design for additive manufacturing, *J. Intell. Manuf.* (2020) 1–14. <https://doi.org/10.1007/s10845-020-01715-6>.
- [264] R. Sandeep, B. Jose, K.G. Kumar, M. Manoharan, N. Arivazhagan, Machine Learning Applications for Additive Manufacturing : State-of-the-Art and Future Perspectives, *Ind. Transform.* (2022) 25–44. <https://doi.org/10.1201/9781003229018-2>.
- [265] J. Qin, F. Hu, Y. Liu, P. Witherell, C.C.L. Wang, D.W. Rosen, T.W. Simpson, Y. Lu, Q. Tang, Research and application of machine learning for additive manufacturing, *Addit. Manuf.* 52 (2022) 102691. <https://doi.org/10.1016/J.ADDMA.2022.102691>.
- [266] G. Mirra, A. Pugnale, Expertise, playfulness and analogical reasoning: three strategies to train Artificial Intelligence for design applications, *Archit. Struct. Constr.* 2022. 1 (2022) 1–17. <https://doi.org/10.1007/S44150-022-00035-Y>.
- [267] J.L. Sandoval Murillo, R. Osen, S. Hiermaier, G. Ganzenmüller, Towards understanding the mechanism of fibrous texture formation during high-moisture extrusion of meat substitutes, *J. Food Eng.* 242 (2019) 8–20. <https://doi.org/10.1016/j.jfoodeng.2018.08.009>.
- [268] P. Wittek, N. Zeiler, H.P. Karbstein, M.A. Emin, High Moisture Extrusion of Soy Protein: Investigations on the Formation of Anisotropic Product Structure, *Foods.* 10 (2021) 102. <https://doi.org/10.3390/foods10010102>.

Curriculum vitae

Personal data:

Name: Manuel Biedermann
Date of birth: April 1, 1991
Place of birth: Ingolstadt, Germany
Nationality: German

Education:

07/2017 – 10/2022 **Doctor of Science (Dr. sc. ETH Zurich)** in Mechanical Engineering, Product Development Group Zurich, ETH Zurich (ETHZ), Switzerland

10/2013 – 05/2017 **Master of Science (M.Sc.)** in Mechanical Engineering, Technical University Munich (TUM), Germany

09/2014 – 01/2015 **Exchange Semester** at the Tsinghua University Beijing (THU), School of Economics and Management, China

10/2010 – 09/2013 **Bachelor of Science (B.Sc.)** in Engineering Science, Technical University Munich (TUM), Germany

09/2001 – 06/2010 **High School Education**, Christoph Scheiner Gymnasium Ingolstadt, Germany

Professional experience:

07/2017 – present **Research Associate**, Product Development Group Zurich, ETH Zurich (ETHZ), Switzerland

Curriculum vitae

- 11/2016 – 04/2017 **Master Thesis and Working Student**, Siemens AG, Corporate Technology, Munich, Assistant for Projects Related to Design for Additive Manufacturing, Title of Master Thesis: “*Simulation-Driven Design for Additive Manufacturing*”
- 01/2016 – 04/2016 **Semester Thesis**, Fraunhofer IWU, Augsburg, Title of Semester Thesis: “*Lightweight Design of an Additive Manufactured Gear Wheel with Integrated Fluid Channels for Lubrication and Cooling*”
- 05/2014 – 08/2016 **Internship**, Dassault Systèmes Corp., SIMULIA, Providence, USA, Assistant for the Development of Optimization Workflows in the Area of Computer-Aided Engineering, Transfer of Knowledge related to Computer-Aided Structural Optimization, and Development of a Training Course
- 09/2012 – 04/2014 **Bachelor Thesis and Working Student**, FE-DESIGN GmbH, Munich, Assistant for Projects Related to Computer-Aided Structural Optimization, Title of Bachelor Thesis: “*Structural Shape Optimization Combining a Controller and Sensitivity-Based Approach*”
- 05/2012 – 08/2012 **Research Assistant**, Technical University Munich (TUM), Chair for Formal Languages, Compiler Construction, Software Construction, Project Work in the Area of Embedded Software Development

List of publications

1. M. Biedermann, P. Beutler, M. Meboldt, Routing multiple flow channels for additive manufactured parts using iterative cable simulation, *Additive Manufacturing*, vol. 56, pp. 102891, Amsterdam: Elsevier, 2022, DOI: 10.1016/j.addma.2022.102891.
2. M. Biedermann, P. Beutler, M. Meboldt, Automated Knowledge-Based Design for Additive Manufacturing: A Case Study with Flow Manifolds, *Chemie Ingenieur Technik*, vol. 94: no. S 7, pp. 939-947, 2022, DOI: 10.1002/cite.202100209.
3. P. Beutler, M. Biedermann, U. Hofmann, R. Rosenbauer, M. Meboldt, Automated Design Workflow for Structural Nodes of Space Frame Structures, 32nd Design in a Changing World (*CIRP Design Conference 2022*), Paris, France, pp.419-424, Amsterdam: Elsevier, March 28– 30, 2022, DOI: 10.1016/j.procir.2022.05.272.
4. M. Biedermann, P. Beutler, M. Meboldt, Automated design of additive manufactured flow components with consideration of overhang constraint, *Additive Manufacturing*, vol. 46, pp. 102119, Amsterdam: Elsevier, 2021, DOI: 10.1016/j.addma.2021.102119.
5. J. Ferchow, M. Biedermann, P. Müller, B. Auchmann, A. Brem, M. Meboldt, Harnessing manufacturing elements to select local process parameters for metal additive manufacturing: A case study on a superconducting solenoid coil, *Additive Manufacturing*, vol. 46, pp. 102140, Amsterdam: Elsevier, 2021. DOI: 10.1016/j.addma.2021.102140.
6. M. Biedermann, M. Meboldt, S. Walker, D. Schwendemann, Rethinking Co-Extrusion: Additive Manufacturing and Simulation-Based Design as a Duo for Extrusion Dies, *Kunststoffe International*, vol. 2021: no. 1, pp. 26-29, München: Carl Hanser Verlag, 2021.

List of publications

7. M. Biedermann, M. Meboldt, S. Walker, D. Schwendemann, Innovation in der Profil Co-Extrusion, *KunststoffXtra*, vol. 2020: no. 11, pp. 18-20, Zug: Sigwerb GmbH, 2020.
8. M. Biedermann, M. Widmer, M. Meboldt, Additive Manufactured Break-Out Cores for Composite Production: A Case Study with Motorcycle Parts, *Munich Symposium on Lightweight Design 2020*, Online, pp.63-73, Berlin; Heidelberg: Springer Vieweg, November 17, 2020. DOI: 10.1007/978-3-662-63143-0_7.
9. M. Biedermann, M. Meboldt, Computational design synthesis of additive manufactured multi-flow nozzles, *Additive Manufacturing*, vol. 35, pp. 101231, Amsterdam: Elsevier, 2020, DOI: 10.1016/j.addma.2020.101231.
10. D. Omidvarkarjan, D. Cipriano, R. Rosenbauer, M. Biedermann, M. Meboldt, Implementation of a design support tool for additive manufacturing using a feature database: an industrial case study, *Progress in Additive Manufacturing*, vol. 5: no. 1, pp. 67-73, Cham: Springer, 2020, DOI: 10.1007/s40964-020-00119-5.
11. M. Biedermann, M. Meboldt, Analyse von Trends in der Implementierung der Additiven Fertigung anhand aktueller industrieller Anwendungen, In *Konstruktion für die Additive Fertigung 2018*, edited by R. Lachmayer, R. B. Lippert, S. Kaiерle, pp. 37-53, Heidelberg: Springer, 2019, DOI: 10.1007/978-3-662-59058-4_3.
12. M. Biedermann, M. Meboldt, Additive Fertigung mit Design-automatisierung, *KunststoffXtra*, vol. 2019: no. 12, pp. 9-12, Zug: Sigwerb GmbH, 2019.

13. R. Kussmaul, M. Biedermann, G. A. Pappas, J. G. Jónasson, P. Winiger, M. Zogg, D.-A. Türk, M. Meboldt, P. Ermanni, Individualized lightweight structures for biomedical applications using additive manufacturing and carbon fiber patched composites, *Design Science*, vol. 5, pp. e20, Cambridge: Cambridge University Press, 2019, DOI: 10.1017/dsj.2019.19.
14. D.-A. Türk, F. Rüegg, M. Biedermann, M. Meboldt, Design and manufacture of hybrid metal composite structures using functional tooling made by additive manufacturing, *Design Science*, vol. 5, pp. e16, Cambridge: Cambridge University Press, 2019, DOI: 10.1017/dsj.2019.16.
15. R. Kussmaul, M. Biedermann, J. Jónasson, M. Zogg, C. Klahn, M. Meboldt, P. Ermanni, Individualized and sustainable lightweight structures from Additive Manufacturing and carbon fiber patched composites, *1st Symposium on Lightweight Design in Product Development (LWD-PD 2018)*, Zurich, Switzerland, pp.60-62, Zurich: CMASLab, ETH Zurich, June 14-15, 2018.
16. M. Biedermann, T. Kamps, C. Kiener, Redesign of a burner tip with multiple integrated flow distributors, *Fraunhofer Direct Digital Manufacturing Conference (DDMC 2018)*, Berlin, Germany, pp. 389, Stuttgart: Fraunhofer Verlag, March 14-15, 2018.
17. M. Biedermann, M. Meboldt, Swiss AM Guide 2018: Exploring new applications in additive manufacturing, Zurich: pd|z; ETH Zurich; AM Network Switzerland, 2018.
18. T. Kamps, M. Biedermann, C. Seidel, G. Reinhart, Design approach for additive manufacturing employing Constructal Theory for point-to-circle flows, *Additive Manufacturing*, vol. 20, pp. 111-118, Amsterdam: Elsevier BV, 2018, DOI: 10.1016/j.addma.2017.12.005.

List of publications

19. M. Biedermann, M. Schoen, M. Meboldt, Design automation for additive manufacturing applied to branched fluid structures, *29th DfX Symposium 2018*, Tutzing, Germany, pp.131-142, Neubiberg: Institut für Technische Produktentwicklung, Universität der Bundeswehr München, September 25-26, 2018.

20. R. Kussmaul, M. Biedermann, J. Jónasson, D. Türk, M. Zogg, C. Klahn, M. Meboldt, P. Ermanni, Combining Additive Manufacturing and Carbon Fiber Patched Composites for Individualized and Sustainable Biomedical Applications, *18th European Conference on Composite Materials (ECCM18)*, Athens, Greece, pp.3058-3065, Patras: Applied Mechanics Laboratory, June 24-28, 2018.

21. M. Chinnakonda, M. Biedermann, S. Eyl, G. Dimitrova, J. Chinnaraju, Coronary Stent Design Optimization Using Parametric and Nonparametric Approaches—A Proof of Concept Study, *Journal of Med. Devices*. Sep 2015, 9(3): 030953, DOI: 10.1115/1.4030583.